UNIVERSITÀ DEGLI STUDI DI TRIESTE

XXXII CICLO DEL DOTTORATO DI RICERCA IN
FISICA

PO FRIULI VENEZIA GIULIA - FONDO SOCIALE EUROPEO 2014/2020

EFFECT OF MODERN RADIOTHERAPY ON PATIENTS WITH CARDIAC IMPLANTABLE ELECTRONIC DEVICES (CIEDs): A COMPREHENSIVE STUDY

Settore Scientifico-disciplinare FIS/07 Fisica Applicata (a Beni Culturali, Ambientali, Biologia e Medicina)

Dottorando:

HOSSEIN ASLIAN

Supervisore:

Dr. MARA SEVERGNINI

Coordinatore & Correlatore:
Prof. FRANCESCO LONGO

ANNO ACCADEMICO 2019-2020

University of Trieste

CYCLE 32 - PHD SCHOOL IN PHYSICS

PO FRIULI VENEZIA GIULIA - FONDO SOCIALE EUROPEO 2014/2020

EFFECT OF MODERN RADIOTHERAPY ON PATIENTS WITH CARDIAC IMPLANTABLE ELECTRONIC DEVICES (CIEDs): A COMPREHENSIVE STUDY

Scientific Discipline FIS/07 Applied Physics (Cultural Heritage, Environment, Biology and Medicine)

Candidate:

HOSSEIN ASLIAN

Research Supervisor:

Dr. MARA SEVERGNINI

Co-supervisor & Coordinator:
Prof. FRANCESCO LONGO

SCHOOL YEAR 2019-2020

"To people with cancer & their loved ones"

Contents

List of Figures

List of Tables

Abstract

According to WHO, 17.9 million people died from Cardiovascular diseases (CVDs) in 2016, representing 31% of all deaths worldwide. During the last decades, cardiac implantable electronic device (CIED) therapy has become first line therapy for those who are at risk for life-threatening ventricular arrhythmias and those survived cardiac arrest. Therefore, there has be a continuous increase in the number of patients with CIEDs, especially in Europe and Italy.

Also, the number of new cancer patients is expected to experience an increase of 53% for 2030. Because radiotherapy (RT) is considered as one of the main component of cancer treatment, approximately 50% of cancer patients will receive at least one course of RT during their treatment. Accordingly, over the last decades, there has been an ever-increasing growth in the number of cancer patients and comorbid cardiovascular disease using CIEDs.

Since the publication of the American Association of Physicists in Medicine (AAPM)-TG34 report, as the earliest guideline published for the management of patients with CIEDs receiving general radiotherapy (RT) in 1994, technologies pertaining to all elements of the chain of RT have progressed. These developments, coupled with advancements in CIED technology, have led to a need for more research on this topic. Due to this fact, many studies have focused on the effect of radiotherapy on patients with CIEDs, and many aspects of this field have been investigated in the literature. However, with the widespread implementation of advanced RT technologies and techniques, the need to consider the different challenges of modern RT techniques when managing patients with CIEDs has arisen.

The main goal of this comprehensive study is to investigate effects of modern radiotherapy on CIED patients.

The thesis is divided in five chapters with an introductory chapter providing a very short explanation of CIED therapy and number of cancer patients with CIEDs.

In the first part of the study, chapter2, a deep review of the literature and analysis study have been conducted. This review and analysis highlighted the available sparse information in the literature and ended up by posing questions for future research.

In the second part of the research, chapter 3, the use of image-guided radiotherapy (IGRT) in patients with CIEDs was investigated. Accordingly, a multicenter dosimetry study to evaluate the imaging dose from Elekta XVI and Varian OBI kV-CBCT systems to cardiovascular implantable electronic devices (CIEDs) was carried out at four centers in the north of Italy, including university hospital of Trieste, Trento, Brescia, and Udine. The results of this study were applied to add new data in the literature and Associazione Italiana di Fisica Medica (aifm) working group.

In the third part, chapter 4, the effect of a stereotactic body radiotherapy (SBRT) using flattening filter-free beams on implantable cardioverter-defibrillators (ICDs), as widespread modern modality for the treatment of cancer, was done. First, a retrospective analysis of patients with CIEDs who underwent radiosurgery SBRT and radiosurgery (SRS) at Peter MacCallum Cancer Centre (the largest cancer research group in Australia) between 2014 and 2018 was performed. This was complemented through a phantom

study through a multidisciplinary study between medical physicists, radiation oncologists and electrophysiologists at the university of Trieste, Peter Mac and Royal Melbourne Hospital. The results of this study were used to update some of the policies applied to manage CIED patients undergoing SBRT/SRS at PeterMac.

In the last part of this comprehensive study, chapter 5, a Monte Carlo (MC) study of out-of-field doses from an ELEKTA 6 and 15 MV photon beam in a homogeneous water phantom at depth of CIED and clinical depth was conducted. Correspondingly, a comparison between the MC results with MONACO treatment planning system (TPS), as a Monte Carlo-based TPS, and radiation dosimetry measurements was carried out to evaluate the accuracy of dose calculation outside the field, where a CIED is usually located.

There has been a tremendous development in non-cardiac implantable electrical stimulation devices such as spinal cord stimulators (SCS), deep brain stimulators (DBS), vagal nerve stimulators (VNS), and sacral nerve stimulators. Therefore, this comprehensive study and its outlines can be considered as a stimulus for future study on the effect of radiotherapy on non-cardiac implantable devices and the potential adverse effects of radiation regarding these devices.

Riassunto

WHO dichiara che 17,9 milioni di persone sono decedute per malattie cardiovascolari (Cardiovascular diseases, CVDs) nel 2016, circa il 31% delle morti mondiali.

Negli ultimi decenni, la terapia tramite i dispositivi cardiologi impiantabili (CIED) è diventata la terapia principale per i pazienti a rischio vita per aritmie ventricolari e per quelli sopravvissuti ad arresto cardiaco. Per questo motivo si assiste a un continuo aumento del numero di pazienti portatori di CIED, specialmente in Europa e in Italia.

Contemporaneamente anche il numero di nuovi pazienti trattati per cancro è in aumento e ci si aspetta che si arrivi al 53% nel 2030. La radioterapia è considerata una delle maggiori componenti nel trattamento del cancro, infatti circa il 50% dei pazienti con cancro viene trattata con almeno un ciclo di radioterapia.

Nello stesso tempo, negli ultimi anni, c'è stato un aumento di pazienti con cancro che hanno anche patologie cardiovascolari portatori di CIED.

La prima linea guida per il trattamento radioterapico in sicurezza di pazienti portatori di device cardiologici è stata pubblicata nel 1994 da parte dell'associazione americana di fisica medica (American Association of Physicists in Medicine (AAPM)-TG34 report).

Le tecnologie in radioterapia sono progredite notevolmente e contemporaneamente ci sono stati sviluppi considerevoli nella tecnologia CIED che sono ad oggi oggetto di ricerca.

Per questi motivi , sono stati fatti molti studi sugli effetti della radioterapia sui pazienti portatori di CIED e molti aspetti sono stati studiati e pubblicati in letteratura.

Vista l'implementazione di tecniche sempre più avanzate in radioterapia è necessario continuare ad indagare le modalità di gestione in sicurezza del trattamento di questi pazienti portatori di device.

Il principale scopo di questo lavoro di dottorato è lo studio degli effetti della radioterapia moderna sui pazienti con CIED.

La tesi è suddivisa in cinque capitoli che seguono un primo capitolo che è un'introduzione con una breve spiegazione della terapia con CIED e con dati statistici relativi ai pazienti CIED malati di cancro.

Nella prima parte dello studio, capitolo 2, è mostrata una revisione della letteratura. La revisione evidenzia e riordina tutte le informazioni sull'argomento e fa emergere nuovi quesiti per la ricerca futura.

Nella seconda parte dello studio, capitolo 3, è stato studiato l'impatto dosimetrico dell'uso delle immagini per il posizionamento del paziente in radioterapia (image-guided radiotherapy (IGRT)) con le due cone beam CT (CBCT) disponibili Elekta XVI and Varian OBI kV-CBCT, sui pazienti portatori di device.

I risultati dello studio studio multicentrico (Trieste, Trento, Brescia, Udine) sono stati pubblicati in collaborazione con il gruppo di lavoro dell'Associazione Italiana di Fisica Medica AIFM.

Nella terza parte, capitolo 4, è stato studiato l'effetto della moderna radioterapia stereotassica FFF (flattening filter-free beams stereotactic body radiotherapy (SBRT)) sui defibrillatori (cardioverter-

defibrillators (ICDs)). Per prima cosa è stata fatta un'analisi retrospettiva dei pazienti con CIED trattati per trattamenti stereotassici (SBRT) o di radiochirurgia (SRS) presso il Peter MacCallum Cancer Centre (il centro australiano per radioterapia più grande) dal 2014 al 2018.

A completamento dello studio sono state effettuate misure in fantoccio per studiare i possibili malfunzionamenti durante l'esposizione di ICD a trattamenti di SBRT e SRS in collaborazione con fisici medici, radioterapisti e elettrofisiologi dell'Università di Trieste e del Peter Mac and Royal Melbourne Hospital.

I risultati sono stati utilizzati per aggiornare le procedure di trattamento nei pazienti portatori di device sottoposti a trattamenti SBRT/SRS al PeterMac.

Nell'ultima parte dello studio, capitolo 5, è stata effettuata la simulazione Monte Carlo (MC) del linac Elekta per i fasci di fotoni di energia 6 e 15 MV e sono state studiate le dosi fuori campo e confrontate con misure sperimentali al fine di stabilire l'accuratezza dei sistemi di pianificazione del trattamento, in dotazione presso la fisica sanitaria di Trieste, nella stima della dose ai CIED.

Si sta assistendo a uno sviluppo considerevole di device impiantabili non cardiologici come stimolatori mi midollo spinale, stimolatori celebrali, stimolatori vagali e stimolatori del nervo sacrale. Questo studio può essere di stimolo per studi futuri sui possibili effetti della radioterapia sui device non cardiologici.

Chapter 1: Introduction into cardiac implantable electronic devices (CIEDs)

1.1 Basic anatomy and internal electrical conducting system of the heart

The heart is considered as a highly efficient pump which lies in the central part of the chest called the mediastinum. The hear composed of four chambers; The bottom chambers are pumping chambers called ventricles namely, left ventricle (LV) and right ventricle (RV). [1–3] LV particularly has a thick muscular wall, because it pumps the blood all around the body into the systematic circulation. RV has a much thinner muscular wall because it only pumps the blood to the lungs which are close to the heart. The upper chambers are filling chambers and called arteria namely, left arteria (LA) and right arteria (RA). In the other words, the heart pumps the blood through the arteries to every last part of the body and supplies the cell with oxygen. In contrast, the venous system task is to transport the deoxygenated blood from the body back to the heart and from there onwards to the lung. There are also four valves namely, the aortic, mitral, tricuspid and pulmonary valves, which regulate blood flow through the heart. [2,3]

The blood coming back through the lungs through pulmonary veins, and this blood is oxygenated. The blood goes through mitral valve into the LV. When the LV contracts, that blood will be ejected through aortic valve into the aorta and then through the body. Then, when it arrives back from the systematic circulation and from the superior (top) and inferior (bottom) venae cavae, is de-oxygenated boold, and drain into RA. Then, blood goes through tricuspid valve to the RV. When RV contracts, the blood will be ejected through pulmonary valve and it will go to each lung. In summary, the LA, RA, LV, RV, pulmonary artery, aorta, superior and interior venae cavae, and pulmonary veins are the basic anatomical part of the heart. [3]

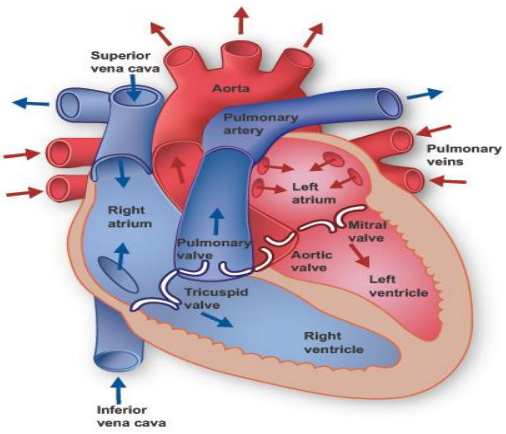

Figure 1: Human heart anatomy schematic [4]

The right side of the heart is important for the implantation of CIEDs, because of their connection with the low pressure venous system through which leads can be passed “transvenously” under fluoroscopic or x-ray control [2]

As mentioned, atria contract first, pushing the blood from atrium chambers through the atrioventricular valves into the ventricles. It has to happen first, in a coordinated way. Then, in an appropriate short period of time the ventricles need to contract. This whole procedure needs to be precisely coordinated and regulated. Just in the right atrium, somewhat near to entrance of the superior venae cavae, there is an area of specialized myocardial tissue which is electrically active. This area is called pacemaker of the heart or the sinoatrial (SA) node. It generates sinus rhythm and depolarize spontaneously around 90-100/mins. There is another electronically active area of the heart between atria and ventricles called AV node. But, its spontaneous depolarization rate is lower than SA node. SA node governs other active tissues and is the physiological origin of the electrical activity required to stimulate myocardial cells in order to generate myocardial contraction. There are electrical path ways take impulses through atrium. These path ways convey at AV node which is known as the collecting node. As impulses go through the AV node, it is delayed about 20-40 ms. This delay is gives the blood mechanically to get through from atria to the ventricles. [2,3,5,6]

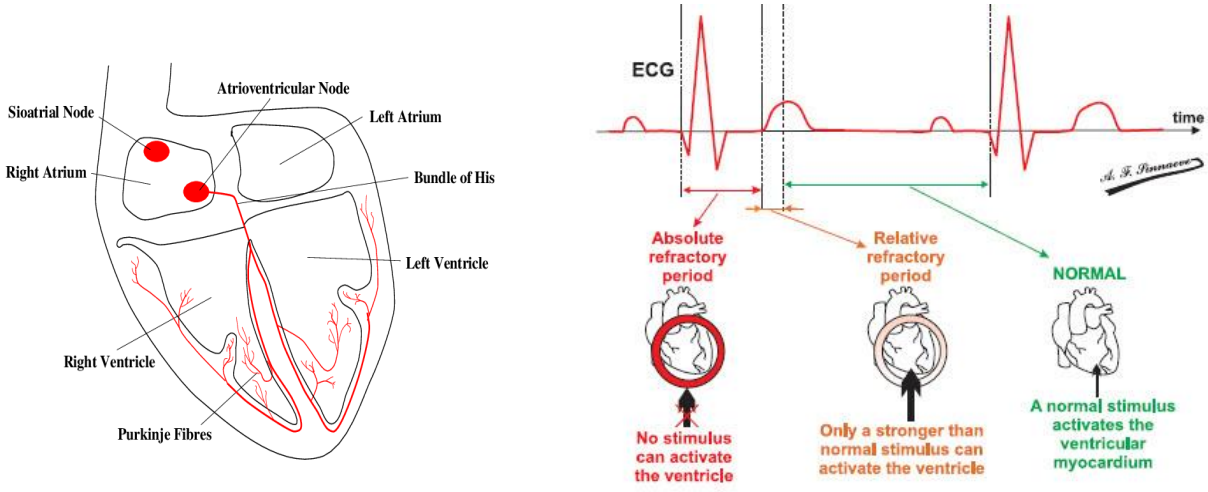

Figure 2: (left) Internal electrical conducting system of the heart [7]*; (right) ECG* [5]

An electrocardiogram (ECG) records electrical potential and conduction generated by the heart. It illustrates several information from the structure of the heart to components of the conducting system. The sinus node is anatomically a very small structure with relatively few cells, so that the sum total of the depolarization potentials is insufficient to register on the surface

electrocardiograph. Atrial muscle depolarization is registered as a small P wave (Figure 2). There is a pause after the P wave before ventricular depolarization or the QRS occurs, called the PR interval. This section is measured from the commencement of the P wave to the commencement of the "Q" or "R" wave and is resultant from the summation of atrial depolarization and the slowing down of the impulse at the AV node. The QRS represents the depolarization of every ventricular cell and usually is completed in <0.1 second emphasizing the conduction speed of the bundle branches and purkinje system. [1,2,5–7]

1.2 Basic concepts in CIED therapy

CIEDs are indicated for electrical disturbances of the heart called arrhythmias which can be slow (bradycardias or bradyarrhythmias) or fast (tachycardias or tachyarrhythmias). These arrhythmias in the worst case scenario, may be lethal without the protection from an implanted CIED and in the best case scenario, the CIED may not only save the recipient's life, but also may markedly improve the patient's quality of life.[2,5,6]

As mentioned, the sinoatrial (SA) node is the heart natural pacemaker. When SA is not able to generate strong and suitable natural biological electrical impulses, an electrostimulation is required. Therefore, this important role might be replaced by external artificial electrical impulses produced by a PM and through leads and needle electrodes to the heart muscles [8,9].

Pacemaker (PM), is an electronic device implanted usually in the left clavicular region to regulate the heartbeat. The PM delivers electrical stimuli over leads with electrodes in contact with the heart. A PM is not designed to deliberate the heart by the delivery of shocks. [2,5]

Implantable cardioverter-defibrillator (ICD) is an electronic device usually implanted in the left clavicular region to prevent ventricular tachycardia. ICDs can also works as a classic pacemaker for bradycardia pacing. But, it is mainly designed to defibrillate the heart by delivering high voltage shocks or to stop malignant tachycardia by anti-tachycardia pacing (short burst of rapid pacing sequence). [2,6]

Another advancement in cardiac pacing is *cardiac resynchronizing therapy (CRT)* using biventricular (left and right ventricles) pacing. This type of pacing is not for a cardiac bradyarrhythmia, but rather a means of altering left ventricular contraction in patients with a congestive cardiomyopathy or severe heart muscle disease. There are two types of CRT devices, namely CRT-P which is cardiac resynchronization therapy pacemaker or a biventricular pacemaker, and CRT-D, which is a cardiac resynchronization therapy defibrillator or a biventricular ICD. [2,6]

The pacing pulse refers to amplitude of the pulses which can generate an action potential in tissue touched by an electrode and it is almost 5.4 Volts.[5]

Sensitivity is a measure of the minimal potential of the wave that is programmed to sense by the PM and it is measured in mV. In other word it is the minimum myocardial voltage required to be detected waves in ECG. [5,6]

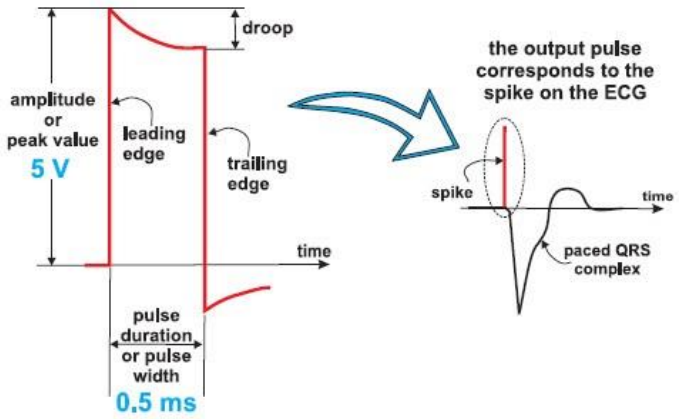

Figure 3: A nominal pacing pulse [5]

The North American Society of Pacing and Electrophysiology (NASPE) and British Pacing and Electrophysiology Group (BPEG) published as a joint effort the pacemaker code known as the NBG pacemaker code. Table 1 identifies the NBG code for CIED [10]. The first and second letters define the chamber paced and sensed and the third letter, the response to sensing. A fourth letter is used if there is rate adaptive pacing which is a means of increasing the pacing rate using a sensor. [2,10]

Table 1: The identification code for cardiac pacemakers

First letter (Chamber being paced)	Second letter (Chamber being sensed)	Third letter (Response to sensing)	Fourth letter
A—atrium V—ventricle D—atrium and ventricle O—no pacing or sensing	A—atrium V—ventricle D—atrium and ventricle O—no pacing or sensing	A—atrium V—ventricle D—atrium and ventricle O—no pacing or sensing	'R' to identify a rate adaptive function.

Very specific hardware is necessary to pace or shock the heart. Generally, a PM includes a low voltage pulse generator for cardiac pacing and a high voltage shock box for defibrillation. These

interface with the heart muscle by insulated wires called leads which require careful implantation in specific areas of the heart. An ICD comprises a pulse generator or shock box, which has three major components: a larger hermetically sealed encapsulating can, an extremely reliable lithium power source and sophisticated microprocessor based electronic circuitry. [2,11,12]

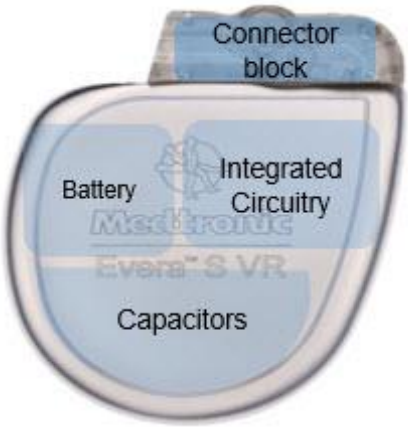

Figure 4: ICD components: integrated circuitry is made of microprossesor, RAMROM, RF link and TM control.

The programmer is a sophisticated, company specific, computer used for programming, interrogating and evaluating CIED. In other words, communication with CIED system which is a complicated procedure conducted by this dedicated computer through radio-frequency telemetry. All pacemakers available today are multi-programmable with memory capability to collect vast amounts of information such as pacemaker usage, arrhythmia documentation, automatic testing and battery status. [1,2,11,12]

Figure 5: Programmers (left); CIEDs on the table (right).

1.3 The number of cancer patients and comorbid cardiovascular disease

According to WHO, 17.9 million people died from Cardiovascular diseases (CVDs) in 2016, representing 31% of all deaths worldwide [13]. During the last decades, cardiac implantable electronic device (CIED) therapy has become first line therapy for those who are at risk for life-threatening ventricular arrhythmias and those survived cardiac arrest [13–15]. Therefore, there has be a continuous increase in the number of patients with CIEDs, especially in Europe and Italy. [16]

Also, the number of new cancer patients is expected to experience an increase of 53% for 2030 [16]. Because radiotherapy (RT) is considered as one of the main component of cancer treatment, approximately 50% of cancer patients will receive at least one course of RT during their treatment. Accordingly, over the last decades, there has been an ever-increasing growth in the number of cancer patients and comorbid cardiovascular disease using CIEDs. [17,18]

CIED therapy is one of the most significant advances in providing care and service to cardiovascular patients, with a life-saving benefit exceeding that of all antiarrhythmic drugs [2,5,6].

Over the last few decades, there has been an ever-increasing number of patients undergoing CIED implantation to improve quality of life and prolong survival among those suffering from cardiovascular disease. As the average patient age increases, the number of cancer patients and comorbid cardiovascular disease also increases.

During the last two decades, implantable defibrillator therapy has become first line therapy for high risk patients for life-threatening ventricular arrhythmias and those survived cardiac arrest and for patients [15,19]. Although CIED implantation is continuously increasing in Europe, the rates in each European country varies with economic factors [15,16,18]. According to a statistic study conducted by Raatikainen, just in Italy there was 62,198 absolute number of CIED impanation in 2013, which was 1,012 per million inhabitants. [15]

Conclusively, over the last few decades there has been an ever-increasing number of patients undergoing CIED implantation to improve quality of life. As patient age and comorbidities increase, the number of patients with CIEDs undergoing Radiotherapy has also increased.

Chapter 2: A literature review and analysis of effect of modern radiotherapy on CIED patients

2.1 Introduction

The number of new cancer patients is expected to experience an increase of 53% for 2030 [17]. Because radiotherapy (RT) is considered as one of the main component of cancer treatment, approximately 50% of cancer patients will receive at least one course of RT during their treatment [18]. Accordingly, over the last decades, there has been an ever-increasing growth in the number of cancer patients and comorbid cardiovascular disease using CIEDs [20].

The American Association of Physicists in Medicine (AAPM) report (TG34) was the earliest guideline published for the management of patients with CIEDs receiving general radiotherapy (RT) in 1994 [21]. Since the publication of the AAPM (TG34) report, technologies pertaining to all elements of the chain of RT have progressed. Also, CIED has undergone significant changes in software and hardware technology. Therefore, there has been a need for more research on this topic and many aspects of how radiotherapy dose affects the CIED have been investigated in the literature [20].

In general, all the citation in the field can be categorised into different groups as following: a) national and international guidelines, recommendations [21–25] and reviews[26][27], b) in-vitro study [28–33], c) in-vivo[34–38] study, d) case repots and clinical studies[39–41], e) related engineering studies [42–45], and f) Monte-Carlo and dosimetry studies [46,47]. In these studies, different aspects were investigated such as how to measure dose to the CIED [48], estimation of CIED dose [49], the effect of direct and indirect exposure reported in *in vivo* and *in vitro* studies, and the assessment of risk [30], mechanism [28], and source [41,50] of CIED malfunctions. Treatment planning techniques for CIED avoidance have also been reported [20,51]

While going through these papers and citations carefully for the purpose of a deep review, we understand that the majority of them focused on the conventional radiotherapy and related challenges and concerns. Subsequently, the published guidelines and recommendation mainly addressed the management of patients with CIEDs undergoing conventional RT. Although some of the recent papers investigated some of the aspects of the modern RT, still of the review papers and recommendation emphasized the imperative need to consider modern radiotherapy, and its related challenges to manage CIED patients [20].

2.2 Materials and methods

A literature search was performed using the following search engines: PubMed, Science Direct and Google Scholar. Search keywords included the following terms: ‘Radiotherapy & Pacemaker’,

'Radiotherapy & Defibrillator', 'Dosimetry & Pacemaker', 'Dosimetry & Defibrillator', 'Electromagnetic Interference & Pacemaker', 'Electromagnetic Interference & Defibrillator', 'Radiation induced & Pacemaker', 'Radiation induced & Defibrillator', 'Neutron & Pacemaker', 'Neutron & Defibrillator', 'Pacemaker & Monte-Carlo', 'Defibrillator & Monte-Carlo', 'Imaging Dose & Pacemaker' and 'Imaging Dose & Defibrillator'. All citations available in the aforementioned databases written in English or an abstract written in English were considered in this review. However, due to the large number of finding, the literature search in Google Scholar was limited to the most cited scholarly works but without any filtration in PubMed and Science Direct. The second step was to examine the citations, regardless of their type (journal paper, conference paper and/or abstract, etc.), that met the following objectives:

a) Scholarly works investigating conventional and modern radiotherapy features that may influence CIED operation/functionality.

b) Scholarly works providing dosimetric data for patients with CIEDs undergoing conventional and modern radiotherapy.

c) Instances (or lack thereof) of CIED failures reported during or after a course of conventional and modern radiotherapy.

The final step was to classify these citations into the aforementioned sections. The classification was performed based on the number, type and methodology of research studies conducted on each section. The Mendeley desktop and online versions, which are free bibliographic software, were used to capture, catalogue and analyse the results.

2.3 Results

A total of 3983 references were identified. After deleting non-relevant publications, 1188 citations remained.

2.3.1 Conventional RT and CIEDs

Table 2 provides a summary of the most cited and/or interesting citation in the classified group, as explained above.

Table 2: Summary of the most cited and/or interesting research in the field

Publication year	Name of the first author	
• National and international guidelines, recommendations and reviews		
1994	Marbach et al. [21]	AAPM Task Group (TG-34)
2012	Hurkmans et al. [22]	Practical guideline in the Netherlands
2015	Gauter-Fleckenstein et al. [23]	DEGRO/DGK guideline
2018	Zecchin et al. [24]	Italian consensus
Online source	*Cancer Institute of New South Wales* [25]	Cancer Institute of New South Wales
2016	*Zaremba et al.*	Review paper
2010	*Hudson et al.*	Review paper
2005	*Hurkmans et al.* [32]	In-vitro
2012	*Hashimoto et al.* [33]	In-vitro
2002	*Mouton et al.* [30]	In-vitro
2014	*Zaremba et al.* [29]	In-vitro
• Case repots and clinical studies		
2008	Munshi et al. [40]	Case study
2013	*Elders et al.*[41]	Clinical Study
2002	*Garofalo et al.* [42]	
• Monte-Carlo and dosimetry studies		
2017,2019	Ezzati [46,47]	Monte Carlo
2010	Studenski *et al.* [48]	Dosimetry
2016	Peet et al. [49]	Dosimetry

2.3.2 IGRT and CIEDs

This literature review showed that there is a lack of clinical and experimental data focusing on possible effects of IGRT such as kV CBCT, portal images on CIED patients. There were only two studies in the form of abstracts published in this topic by Wronski et al. [17] and Ming et al. [18].

In the first study the authors investigate imaging dose from kV CBCT to CIEDs using MOSFET dosimeters and in the second, Ming et al. [18] reported Monte Carlo (EGS4) simulated CIED doses due to kV-CBCT. However, there was no detailed information regarding their protocols and kV-CBCT systems and analysis. Therefore, more investigation needs to add new clinical data and enrich the sparse data [20].

2.3.3 SBRT/SRS and CIEDs

The updated literature showed that among modern RT, there are also lack of experimental data on management of CIED patients treated with stereotactic body radiotherapy (SBRT)/SRS[20].

SBRT is increasingly used due to the possibility of achieving a highly localised dose distribution facilitated by the common use of non-coplanar beam deliveries, the explicit inclusion of motion management and the use of image guidance [52]. It is an effective technique to treat different malignancies, including both primary and metastatic lung, liver, brain, vertebral, kidney and pancreatic tumours [53]. Most of the aforementioned features may be particularly challenging when SBRT/SRS is adopted for treating patients with cardiac implantable electronic devices (CIEDs) [20].

In this literature review we found that, only 12 related scholarly works related to patients with CIEDs undergoing SBRT/SRS have been reported since 2000; these citations include only three case studies, two abstracts and one conference paper directly focused on this topic. The remaining articles are general studies addressing different numbers of patients with CIEDs who received stereotactic RT in their total datasets without reporting detailed information regarding these patients [20].

Available data regarding SBRT and SRS in patients with CIED are limited with respect to delivery systems and techniques, as well as patient datasets. According to our review, only one study reported on the use of a Gamma-Knife to treat patients with CIEDs (10 out of 215 patients with CIEDs), with no additional details about these patients [54]. Additionally, only one case study reported the use of tomotherapy SBRT [55], and four studies reported the use of a CyberKnife to treat patients with CIEDs [56–59]. Similarly, clinical data regarding conventional linac-based SBRT and SRS are scarce [56,60,61]. The only study found for this review regarding SBRT treatment plans and/or plan optimisation for patients with CIEDs was a conference proceeding paper [62] [20].

Table 3: A summary of studies considering stereotactic radiotherapy for patients with CIEDs

Publication year	Name of the first author	A brief summary and specific outcomes
• Patient studies		
2015	Prisciandaro et al [60]	✓ 6 lung cancer patients with CIEDs were treated with conventional linac-based SBRT and 1 CIED patient with conventional linac-based SRS ✓ CIEDs distance to treatment fileds ranged from 1.5 cm to 40cm ✓ Reported CIED dose *0.54-1.81 Gy* ✓ Functionality of the CIEDs during RT was reported, and 2 failures (ICD partial-resets) occurred; both were associated with a higher energy (16 MV), but it is not clear whether these beams were associated with the SBRT/SRS treatments.
2014	Ahmed et al [61]	✓ A case study (lung) cancer patient were treated in 3 different RT techniques including SBRT ✓ CIED was inside fields ✓ Dmax=52.4 Gy. ✓ Functionality of the AICD during and after RT was assessed, and no failures occurred
2011	Soejima et al [56]	✓ 4 lung cancer patients with CIEDs treated with conventional linac-based SBRT and 2 brain cancer patients were treated with conventional linac-based SRS ✓ CIEDs were outside the SBRT fields ✓ Functionality of the CIEDs during and after RT was reported, and no failures occurred due to SBRT/SRS.
• Treatment planning system calculations and optimisation		
2012	*Chow and Jiang* [62]	
2002		
• Tomotherapy, CyberKnife, VERO, and Gamma-Knife		
2015	Scobioala et al [55]	✓ A case study (lung) cancer patient treated with 3DCRT and SBRT using tomotherapy ✓ Patient has PM and ICD and they were inside the SBRT field

		✓ *ICD: D_{max}=15.58 Gy* and *PM: D_{max}=2.74 Gy* ✓ Functionality of CIEDs during and after RT was assessed, and no failures occurred due to SBRT/SRS
2008	Bianchi et al [57]	✓ 2 (lung & thymus) cancer patients with CIEDs treated with CyberKnife ✓ Functionality of CIEDs during and after RT was assessed, and a malfunction during the first fraction of the second patients (defibrillator was triggered) occurred
2015	Grant et al [54]	✓ 10 cancer patients with CIEDs treated with Gamma-Knife ✓ Functionality of CIEDs during and after RT was assessed, and no failures occurred due to SBRT/SRS.
2012	Çakmak et al [59]	✓ A case study lung cancer patient treated with CyberKnife ✓ CIEDs were outside the fields ✓ Functionality of ICD after RT was assessed, and it was found that 5 ICD inappropriate shocks during treatment had occurred.
2018	Riva et al [58]	✓ 35 (chest, head &neack, abdomen and pelvis) cancer patients with CIEDs treated with CyberKnife and VERO system ✓ Functionality of CIED during and after (only for 73% of all patients) RT was assessed, and no failures occurred due to SBRT/SRS
• Proton-SBRT therapy		
2012	Westover et al [63]	✓ A lung cancer patient treated with Proton SBRT ✓ CIEDs were outside the fields ✓ Functionality of CIED during and after RT was not reported at all.
2016	Ueyama et al [64]	✓ A lung cancer patient treated with Proton SBRT ✓ CIEDs were outside the fields ✓ The measured neutron dose=154.6 mSv ✓ Functionality of CIEDs during and after RT was assessed, and a change in the PM mode for patient 1 on treatment day 8 occurred ✓

2.4 Discussion

This in-depth review of literature showed that the previous published studies and citation mainly addressed the management of patients with CIEDs undergoing conventional radiotherapy. However, there are new challenges and concerns of modern RT for the management of CIED patients receiving such techniques and technologies. This is not only because of widespread use of modern techniques such as conventional and hypo-fractionated intensity modulated radiotherapy (IMRT) and volumetric modulated radiotherapy (VMAT), but also because the increasing installation of modern linac (eg,. CyberKnife) and hybrid technology (e.g., hybrid Linac-MR system) [20].

Therefore, the results indicated that as the clinical use of advanced RT technologies and techniques increases, the need to consider the different challenges of these techniques when managing patients with CIEDs has arisen [22]. Compared to conventional radiation therapy, in modern radiotherapy technologies and techniques there are characteristics that might demand special considerations for the safety of patients with CIEDs. The following are some of these characteristics:

1. Image-guided Radiotherapy (IGRT).
   IGRT is commonly used in modern techniques and there is a lack of clinical data on effects of IGRT on patients with CIEDs. The question may arise here is whether the additional imaging dose to CIEDs is negligible or considerable. If it is considerable, the question is how could this additional imaging dose be managed? What about the portal imaging dose from MV X-rays to CIEDs? [20]

2. Hypo-fractionated radiotherapy.
   Higher doses delivered in few fractions result in a higher dose per fraction for a CIED [20].

3. Dedicated Treatment Technologies.
   Apparat from conventional linacs, there are other dedicated treatment units such as CyberKnife, Gamma-Knife, Tomotherapy and VERO system. Limited data focusing on CIED patients treating with these systems were found in the literature [20].

   There are several *in vitro* studies of CIED irradiation using conventional linacs have been conducted. Two of the most cited *in vitro* studies performed by Mouton et al [30] and Hurkmans et al [32]. In these studies, CIEDs were exposed to high dose fractions with incremental dose deliveries (from 0.05 Gy and 0.5 Gy up to 20 Gy). However, there is no specific *in vitro* or *in vivo* data on irradiation of different ICDs and PMs and dose fractionations using CyberKnife and Gamma-Knife units are available [20].

4. Different delivery technique.
   Modern delivery technique, such as segmental-MLC (multi-leaf collimater) IMRT, dynamic-MLC IMRT and VMAT, multiple static fields or arcs, and non-coplanar geometries to achieve dose conformity. Different challenges may be involved [65] compared to those associated with conventional radiotherapy [20].

   As explained earlier, there might be different challenges related to modern delivery techniques when it comes to manage CIED patients. For example "fingers of death", which is a streak of unexpectedly high doses in unexpected places. This is an issue during a non-isocentric robotic SBRT using a CyberKnife describe by Berlach et al [20,65]

5. Different out-of-field Doses. Different delivery devices and beam modifiers lead to different out-of-field doses [66]. Additionally, more leakage and higher collimator scatter occur due to higher monitor units (MUs) in modulated techniques (such as intensity modulated radiotherapy (IMRT)and volumetric modulated arc therapy (VMAT)) [20].
   In a study by Covington et al [67], the athour focused on out-of-field doses for FFF photon beams. They prepared a comprehensive out-of-field dose dataset for various field sizes and distances from the field edge for 6 FFF and 10 FFF beams. Although the clinical the clinical implementation of this dataset was demonstrated by taking a patient with CIED treated with a 6 FFF beam as an example. However, according to the authors caution should be taken in case of modulated fields bacasue applying this model to these fileds could result in greater uncertainty [20].

6. Flattening-Filter-Free (FFF) Beam Modes.
   More modern linacs with FFF functionality have been installed and compared with conventional FF beam, FFF beams have several unique features such as different beam profiles, different head scatter properties, and a higher dose rate [68,69]. Though they are potentially advantageous characteristics for patients with CIEDs, there is lack of information regarding its potential issue [20].

In a study by Rodriguez et al [70], they found that radiation-induced photocurrents generated by a high dose rate van result in a transient effect on CIED. According to their results, the effect can become appreciable with a pulse dose rate greater than 10^4Gy/sec. In that case, the effect of the pulse dose rate might be much more significant [70].
In a comprehensive national practical guideline to manage CIED patients by Hurkmans et al [22], the authors stated that high dose rate may cause possible abnormal functionalities in some parts of CIEDs. However, they emphasized that for conventional FF beams, the dose rate effect (e.g., ranging from 1 Gy/min – 6 Gy/min at depth of maximum dose at reference distance) on CIEDs is

not significant because the dose rate at the CIED location is lower than the recommended maximum acceptable value (0.2 Gy/min) [30]. They estimated that for FFF beams, the dose rate would be lower than 1 Gy/min, provided that the CIED is located outside of the treatment field. Thus, dose rate effects might not be frequent [20].
The effect of pelvic and thoracic FFF-VMAT on 76 ICDs were studied by Gauter-Fleckenstein et al [71]. In their experimental study, the authors irradiated the ICDs in 5 sets with a cumulative dose of up to 150 Gy [10 Gy*3 fractions] in the isocentre. The beam energies were 6-, 10- and 18-MV beams and dose rate was up to 2500 cGy/min. Different unpredictable incidents, including inadequate defibrillation, reset and data loss at 10 MV and 15 MV were reported [20].
In modern linear accelerators, the dose rate for flattening filter-free SBRT can reach up to 24 Gy/min. For this dose rate, the question arises as to whether the effects of such high dose rates on CIEDs are still rare. The second questions is whether one needs to consider dose/min, dose/sec, and dose/pulse and their effects [20].

7. Electromagnetic Interference (EMI).

EMI rarely causes advert event in CIEDs patients treating with conventional linac. There are limited data focusing on potential EMI in other systems. Electromagnetic field fluctuations are specific to repeated beam hold states (e.g., step-and-shoot IMRT and gating techniques) or non-conventional linac-based technologies (e.g., continuous motion of couch and gantry in tomotherapy with a shorter source-to-axis distance (SAD=85 cm) instead of the usual 100 cm in conventional accelerators or the proximity/motion of CyberKnife linac relative to patients compared to conventional linac treatments) [20].

Also Magnetic resonance imaging (MRI) may cause some transient effect on CIEDs due to EMI. As such, the evaluation of EMI and strategies for minimising the associated risks are highly recommended for cancer patients with CIEDs. To mitigate the risk of EMI affecting CIED functionality, device program-change protocols have been employed or a vendor-supplied external static magnet has been applied to minimise inappropriate activation or inhibition of brady-/tachyarrhythmia therapies [72].

Also the recent advancements in the technology of MR-conditional CIEDs mitigate the hazards associated with EMI and minimise the risk of device malfunction, as well as the clinically significant adverse events to some extent.

Currently the use of integrated MRI-linacs , which provide high precision and accurate dose delivery, is increasing [73]. Thus, the potential risks associated to such systems should be addressed due to concerns of the interaction between MRI fields and CIEDs [20].

In the literature there are no reported instances of clinically significant adverse events as a result of EMI induced by the conventional linac system from previous studies [72], but some evidence of transient complications such as pacing inhibition and inappropriate detection of ventricular arrhythmia during the treatment has been reported [54,72]. Therefore, the restrictions on the electromagnetic exposure of cancer patients with CIEDs might be justifiable [20].

The recent advancements in CIED technology and the introduction of clinical safety protocols during RT (such as accessing special programming modes via the CIED clinic or with the application of a vendor-supplied external static magnet) can potentially minimise the risk of an EMI-related malfunctions [72,74].

2.5 Conclusion

As patient age and comorbidities increase, the number of studies focusing on the management of patients with CIEDs undergoing RT has also increased. However, the number of publications that specifically address the issue of modern RT and CIEDs is not high.

Conclusively, we identified that with the ever-increasing use of advanced RT technologies and techniques, the different characteristics of such techniques should be considered when managing patients with CIEDs [20].

The updated literature showed that although there has been a tremendous development in non-cardiac implantable electrical stimulation devices such as spinal cord stimulators (SCS), deep brain stimulators (DBS), vagal nerve stimulators (VNS), and sacral nerve stimulators, there is still lack of studies regarding the effect of radiotherapy on non-cardiac implantable devices and the potential adverse effects of radiation regarding these devices. Therefore, this comprehensive study and its outlines can be considered as a stimulus for future study.

Chapter 3: Image-guided radiotherapy (IGRT) in patients with CIEDs

3.1 Introduction

The ultimate goal of radiotherapy is to precisely delivery of a prescribed dose to the target volume while sparing adjacent normal tissues. To achieve this fundamental goal, all elements in the chain of radiotherapy process have been and are still being developed [75]. Correspondingly, IGRT has been introduced to achieve these goals. An accepted definition for the term "IGRT" is to "use of frequent imaging within the radiation treatment room, with decisions based on imaging to improve precision of radiation therapy delivery i.e., process of in-room imaging guiding radiation delivery" [76–78].

There are several forms of image-guidance based on the imaging method which can be divided into two main categories namely, a) non-irradiation based system (e.g., ultrasound-systems, camera-based or optical tracking systems, etc.), b) radiation based systems (e.g., electronic portal imaging devices (EPID), KV or MVCone Beam CT (CBCT), etc.) [79].

With the advent of the cone beam computed tomography (CBCT) system, radiotherapy and, more specifically, patient positioning have undergone significant changes [78]. Because of noteworthy advantages of this system, including three-dimensional visualization of the body and enhanced visualization of soft tissue, it has become an important component of modern linear accelerator (LINAC) [78,80–82]

There are potentially two issues caused by kV CBCT system, when it comes to manage CIED patients. The first one is dose-rate effects and the second one is additional imaging dose [78]. In general, ever-increasing use of daily CBCT leads to additional imaging dose delivered to the patient. Accordingly, there has been an increase in the number of research studies focusing on imaging dose due to CBCT in radiotherapy. Many aspects of this field have been investigated, ranging from dose measurements and calculations to cancer risk related to imaging dose [83–90]. A review study by Alaei and Spezi [81] presented a comprehensive systematic review of imaging dose associated with CBCT including various methods for the measurements of imaging dose delivered by kilovoltage CBCT systems [78].

Our study, however, showed that the precise range of imaging dose from different kV CBCT systems to CIEDs is ill-defined and there is a lack of clinical and experimental data focusing on imaging dose to cardiovascular implantable electronic devices (CIEDs) from the CBCT systems [78].

As highly recommended by international and national guidelines for the management of patients with CIEDs receiving radiotherapy, the cumulative dose received by CIEDs should be kept as low as possible, and a safe threshold based on patient risk classification needs to be respected [22,23,91,92]. Patients with CIEDs are usually categorized for risk on the basis of cumulative dose and pacing dependency into low (CIED dose is less than 2 Gy and the patients are not pacing dependent), medium (CIED dose is between 2 Gy and 10 Gy and the pacing-dependent patients receive a CIED dose less than 2 Gy), and high risk groups (patients who receive a CIED dose of 10 Gy or above)[22].

Based on the aforementioned issues caused by kV CBCT, there might be two questions to answer. The first question is how possible risk associated with dose rate effect should be defined. The second question that arises is whether the additional imaging dose from kV-CBCT is significant when considering its potential contribution to the CIED cumulative dose[93–95].

The goal of this part of the study is to investigate the second question and add new clinical data and enrich existing data [93–95] on imaging dose to the CIEDs [95]. In order to answer this question precisely, two main commercial radiotherapy CBCT systems, namely the X-ray Volumetric Imager (XVI, Elekta Oncology Systems) and the On-Board Imager (OBI, Varian Medical Systems), using three different dosimetric measurement methods including Gafchromic films, metal-oxide-semiconductor field-effect transistor (MOSFET), and thermoluminescence dosimeters (TLDs) were used in a multicenter study.

3.2 Materials and methods

3.2.1 CBCT Systems in the centers

Four radiation therapy centers in the north of Italy: Triste titled (C1) throughout this chapter, Trento (C2), Udine (C3), and Brescia (C4) participated in this study. In this study, all measurements were performed using the two kV-CBCT systems, namely the X-ray Volumetric Imager (XVI) mounted on the Elekta Synergy linear accelerator (Crawley, United Kingdom) and the On-Board Imager (OBI) mounted on the Varian Clinac-iX linear accelerator (Palo Alto, CA). The measurements were acquired on three Elekta-XVI (C1, C2, C4) and one Varian-OBI (C3), which consist of a kV x-ray tube and an amorphous-silicon flat panel detector. In C1 and C4, the manufacturer's default CBCT protocols, using the exposure factors and reconstruction parameters as suggested by vendor, were utilized. But, in C2 andC4, the CBCT protocols were optimized based on their clinical experience to have optimal image quality whilst minimizing image dose. [78]

3.2.2 Anthropomorphic Phantom

To determine the imaging dose delivered to the CIEDs at each center, an anthropomorphic phantom was used to simulate almost the exact situation of a real patient. In the first and fourth center, two old Alderson multi-section RANDO average-man phantoms (Alderson Research Laboratories, USA) composed of a natural human skeleton embedded in a synthetic isocyanate rubber and compounded to be sensibly tissue-equivalent over the range of commonly used x-ray energies [96], were used. The new modified and improved version of this phantom is named the Alderson Radiation Therapy Phantom (ART) fabricated using detailed polymer skeleton and tissue equivalent materials based on ICRU-44 [97] standards which is available in male and female version [98]. In the second and third center, two male ART phantoms were used. The CIEDs were placed in the phantom's left clavicular region. Because the CIED is usually located at 0.5-1.5 cm below the patient's skin [99], a 1-cm thick bolus (mean value) was used to simulate the patient's tissue in this study. It should be noted that in order to have almost the same setup at each center, similar sample pictures illustrating the phantom and CIED positioning were used at each center (Figure 7).

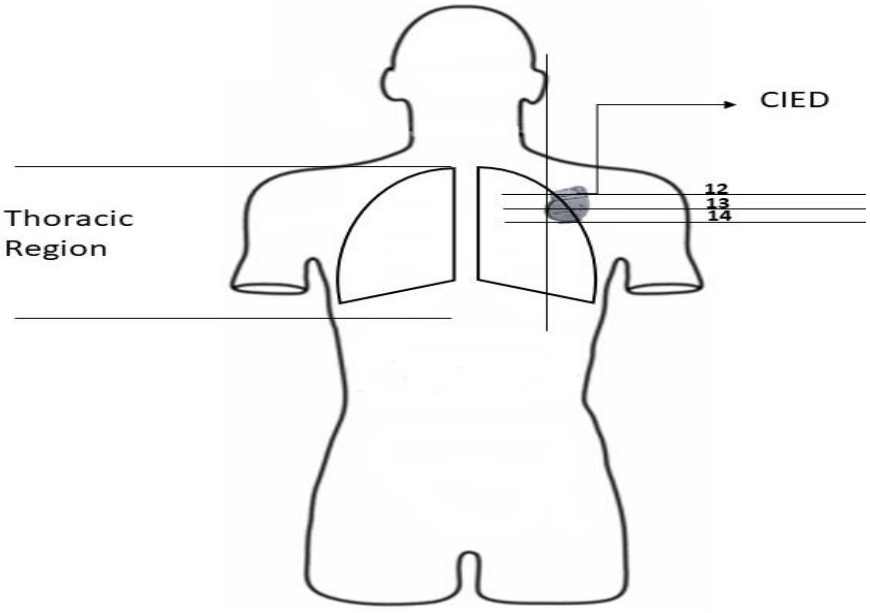

Figure 6: Schematic illustration of setup with anthropomorphic phantom (left); [78]

Figure 7: Experimental setup with a 1-cm thick bolus-(C1:top right, C3: bottom right).

3.2.3 Dosimetry Systems and calibration of dosimeters

The first dosimeter was used in this study was Gafchromic XR-QA2 films (International Specialty Products, Wayne, NJ). This study is suited for kV photon beams and sensitive for 0.1-20 cGy. The batch numbers of utilized Gafchromic XR-QA2 films were (#01041702, used at C1,C3), (#A10121202, used at C2), (#10261501, used at C4). A solid state detector (CT Dose Profiler DP2, RTI Electronics, Mölndal, Sweden) at C4 and three ionization chambers (Radcal 9015 and 9660, 10x6-5 and 10X6-6 chambers; Radcal Corp., Monrovia, CA, USA) at C1, C2 and C3 were applied to record the related dose values from which the calibration curve was constructed. The methods used for generating calibration curves were based on studies by Tomic et al and Giaddui et al [82][100], and the handling of the film was in compliance with the AAPM TG-55 protocol [101].

Gafchromic films were cut into pieces and irradiated free-in-air for different kV-CBCT settings that were frequently used in each center: for the XVI, 100 kVp/F0 (no filter) and 120 kVp/ F0 & F1 (with Bowtie filter), and for the OBI, 100 kVp/FF (full Bowtie filter) and 110&125 kVp/HF (half Bowtie filter) at the isocenter and perpendicular to the surface of the film. Twenty-four hours after irradiation, all film pieces were read with two EPSON Expression 10000 XL (used at C1 and C3) and two EPSON V750 PRO (used at C2 and C4) scanner. To include reproducibility of the response of the scanner in the uncertainty analysis each sample was scanned three times and to avoid off-axis scanner non-uniformity, the film pieces were placed on the center of the flat-bed document scanner [102], and film reading was performed with the following parameters: reflection scanning mode with all filters and image enhancement options turned off, 72 dpi, and 48-bit RGB mode (16 bits per color). Film images were saved in tagged image file format (TIFF). The red components of all RGB scanned images were extracted and analyzed with ImageJ software (National Institutes of Health, USA). Several fitting curves were tested using either Excel (Microsoft, USA) or LAB Fit (Silva, W.P. and Silva, C.M.D.P.S., Brazil) software, and the best R^2-value of the fitted curves were chosen accordingly. [78]

Moreover, the high bias and high sensitivity micro-MOSFET dosimeters (TN-1002RDM-H, Best Medical Canada) were used for measuring the imaging dose in the first center (C1). The beam qualities were matched for the required KV range with those of the XVI CBCT system and protocols.
The MOSFETs were calibrated for surface dose measurements by simultaneous MOSFETs and Radcal ionization chamber exposure free-in-air, under the identical X-ray irradiation conditions. The dosimeters were positioned in parallel, opposite directions along the same axis, and equally placed 1 cm from the X-ray beam axis. More detailed information of calibration methodologies for MOSFET have been proposed and published by Brady and Kaufman [103].

Also, Lithium fluoride thermo-luminescent dosimeters (Harshaw TLD-100 LiF, Square Rod) with dimensions of $6 \times 1 \times 1$ mm^3 were used in the second center (C2) to measure the imaging dose. They were read in a 3500 Harshaw Bicron TL reader, and the pre-irradiation annealing procedure was 1 hour at 400°C, followed by 2 hours at 100°C, and then post-reading annealing was 10 min at 100°C. The TLD calibration procedure was carried out free-in-air using the X-ray tube in the XVI system and the air kerma was measured with a Radcal 6cc Ion Chamber. The TLD signal was quantified as the mean value of three TLD rods, subtracting the background radiation, and estimated with three unexposed dosimeters.

3.2.4 Dose uncertainty analysis

The principles of measurement uncertainty analysis in Gafchromic film dosimetry have been studied in detail by Tomic et al [82], Devic et al [104,105], and Aldelaijan et al [106], considering experimental uncertainty (such as scan reproducibility, film, and scanner non-uniformity) and

curve fitting uncertainty (associated with fitting quality). In our study, the total relative uncertainty (experimental and fitting) for each kV XVI or kV OBI point dose of each calibration curve as a function of air kerma was calculated using the formalism and procedure proposed by Tomic et al [82] formulated as following:

$$\nabla R^i = R^i_{before} - R^i_{after} = \frac{1}{2^{16}}[PV^i_{before} - R^i_{after}]$$

(Equation 3.1)

$$\sigma_{\nabla R^i} = \frac{1}{2^{16}}\sqrt{(\sigma(PV^i_{before}))^2 + (\sigma(PV^i_{after}))^2}$$

(Equation 3.2)

$$\sigma_{(K^{film}_{air})^{air)\,\exp(\%)}} = \frac{b[\frac{\ln(net\Delta R) - 1}{\left(\ln\left(net(\nabla R)\right)\right)^2}]\sigma_{net\nabla R}}{(K^{film}_{air})^{air}} \times 100$$

(Equation 3.3)

$$\sigma_{(K^{film}_{air})^{air)\,\mathrm{fit}(\%)}} = \frac{[\frac{(net\Delta R)}{\ln\left(net(\nabla R)\right)}]\sigma_b}{(K^{film}_{air})^{air}} \times 100$$

(Equation 3.4)

$$\sigma_{(K^{film}_{air})^{air)\,\mathrm{fit}(\%)}} = \frac{\sqrt{(\frac{(net\Delta R)}{\ln\left(net(\nabla R)\right)})^2\sigma_b^2 + b^2(\frac{\ln(net\Delta R) - 1}{\left(\ln\left(net(\nabla R)\right)\right)^2})^2\sigma^2_{net\nabla R}}}{(K^{film}_{air})^{air}} \times 100$$

(Equation 3.4)

Where ∇R^i is changes in reflectance, $\sigma_{\nabla R^i}$ is corresponding standard deviations over ROI, PV is abbreviation of pixel value and represents 16 bit deep pixel value over ROI (before irradiation or after irradiation) [82].

Further, the uncertainty in the TLD and MOSFET measurements was estimated from at least three repeated measurements.

3.2.5 kV-CBCT protocols

Table3-6 also shows the important parameters of imaging protocols that are commonly used at each participating center.

Table 4: kV-CBCT system and the corresponding important parameters investigated at C1

	CBCT System	Scanning Protocol					
Trieste		Name	Fan Type	Tube voltage	Total mAs	Frames	Tube Start/Stop angle
	Elekta XVI	H&N S10	S10/F1	100	36.6	366	320/160
		H&N S20	S20/F1	100	36.6	366	320/160
		ChestM20	M20/F1	120	264	660	180/180
		Pelvis M20	M20/F1	120	1056	660	180/180
		Symmetry Left	M20/F1	120	312	975	180/20
		Symmetry Right	M20/F1	120	312	975	180/20
		Prostate M10	M10/F1	120	1689.6	660	180/180
		Prostate M15	M15/F1	120	1689.6	660	180/180

Table 5: kV-CBCT system and the corresponding important parameters investigated at C2

	CBCT System	Scanning Protocol					
Trento		Name	Fan Type	Tube voltage	Total mAs	Frames	Tube Start/Stop angle
	Elekta XVI CBCT	H&N S10	S10/F1	120	60.8	190	-130/70
		H&N S20	S20/F1	120	60.8	190	-130/70

	Chest M15 central	M15/F1	120	528	330	-180/180
	Chest M15 left	M15/F1	120	528	330	-180/180

Table 6: kV-CBCT system and the corresponding important parameters investigated at C3

Udine	CBCT System	Scanning Protocol					
		Name		Tube voltage	Total mAs	Frames	Tube Start/Stop angle
	Varian OBI	Pelvis	half	125	702	438	182/178
		Thorax	half	110	271	678	182/178
		Thorax	half	110	269	678	182/178
		Head&Neck-high dose	Full	100	750	375	22/178
		Head&Neck-high dose	Full	100	750	375	22/178
		Head&Neck-low dose	Full	100	75	375	22/178

Table 7: kV-CBCT system and the corresponding important parameters investigated at C4

Brescia	CBCT System	Scanning Protocol					
		Name	Fan Type	Tube voltage	Total mAs	Frames	Tube Start/Stop angle
	Elekta XVI CBCT	H&N S10	S20/F0	100	36.6	366	320/160

H&N S20	S20/F0	100	36.6	366	320/160
Chest M20	M20/F1	120	264	660	180/180
Prostate M15	M15/F1	120	1689.6	660	180/180

3.3 Results

3.3.1 Dose Uncertainty analysis

For all beam qualities used in C1, C2, C3, and C4, the variation in the percentage total relative uncertainties for Gafchromic XRQA2 film are presented in Figure 8. The results indicated that the uncertainty ranged between 4% and 6% at a dose above 20 mGy. However, the uncertainty was higher at low doses and might be as high as 17%.

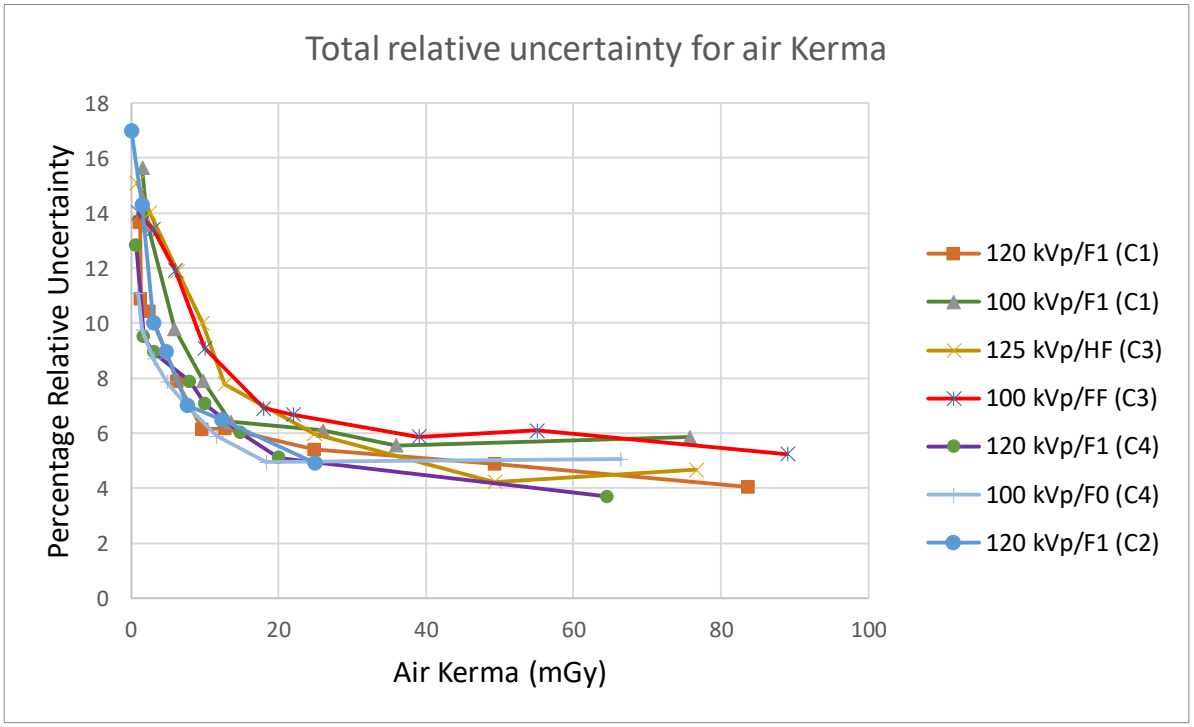

Figure 8 :Results of uncertainty analysis for Gafchromic film for different beam qualities used in three centers. [78]

It should be noted that the effect of control film pieces on uncertainty of the dose measured using a radiochromic film has been considered in the formalism proposed by Tomic et al [82]; however, we did not evaluate this factor in our uncertainty analysis due to the fact that the magnitudes of the measured signals by the control film pieces were negligible (less than 1%).

The uncertainties of MOSFET measurements ranged between 7% (for higher doses) and 16% (below 0.1 cGy), and overall uncertainty in TLD was approximately 6%.

3.3.2 CIED doses associated with different KV-CBCT protocols

Table 8-10 illustrates the full results of the mean imaging dose to the CIEDs measured at four centers by using three different dosimeters. The uncertainty in the measurements (one standard deviation [SD]) estimated from at least three repeated measurements.

The maximum values of imaging doses were found once CIEDs were inside the CBCT field, and they had the following values: Head and Neck (HN)-S20 (XVI):2.57 mGy/100 mAs, Thorax (OBI):2.92 mGy/100 mAs, Chest M15-left (XVI): 1.52 mGy/100 mAs, Symmetry-left (XVI): 5.67 mGy/100 mAs. However, they received a much lower dose once the CIEDs were not inside the field.

The results measured at the first center using both the micro-MOSFET point-dose and Gafchromic film XR-QA2 indicated some disagreements that ranged between 10% and 28%. These discrepancies were higher when the ICD was out of the CBCT field (in the prostate and pelvis) and in the border of the field (in the head and neck). However, there was quite good agreement between the results when the ICD was inside the CBCT field (symmetry). Further, such discrepancies were observed between results obtained by TLD and XRQA2 at C2 when PM was in the border of the field (up to 24%), while the average PM doses were in good agreement when PM was inside the CBCT field. [78]

Measured imaging doses to CIED by by XRQA2 film, TLD, and MOSFET at each center were tabulated in the tables.

Table 8: Imaging dose to CIED measured by XRQA2 film, and MOSFET at C1. Uncertainties represent one standard deviation from repeated measurements.

Trieste	Position of CIEDs (In terms of CBCT-FOV)	Average ICD dose					
		mGy				mGy/ 100 mAs	
		XRQA2	SD%	MOSFET	SD%	XRQA2	MOSFET
H&N S10	Outside	0.13	9.1%	-	7.5%	0.36	-
H&N S20	Partially Inside	0.38	10.3%	0.47	14.9%	1.04	1.28
ChestM20	Fully Inside (center)	3.86	3.7%	3.36	6.7%	1.46	1.27
Pelvis M20	Outside	0.59	6.3%	0.48	8.3%	0.06	0.05
Symmetry Left	Fully Inside (center)	17.7	5.8%	15.9	9.1%	5.67	5.10
Symmetry Right	Fully Inside (Peripheral part)	9.11	6.1%	10.16	9.8%	2.92	3.26
Prostate M10	Outside	0.20	3.6%	-	-	0.01	-
Prostate M15	Outside	0.22	2.2%	0.172	7%	0.01	0.01

Table 9: Imaging dose to CIED measured by XRQA2 film, and TLD at C2. Uncertainties represent one standard deviation from repeated measurements.

Trento	Position of CIEDs (In terms of CBCT-FOV)	Average PM dose					
		mGy				mGy/ 100mAs	
H&N S10		XRQA2	SD%	TLD	SD%	XRQA2	TLD
H&N S20	Outside	-	-	0.03	3%	-	0.02
Chest M15 central	Partially Inside	1.13	8%	1.40	3%	1.86	2.30
Chest M15 left	Fully Inside (Peripheral part)	6.18	4.7%	5.50	6%	1.17	1.04
H&N S10	Fully Inside (center)	7.48	7.5%	7.99	8%	1.42	1.52
Pelvis M15	Outside	-	3.6%	0.21	8%	-	0.04
Prostate S10	Outside	-	2.3%	0.05	5%	-	0.01

Table 10: Imaging dose to CIED measured by XRQA2 film at C3. Uncertainties represent one standard deviation from repeated measurements.

Udine	Position of CIEDs (In terms of CBCT-FOV)	Average PM dose		
		mGy		mGy/ 100 mAs
		XRQA2	SD%	
Pelvis	Outside	0.9	12%	0.12
Thorax	Outside	1.52	7.6%	0.56

Thorax	Fully Inside (center)	7.86	4.9%	2.92
Head&Neck-high dose	Outside	1.6	10.3%	0.21
Head&Neck-high dose	Fully Inside (Peripheral part)	3.2	7.6%	0.42
Head&Neck-low dose	Fully Inside (Peripheral part)	1.11	4.3%	1.48

Table 11: Imaging dose to CIED measured by XRQA2 film at C4. Uncertainties represent one standard deviation from repeated measurements.

	Position of CIEDs (In terms of CBCT-FOV)	Average PM dose		
		mGy		mGy/ 100 mAs
		XRQA2	SD%	
H&N S10	Outside	0.05	7.8%	0.14
H&N S20	Partially Inside	0.94	11%	2.57
Chest M20	Fully Inside (Center)	2.1	6.8%	0.80
Prostate M15	Outside	0.09	8%	0.01

3.4 Discussion

A comparison between results obtained by the same CBCT system (XVI) at three geographically separated centers (C1, C2, and C4) using similar dosimeters (XRQA2) (although there was a slight difference in imaging scenario) showed variations in CIED dose. This can be explained by several factors such as using a filter or without filter in HN (HNS10,20 F0 &F1), a difference in the size of the collimator in the chest (chest M15 and chest M20), and size differences between ICD (used at C1) and PM (used at C2 and C4). However, another factor is that the CIED doses also depend on the distance between the CIED and scan center. The dose profiles obtained in symmetry at C1 are presented in Figure 9 by using XRQA2. As illustrated, dose distribution was not homogeneous, and there was some asymmetry especially in the lateral profile, because the tube did not have a full rotation (only 200 degree of gantry rotation). Figure 10 shows the mean dose to ICD against distance to the scan center for chest M20 by using MOSFET in a craniocaudal direction, which decreases exponentially. In addition, measuring the imaging dose outside the FOV along the craniocaudal direction showed a large penumbra region and a dramatic decrease in imaging dose by increasing the distance between the CIEDs and field edge. A less dramatic decrease along the mediolateral direction was seen. [78]

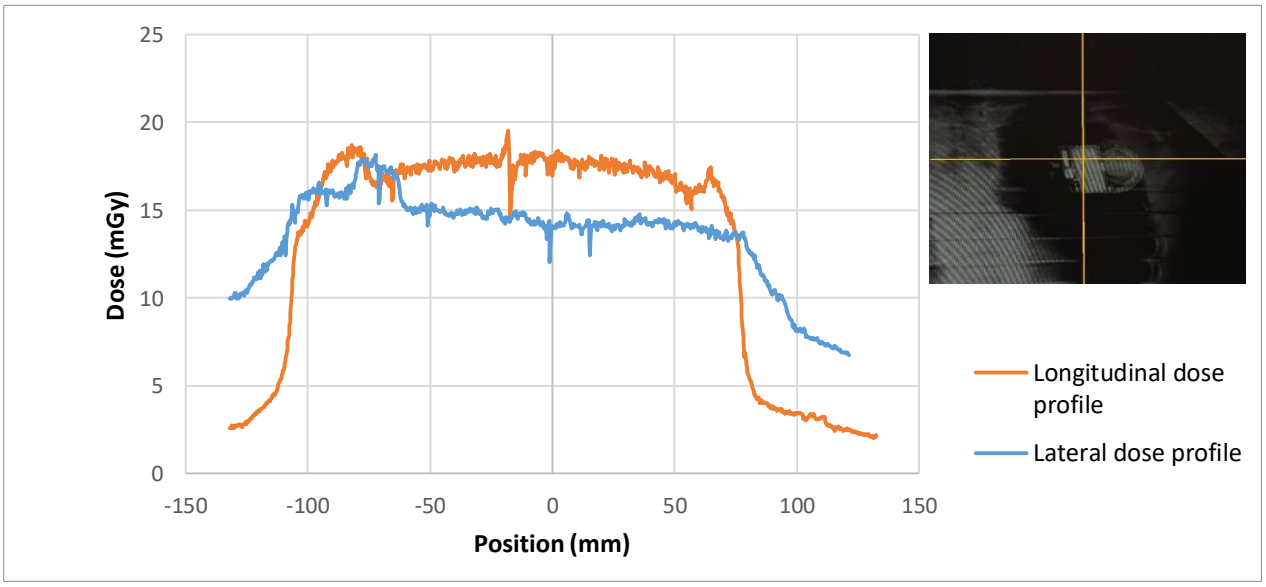

Figure 9. Dose profiles during symmetry scan in both longitudinal and lateral directions using gafchromic film (at C1). [78]

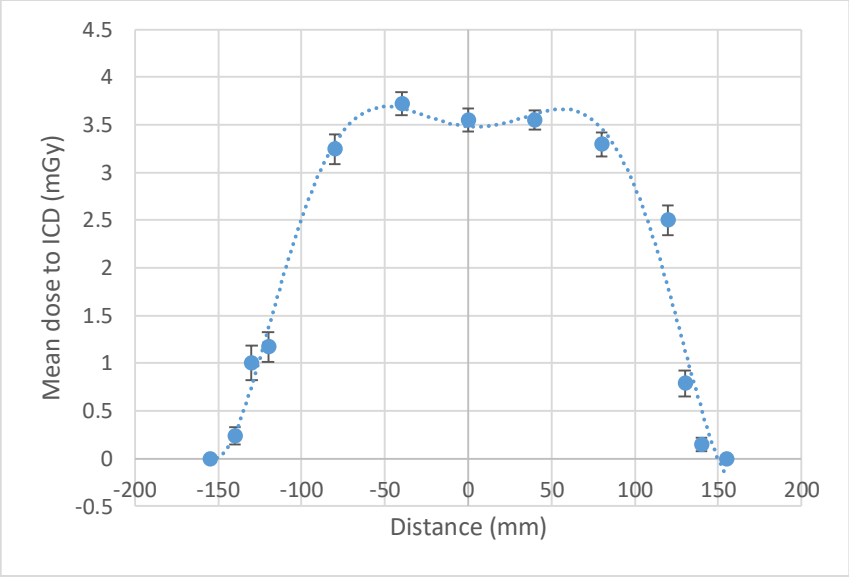

Figure 10. Mean doses to ICD were measured for Chest M20 scan as a function of the MOSFET position in the craniocaudal direction (at C1). [78]

To the best of our knowledge, only two studies in the form of abstracts have published the imaging dose to CIEDs from kV CBCT. In the first study, Wronski et al [93] measured CIED dose both inside and outside the FOV in an anthropomorphic phantom by using MOSFET dosimeters. In the second, Ming et al [94] reported Monte Carlo (EGS4) simulated CIED doses due to kV-CBCT. Their results are listed in Table 11.

Table 12: Studies focusing on imaging dose to CIED from kV-CBCT systems [78]

Author (Ref) / year	*CBCT Protocol*	*PM or ICD*	*Position of device relative to CBCT field*	*Imaging dose to CIED from each fraction*
Wronski et al [93] / 2011	Standard clinical protocols (not mentioned specifically)	PM and ICD	Inside	PM: 0.8-1.9 cGy. ICD: 2.2-4.3 cGy.
Ming et al [94] / 2013	Low-dose thorax	Type of CIED was not mentioned.	Inside	1.5 cGy
	Pelvis			6.2 cGy
	High quality head			0.9 cGy

Although, there was no detailed information regarding their protocols and kV-CBCT systems, in general, the range of imaging doses from the first study are much higher than our findings, while the average results of the second investigation for head and thorax protocols are more consistent

with our results. In case of pelvis the reported imaging dose is very high, this is because the authors measured CIED dose inside the FOV for pelvis.

The major portion of the total cumulative dose to CIEDs is due to radiotherapy and this is influenced by several factors, some of which are the total prescription dose, the beam energy, the distances from the treatment field edge to the CIEDs and treatment technique. However, based on the findings of this study, another factor that can sometimes be influential is additional imaging dose to CIED.

Table 12 provides some clinical information and therapeutic doses to the CIEDs in four different sites. The last column reports the maximum imaging doses from kV-CBCT to the CIEDs measured in this study in order to provide an estimate of the potential contribution of corresponding imaging dose to the CIED cumulative dose.

Table 13: Some clinical information and therapeutic doses to the CIEDs in four different sites along with the maximum imaging doses measured in this study [78]

Author (Ref) / year	Pt. #	Site	Prescribed dose (cGy)	Energy (MV)	Treatment technique	Distance from CIED to treatment fields (cm)	Dosimeter	Total CIED dose due to RT (cGy)	CIED dose per fraction due to RT (cGy)	The maximum imaging dose to CIED measured in this study per CBCT scan (cGy)
Prisciandaro et al [60] / 2015	58	Breast & Thorax	5,000	6X/ 16X	SBRT	2	TLD	75	*9.37	0.786 Thorax (C2)
Prisciandaro et al [60] / 2015	45	Head & Neck	7,000	6X	IMRT	3	TLD	169	4.8	0.32 Head&Neck-high dose (C3)
Bourgouin et al[107] / 2015	3	Lung	4,500	n/a	IMRT	11.6	PSD	113	*3.76	1.77 Symmetry-4D CBCT for Lung (C1)
Peet et al [49] / 2016	5	Lung	6,000	6X	VMAT	5	OSLD	22	4.4	1.77 Symmetry -4D CBCT for Lung (C1)

Pt. #: Patient number, RT: Radiotherapy, TLD: Thermoluminescence Dosimeters PSD: Plastic Scintillation Detector, OSLD: Optically Stimulated Luminescent Dosimeter

**The number of fractions has not been mentioned (assume 8 fractions for SBRT and 30 fractions for IMRT).*

Even though the magnitude of the imaging dose to CIEDs per CBCT scan for HN and thorax is small, compared to that of therapeutic dose, the additional imaging dose in 4D symmetry protocol for lung is not negligible. Moreover, the reported therapeutic doses to the CIEDs for modern radiotherapy techniques, which were sparsely scattered throughout the literature, can be altered due to the aforementioned factors. Therefore, when CIEDs are inside the CBCT-field, estimation of dose contribution from kV-CBCT to total cumulative dose of CIED is justifiable.

There are different CBCT imaging dose reduction methods, including optimization of exposure parameters (e.g. tube current-exposure time [mAs]), optimizing the number of image acquisition and using a filter [108–110] More specifically, some of the strategies to reduce imaging dose from CBCT to CIED are as follows.
a) Excluding the CIED from CBCT-field as a general method, if possible. As can be seen in Table 9, at C3 for the same protocol (Head & Neck-high dose and Thorax), when the CIED is inside and outside the CBCT-FOV imaging dose can be reduced by a factor of 2 and 5, respectively.
b) Manipulating scanning parameters. Wronski et al [93] evaluated imaging dose of a partial-angle scan protocol. They reduced the scan length from a full 360-degree scan to a posterior 180-degree and could decreased imaging dose to CIED by a factor of 8. But, a trade-off between image quality and imaging dose should be achieved.

c) Shielding; Yan et al [99] in their recent study suggested that a bolus of 1-2 cm during radiation therapy could be used for reducing the dose to the CIED, provided that the CIED is implanted at a depth of no more than 2 cm from skin surface. However, this is not an effective approach to reduce the imaging dose to the CIED. Nevertheless, shielding with copper decreased the imaging dose from CBCT to the CIED. The measured doses using MOSFET (at C1) and applying a symmetry protocol with two different thicknesses of copper (1 mm and 2 mm) showed that the imaging doses were reduced from 1.59 cGy to 0.53 cGy and 0.37 cGy, respectively. However, the presence of the copper degraded quality of the entire image, especially in the location of the CIED, and it caused an increase of image noise up to 43% (in tissue region). Therefore, there should be a reasonable compromise between noise and imaging dose.

3.5 Conclusion

With the increasing use of CBCT in radiotherapy, there has been a corresponding focus on the additional imaging dose delivered to the patient. This growing consideration could also be important when we treat patients with CIEDs. This is because in this group of patients, the maximum accumulated dose to the devices needs to be limited.
Although the major portion of the total dose to CIEDs is due to radiotherapy, another factor that can sometimes be influential is additional imaging dose to CIED.
This study showed that when CIEDs are inside the CBCT field, special attention should be paid to the imaging dose, and an estimation of dose distribution should be made. This is particularly

important for image guidance technique in radiotherapy on a daily basis over a long treatment course. For example, the overall imaging dose delivered from a daily kV-CBCT in a 30-fraction (for a symmetry protocol) could reach as high as 50 cGy. Therefore, this additional imaging dose is sometimes not negligible and should be taken into consideration in the classification of risk. In that case, we suggest applying a dose reduction strategy, wherever it is possible and reasonable.

Chapter 4: Stereotactic body radiotherapy and radiosurgery using FFF in patients with CIEDs

4.1 Introduction

Stereotactic radiosurgery (SRS) was first conceptualized by Lars Leksell [111,112] in 1950 as a single-fraction ablative radiotherapy for intracranial tumors. Years later, in 1991, an extension of this concept was applied to extracranial tumors by Bromgren and Lax[111,112], called stereotactic body radiation therapy (SBRT), which has recently been renamed stereotactic ablative body radiotherapy (SABR). Today, SBRT has become an effective, widespread modality for the treatment of both primary and metastatic cancers[113,114].

Over the last few decades, there has been an ever-increasing number of patients undergoing cardiac implantable electronic device (CIED) implantation to improve quality of life and prolong survival among those suffering from cardiovascular disease[115]. As the average patient age increases, the number of cancer patients and comorbid cardiovascular disease also increases.[116] Due to this fact, many studies have focused on the effect of radiotherapy on patients with CIEDs, and many aspects of this field have been investigated in the literature[49–51]. However, guidelines[23,24] and reviews[27,50] mainly address the management of patients with CIEDs undergoing conventional radiotherapy.[20,78] The only recommendation from the AAPM on the management of radiotherapy patients with CIEDs dates back to 1994 (TG34)[21], but according to the AAPM website, an update to this document is expected in December 2019.

A recent review[20] discussed some of the different characteristics of SBRT/SRS compared to conventional radiotherapy that might indicate that special considerations are required for the safety of patients with CIEDs. These features are a) higher dose per fraction in SBRT, which might result in a higher dose per fraction for a patient with a CIED, b) SBRT-dedicated treatment technologies (e.g., CyberKnife, Gamma-Knife and VERO), c) different techniques to achieve conformal doses (such as multiple static fields/arcs and noncoplanar geometries), d) different out-of-field doses[66], higher monitor units (MUs) in modulated techniques (e.g., intensity-modulated radiotherapy (IMRT)-SBRT and volumetric-modulated arc therapy (VMAT)-SBRT), e) electromagnetic field fluctuations in SBRT that are specific to repeated beam holds (e.g., step-and-shoot IMRT and gating techniques) or nonconventional linac-based technologies (e.g., continuous motion of the couch and gantry in tomotherapy with a shorter source-to-axis distance (SAD=85 cm) instead of the usual 100 cm in conventional accelerators or the proximity/motion of CyberKnife linac relative to patients compared to conventional linac treatments), and f) extensive use of image-guided radiotherapy (IGRT).

In the context of high dose per fraction, SBRT flattening filter-free (FFF) beams have gained popularity.[68,69,117] FFF beams have several unique features, including a lower out-of-field dose, a sharper penumbra, and less head scatter, which are potentially advantageous characteristics for patients with CIEDs.[20] Additionally, FFF photon beams make a higher average dose rate possible, with a 2–6-fold increase in the instantaneous dose rate for the dose pulses compared with conventional FF photon beams.[118]
Rodriguez et al.[70] found that a transient effect on CIED can occur due to radiation-induced photocurrents generated by a high dose rate. According to Hurkmans et al.[22], based on the theoretical failure mechanism, the effect of the pulse dose rate might be much more important than the average dose rate. However, the authors concluded that for conventional beams with flattening filter (FF) beams, the dose-rate effect on CIEDs is not significant. [22,70]

Several in vitro studies have been reported in the literature investigating the effect of RT with FF beam on CIEDs[28–33], but there is a lack of robust data focusing on the effect of FFF beams using modern RT techniques on CIEDs.[71] Additionally, given the increasing use of SBRT for both lung tumors and metastases, a study that specifically investigated CIED function during and after FFF beam irradiation would be of value.

In this study, a retrospective analysis of patients with CIEDs who underwent SBRT/SRS at Peter MacCallum Cancer Centre (abbreviated PeterMac) between 2014 and 2018 was performed. This was complemented through a phantom study to evaluate the effect of SBRT using FFF beams on implantable cardioverter-defibrillator (ICD) function.

4.2 Methods and materials

3.1 Retrospective study

A retrospective review of patients with CIEDs who underwent RT at the five campuses of PeterMac between 2014 and 2018 was performed. Then, data from CIED patients treated with SBRT/SRS, such as patient characteristics, type of CIEDs, irradiation sites, treatment plan specifications, and reports, were extracted from the MOSAIQ (Elekta AB, Stockholm, Sweden) database and Eclipse treatment planning system. Radiation oncologists were also asked to check their medical records and clinical notes to determine if any patients had a CIED malfunction and/or treatment complications during and/or after RT.

3.2 Experimental study

3.2.1 Device selection and programming

Recently explanted ICDs from the Royal Melbourne Hospital Cardiology Department were analyzed to ascertain whether they had full functionality and a suitable battery life. Of these,

26 ICDs were selected from two different manufacturers (Medtronic and St. Jude Medical [now Abbott]). None of the ICDs were previously exposed to irradiation, and they could have been explanted for any reason except malfunction. All the ICDs were programmed to a maximum and minimum frequency of 120 pulse per minute (ppm) and 60 ppm, respectively. The voltage and pulse width were also programmed to a fixed setting consistent with clinical outputs, and the sense threshold was set to the most sensitive level, approximately 0.2-0.3 mV. Shock therapy was deactivated.

3.2.2 Interrogation before, during and after radiation

To interrogate the devices, manufacturer-specific programmers and a 4-channel oscilloscope were used in this study. Before irradiation, parameters such as battery status and information including mode, longevity, and pacing pulse characteristics were obtained. Additionally, the sensing of each ICD was tested by injecting a 40 ms sine-squared pulse or an ECG wave using a signal generator and an oscilloscope (figure 11).[44]

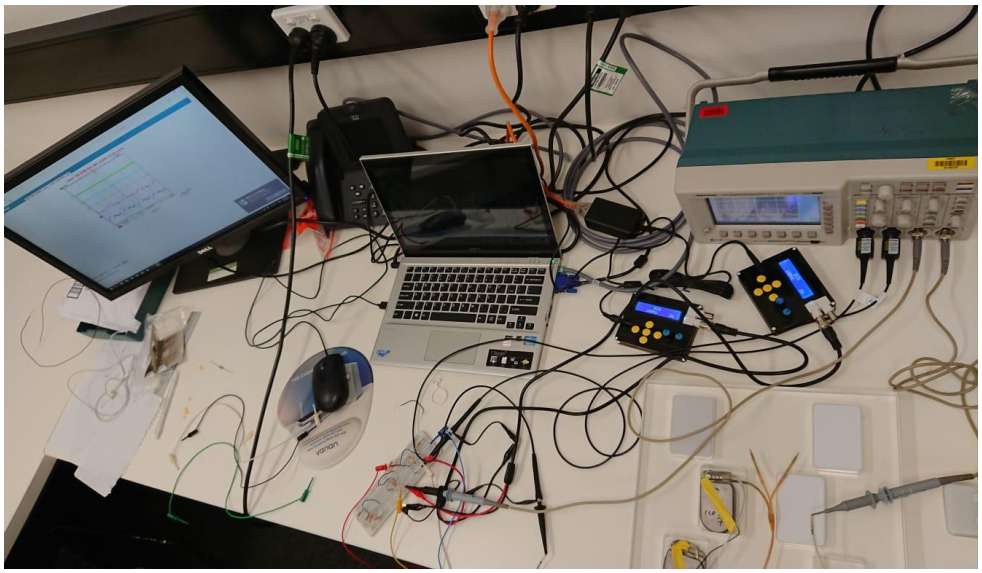

Figure 11: Sensitivity testing of CIEDs by injecting signal and interrogation of pacing parameters before irradiation using oscilloscope

The pacing output and sensitivity during irradiation were monitored by programmers and an oscilloscope to analyze the dose-rate effect. An electrical load circuit was used to simulate myocardial resistance, and isolation circuitry between the load and oscilloscope was used, as recommended by the manufacturer's principal R&D engineer (figure 12). The manufacturer-specific programmers and oscilloscope were present in the bunker room to monitor the signal

during irradiation. The oscilloscope was connected to a laptop placed in a control room through a long ethernet LAN cable. Additionally, the ICD marker channels were printed out using the programmer's internal printer and were monitored using cameras in the radiotherapy bunker room.[119] Finally, the ICDs were interrogated after irradiation using the programmers and oscilloscope to check for any kind of malfunction (e.g., a loss of data or a reduction in the battery capacity) and any significant changes in the programmed ICD parameters (e.g., in the pulse voltage or in the pacing frequency).

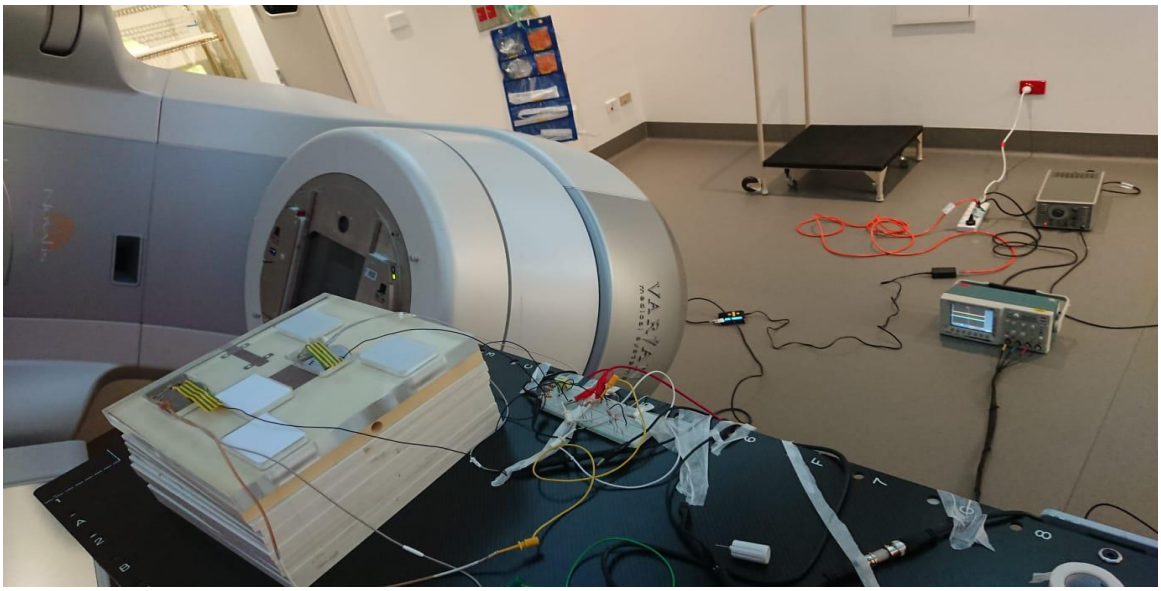

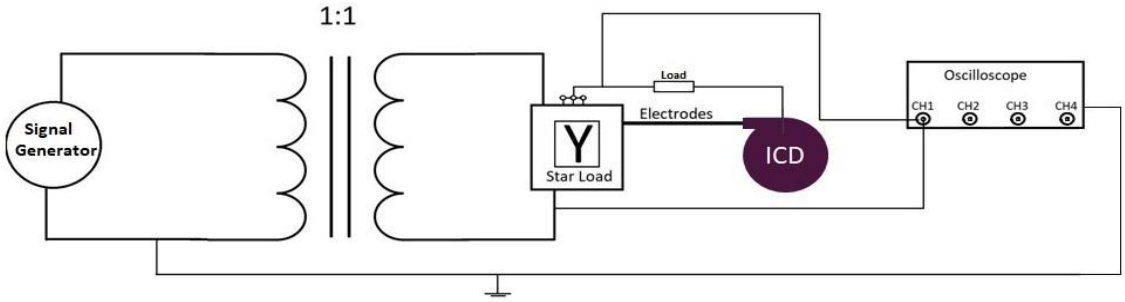

Figure 12: Testing setup of the experiment(top); The isolation circuitry between the load and the oscilloscope was used to monitor the ICD during irradiation. A star load configuration with the electrodes, except the case, was tied to a common node through 250-ohm resistors. The common node is tied back to the case via a 10-ohm resistor (bottom).

3.2.3 Experimental setup, planning and irradiation

Figure 13 depicts the experimental setup. The phantom included a 10-cm water-equivalent slab to provide full backscatter conditions. Then, an acrylic solid slab was designed to position the ICDs. On top, a 1-cm-thick slab was used to simulate the patient's tissue. The size of the solid slab was 30 cm x 30 cm x 30 cm.

Irradiation was performed using a Varian TrueBeam STx linac (Varian Medical Systems, Palo Alto, CA, USA) at PeterMac, Melbourne, Australia. First, a dose-rate test (DRT) including a range of beam pulse frequencies was conducted to determine when inappropriate sensing (either oversensing or inhibition) occurred. In this test, the ICDs were placed at a depth corresponding to the maximum dose and were directly irradiated with both 6-MV FFF and 10-MV FFF beams using a 10 x 10 cm^2 field. The irradiation started with a low dose rate up to the highest value and delivered small doses to avoid exceeding the ICD's total dose tolerance. Additionally, a few initial tests were performed with the device out of, but still near, the beam by moving the jaws to determine whether inappropriate sensing was due to electromagnetic interference (EMI).

The second part of the irradiation process involved delivering four clinical treatment plans (CTPs) to the phantom. A solid slab was designed to place the ICDs into six specific holes. The dimensions of the holes were based on the maximum dimensions of the selected ICDs. Four holes were designed to be 3 cm away from the planning target volume (PTV), and two holes were designed to be placed partially inside the PTV. All the ICDs were oriented and placed in such a way that their integrated circuitry was the most proximal part of the device to the PTV (figure 13).

Table 13 illustrates the details of multifraction SBRT and single-fraction SBRT treatment plans (SAFRON II)[120] with FFF beams, which are frequently used at PeterMac for the treatment of lung tumors. It also presents a summary of thee dose-rate tests (DRTs) conducted in this study. The CT scan of the phantom was imported into the Varian Eclipse treatment planning system (version 15) with an Acuros XB algorithm (AXB1511). The ICDs were contoured and overridden to an extended HU scale to perform the dose calculations.[121]

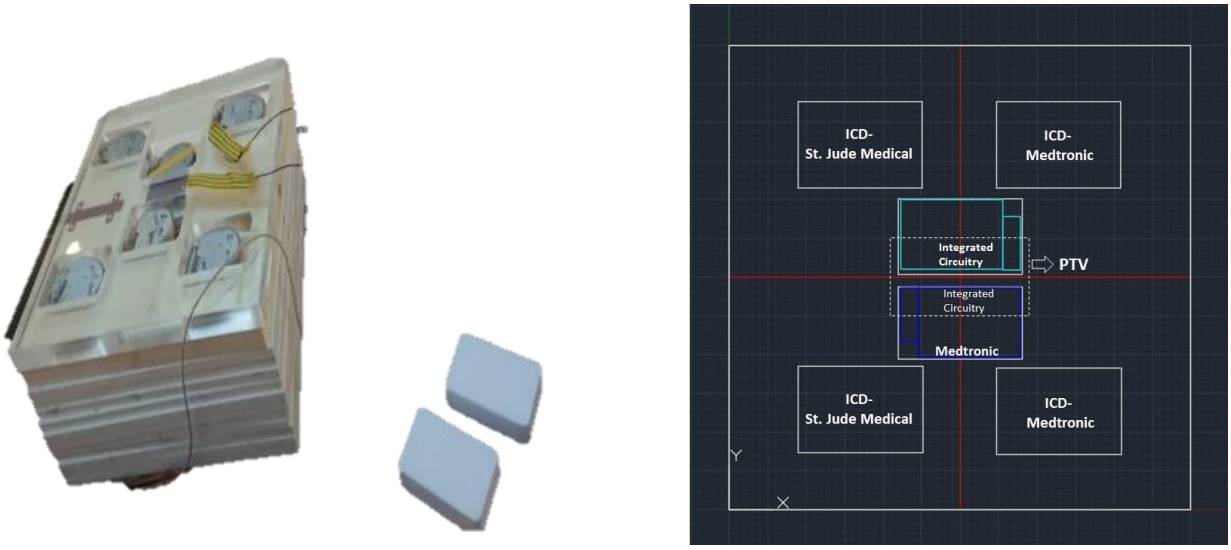

Figure 13: (Left) The experimental setup; (Right) top view of the acrylic slab designed to position the ICDs into six specific holes. Four holes were designed to be 3 cm away from the planning target volume (PTV), and two holes were designed to be placed partially inside the PTV.

Table 14: Clinical treatment plans (CTPs) and dose-rate tests (DRTs)

	DRT #1	DRT #2	CTP #1	CTP #2	CTP #3	CTP #4
Site	--	--	Lung&Chest	Lung&Chest	Lung&Chest	Lung&Chest
Delivery technique	Open field irradiation at iso-center	Open field irradiation at iso-center	VMAT-SBRT	VMAT- SBRT	VMAT- SBRT	3DCRT- SBRT
Energy & Beam mode	6MV-FFF	10MV-FFF	10 MV-FFF	6 MV-FFF	10 MV-FFF	6MV-FFF
Dose/Fx	From 50 MU up to 150MU	From 50 MU up to 200MU	28 Gy/1Fx	28 Gy/1Fx	48 Gy/4Fx	48 Gy/4Fx
The maximum dose rate at iso-center	• 600 MU/min • 800 MU/min • 1000 MU/min • 1200 MU/min • 1400 MU/min	• 400 MU/min • 800 MU/min • 1200 MU/min • 1600 MU/min • 2000 MU/min • 2400 MU/min	2400MU/min	1400 MU/min	2400MU/min	1400 MU/min
Position of integrated circuits to PTV	▪ Inside	▪ Inside	○ Partially inside	○ Partially inside	○ Partially inside	○ Partially inside

			• Outside: 3cm away	• Outside: 3cm away	• Outside: 3cm away	• Outside: 3cm away
ICD #	▪ 2 ICDs (Inside) **ICD #1:** Medtronic-Maximo VR 7232 **ICD #2:** St. Jude Medical- Current VR RF 1207-36	▪ 2 ICDs (Inside) **ICD #3:** Medtronic-Secura VR D234VRC **ICD #4:** St. Jude Medical- Ellipse VR CD1377-36QC	○ 2 (Partially inside) **ICD #5:** Medtronic-Maximo II VR D284VRC **ICD #6:** St. Jude Medical-Ellipse DR CD2377-36QC • 4 (Outside) **ICD #7:** Medtronic-Maximo II VR D284VR **ICD #8:** St. Jude Medical-Quadra Assura MP CD3371-40QC **ICD #9:** Medtronic-Secura DR D234DRG **ICD #10:** St. Jude Medical-Fortify ST DR. CD2235-40Q	○ 2 (Partially inside) **ICD #11:** Medtronic-Evera MRI XT DR SureScan DDMB2D4 **ICD #12:** St. Jude Medical-Ellipse VR. CD1377-36QC • 3(Outside) **ICD #13:** Medtronic-Evera MRI XT VR SureScan DVMB2D4 **ICD #14:** St. Jude Medical-Current Accel VR. CD1215-36 **ICD #15:** Medtronic-Evera MRI S VR SureScan Model DVMC3D4	○ 2 (Partially inside) **ICD #16:** St. Jude Medical-Current VR. CD1207-36Q **ICD #17:** Medtronic-Evera S DR DDBC3D1 • 4 (Outside) **ICD #18:** St. Jude Medical-Quadra Assura MP CD3371-40QC **ICD #19:** Medtronic-VR SureScan DVFC3D1 **ICD #20:** St. Jude Medical-Unify Assura CD3361-40C **ICD #21:** Medtronic-Viva XT CRT-D DTBA2D1	○ 2 (Partially inside) **ICD #22:** St. Jude Medical-Current VR RF 1207-30 **ICD #23:** Medtronic-Viva XT CRT-D DTBA2D1 • 3 (Outside) **ICD #24:** St. Jude Medical-Fortify Assura CD2359-40QC **ICD #25**: Medtronic-Secura DR D234DRG **ICD #26:** St. Jude Medical-Current + VR 1211-36

DRT Dose-rate test, *CTP* Clinical treatment plan, FFF beam Flattening-filter-free beam, *VMAT-SBRT* Volumetric-modulated arc therapy-Stereotactic body radiotherapy, *PTV* Planning target volume*, MU/min* Monitor unit per minutes*, ICD* Implantable cardioverter defibrillator*.*

4.3 Results

4.3.1 Retrospective study

In total, 523 patients with CIEDs who received at least one course of RT at the five campus of PeterMac between 2014 and 2018 were included in the study.

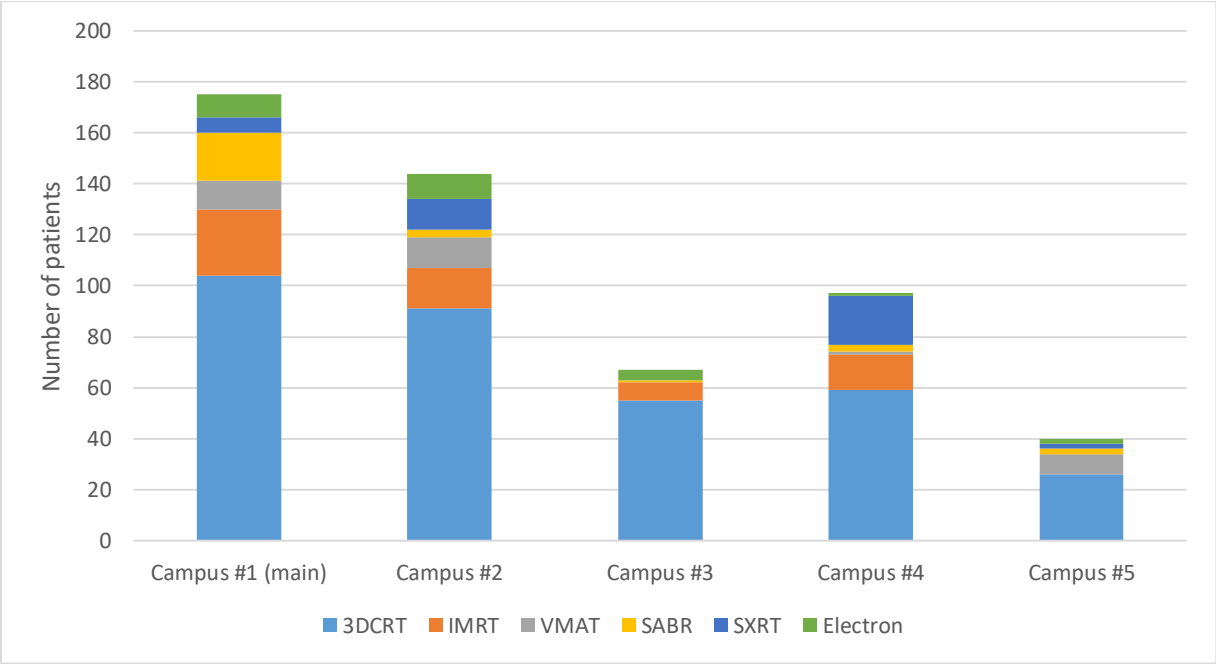

Figure 14: Patients with CIEDs underwent radiotherapy at Peter MacCallum Cancer Centre between 2014 and 2018

As shown in figure 14 and 15, although the majority of CIED patients were treated with three-dimensional conformal radiotherapy (3DCRT) during the study period, there was a continuous increase in the number of patients who had CIEDs and underwent SBRT/SRS. For comparison, the total number of patients treated across the five campuses has been reasonably steady at 6500 per year which highlights the significant increase in the fraction of patients presenting with implantable devices. This yields an increase from 0.5 to 2% of patients needing consideration for CIEDs.

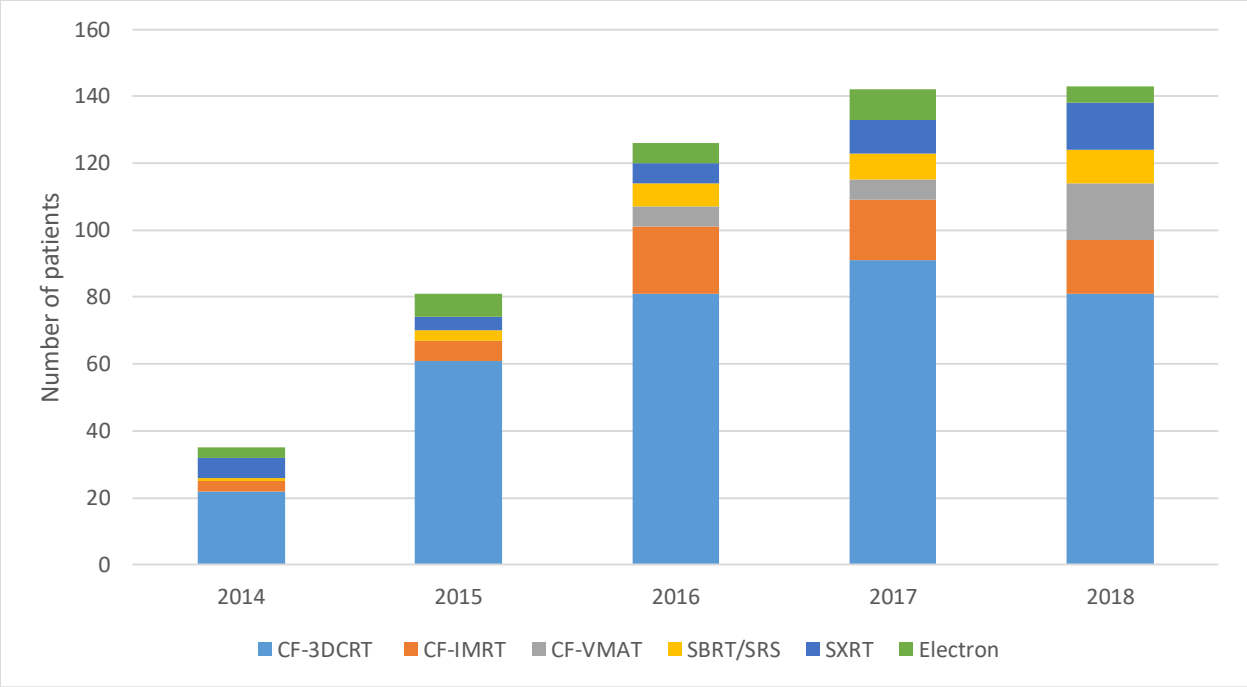

Figure 15: A retrospective analysis of patients with CIEDs undergoing radiotherapy at PeterMac between 2014 and 2018; CF-3DCRT: Conventionally-fractionated three-dimensional conformal radiotherapy, *CF-IMRT:* Conventionally-fractionated intensity modulated radiotherapy, *CF-VMAT:* Conventionally-fractionated volumetric modulated arc therapy, *SBRT/SRS:* Stereotactic body radiotherapy/Stereotactic radiosurgery, *SXRT:* Superficial x-ray radiation therapy

The characteristics, treatment plans and calculated CIED doses of patients and their device characteristics who were treated with SBRT/SRS are summarized in Table 14. Among the cohort, 11 cases were treated with FFF beams at an average dose rate of 2400 MU/min, and 17 cases were treated with FF beams at an average dose of 600 MU/min. All of the devices were positioned outside the treatment field at a distance greater than 5 cm with the exception of one case where the distance was 4 cm. The median (range) calculated dose the CIEDs were exposed to was 0.2 (0-1.86) Gy (figure 16). The functionality of the CIEDs during and after RT was investigated, and no failures were reported due to SBRT/SRS.

Table 15: Summary of the dose-rate test, the clinical treatment plans and their related features

Characteristics	Study population	SBRT/SRS with FFF	SBRT/SRS with FF
No. (%)	28	11	17
Patient age, median (range), y	80 (57-93)	-	-
Type of CIED, No. (%)			
PM	23	9	14
ICD	4	1	3
CRT-D	1	1	0
Site of irradiation, No. (%)			
Lung and Chest	17	9	7
Brain	2	0	2
Liver	2	1	1
Kidney	5	0	5
Spine	1	0	1
Pelvis	1	1	1
Treatment Plan specification			
Photon Energy			
6MV	17	0	17
10MV	11	11	0
Number of fraction, median (range)	3 (1-5)	-	-
Dose/fraction, median (range), Gy	29 (28-54)		
Dose rate (MU/Min)			
2400 (MU/Min)	11	11	0
1400 (MU/Min)	0	2	0
600 MU/Min	15	0	15
Distance between ICD and closest treatment field edge			
less than 5 cm	1	1	0
5cm-10 cm	4	0	4
More than 10 cm	23	10	13

SBRT delivery technique			
VMAT	11	4	7
3DCRT	17	4	13

CIED Cardiac implantable electronic device*, PM* Pacemaker*, ICD* Implantable cardioverter defibrillator*, CRT-D* Cardiac resynchronization therapy*, SBRT* Stereotactic body radiotherapy*, SRS* Stereotactic radiosurgery*, FFF beam* Flattening-filter-free beam*, FF beams* flattened beams.

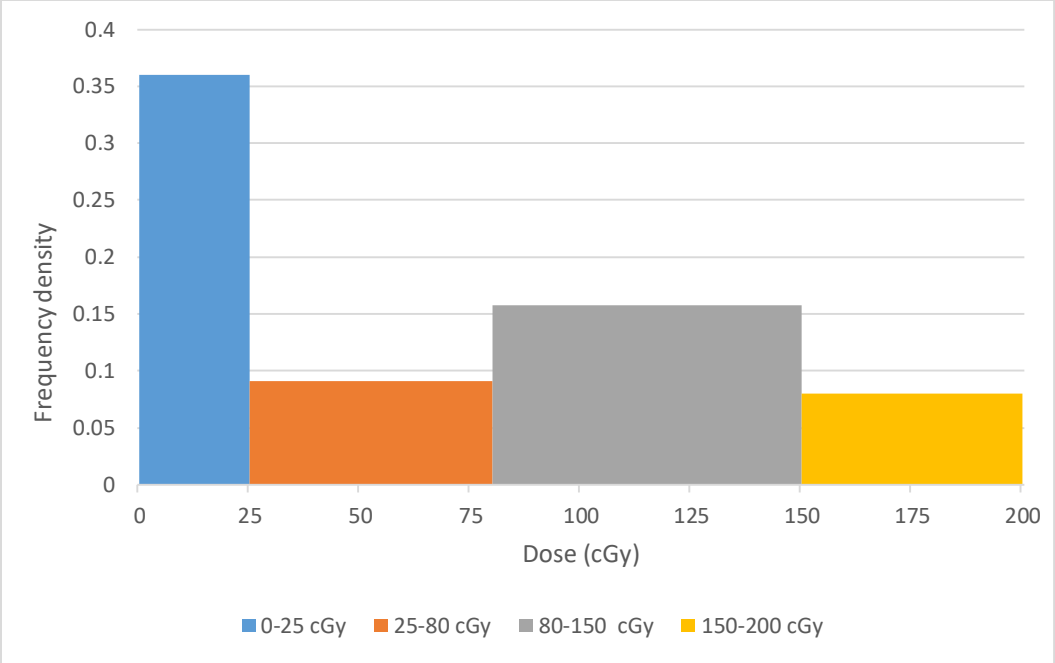

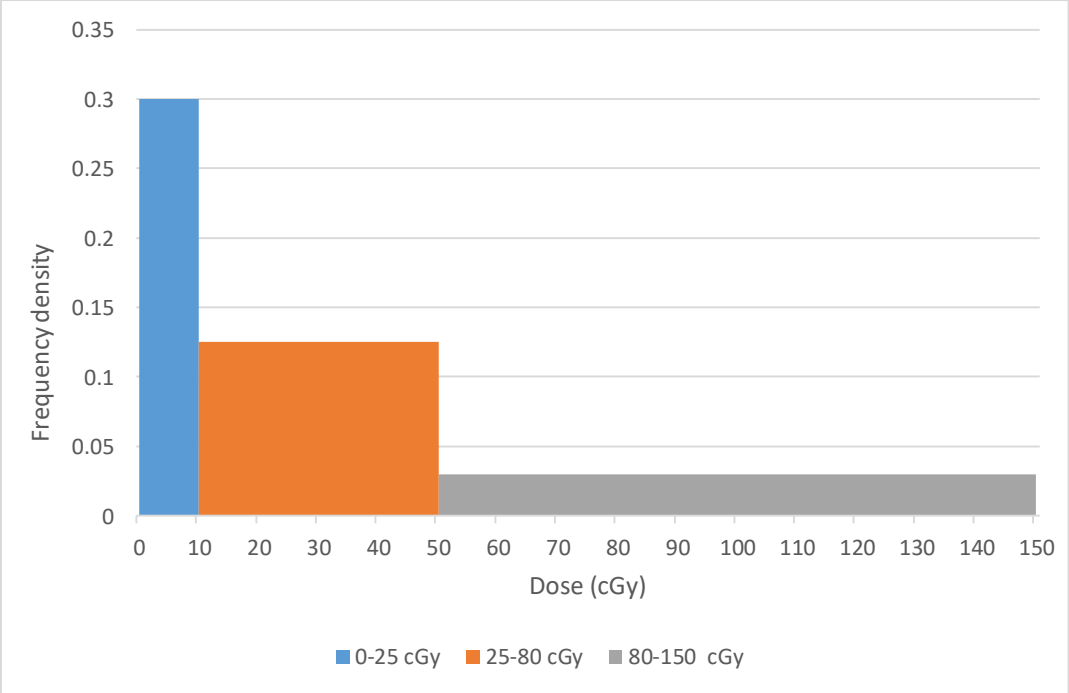

Figure 16: Histogram with non-uniform class width of CIED dose show estimated dose to CIEDs from FF and FFF beams. The median (range) calculated dose to CIEDs was 0.11 (0-1.5) Gy for FFF beams and was 0.22 (0.01-1.86) for FF beams.

4.3.2 Experimental study

4.3.2.1 Dose-Rate Tests (DRTs)

An average dose rate of less than 1200 MU/min for both the 6-MV FFF and 10-MV FFF beams did not affect the sensing function of the selected ICDs. Inappropriate sensing occurred with 10-MV FFF beams, starting at a dose rate of 1200 MU/min in ICD #3 and at 1400 MU/min in ICD #4, but was rare with 6-MV FFF beams and occurred at only a dose rate of 1400 MU/min in ICD #2. (figure 17)

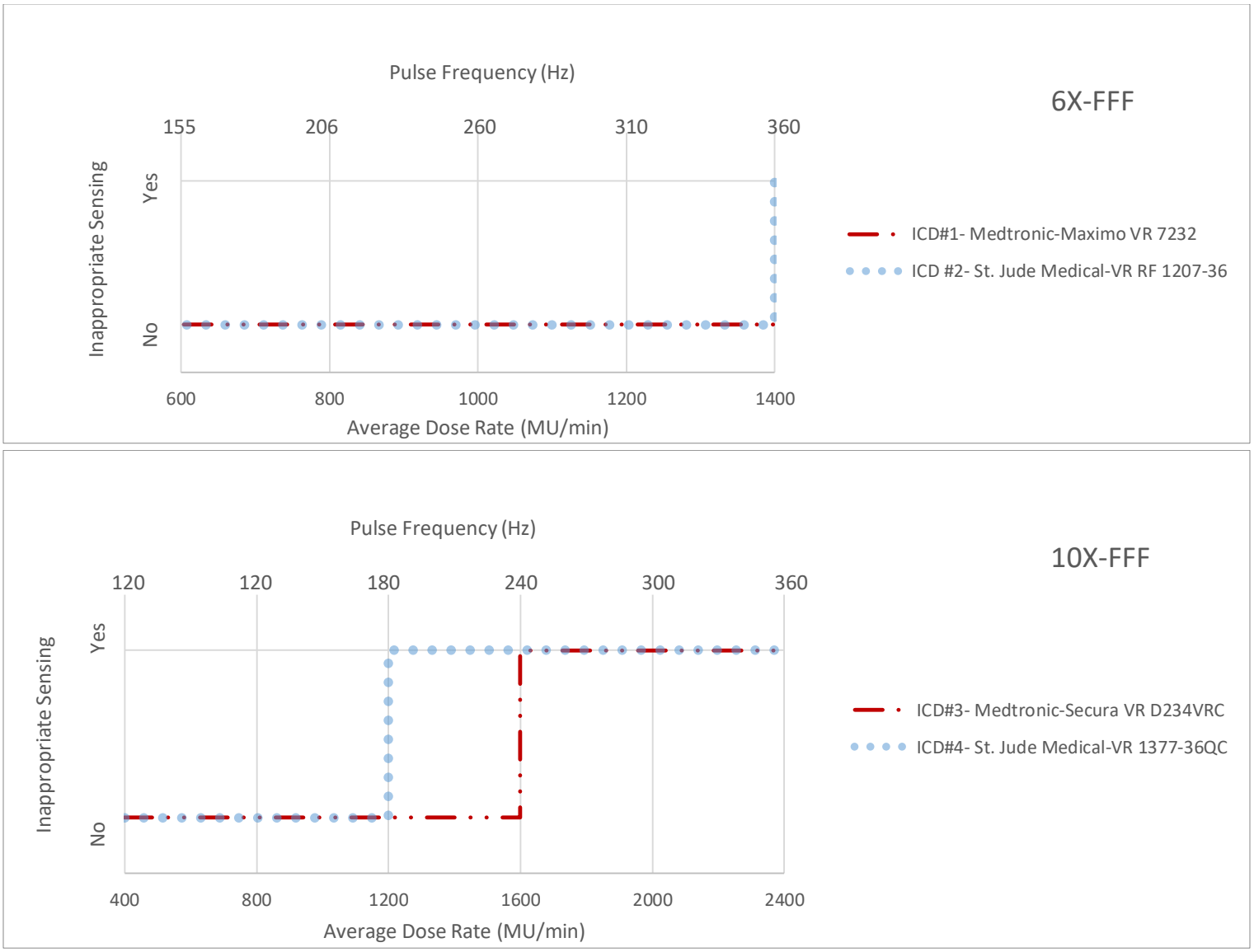

Figure 17: Results of the dose-rate tests for 6-MV FFF (up) and 10-MV FFF (down) to determine when inappropriate sensing (either over-sensing or inhibition) occurs.

4.3.3 Clinical treatment plans (CTPs)

The ICD dysfunctions observed during and after delivering lung SBRT to the phantom are summarized in Table 15. No errors were observed in the ICDs that were irradiated using CTP #2 and CTP #4 with 6-MV FFF photon beams. During the delivery of CTP #1 and CTP #3 with 10-MV FFF photon beams, inappropriate sensing occurred in ICD #6, ICD #9, and ICD #16 (figure 18). Note that over-sensing was minor and did not meet criteria for a shock. Interrogation after irradiation showed changing in programmed parameters such as pacing mode, ventricular pacing threshold, pacing rate and pulse amplitude (figure 19). Inadequate shock therapy (in spite of deactivation) and battery voltage changes/longevity were not detected by the programmers. Additionally, no permanent damage to the ICDs was reported.

Table 16: Types of ICD errors

ICD #	CTP #	Position of electronic circuit of ICD to PTV	Inappropriate sensing during irradiation	Interrogation after irradiation	Total calculated dose to	
					the part of device inside the field including integrated circuits (Gy)	the part of device outside the field (Gy)
5	1	Partially inside	No	Reprogramming of pacing rate	Dmax: 26.1 Dmean: 16.2	Dmax: 17.8 Dmean: 5.6
6	1	Partially inside	Yes	Reprogramming of pacing rate	Dmax: 28 Dmean: 16.9	Dmax: 18.7 Dmean: 2.8
16	3	Partially inside	Yes	A decrease in pulse amplitude after delivering the last fraction	Dmax: 46.4 Dmean: 28.8	Dmax: 30.7 Dmean: 9.6
17	3	Partially inside	No	Reprogramming of ventricular pacing threshold	Dmax: 42.7 Dmean: 28.4	Dmax: 29.2 Dmean: 4.8
					Total calculated dose to the ICD (Gy)	
9	1	Outside	Yes	Change in pacing mode	Dmax: 0.89 Gy Dmean: 0.66 Gy	
20	3	Outside	No	Change in pacing mode	Dmax: 0.96 Gy Dmean: 0.85 Gy	

CTP Clinical treatment plan*, ICD* Implantable cardioverter defibrillator*, PTV* Planning target volume.

Figure 18: The ICD electrogram demonstrates inappropriate sensing during the delivery of CTP #1 in ICD #9.

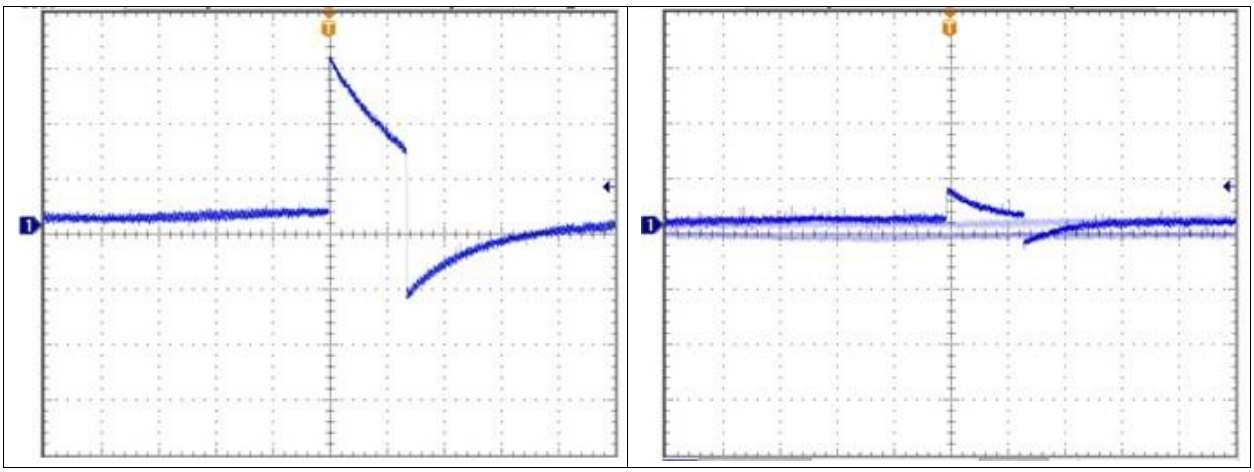

Figure 19: Amplitude deviation for ICD#17 after delivering the last fraction of CTP3.

4.4 Discussion

With the widespread implementation of advanced RT technologies and techniques, including SBRT treatments with FFF beams, the need to consider the different challenges of these techniques when managing patients with CIEDs has arisen[20].

Different factors, such as the CIED cumulative dose[30], the radiated EMI problem, and the ICD model and manufacturer, should be taken into account to accurately evaluate dose-rate effects. Given that we cannot generalize the obtained threshold dose rate beyond which inappropriate sensing occurs in all ICD models and treatment conditions.

Inappropriate sensing includes both over- and under-sensing. In our test, it was observed that over-sensing was more frequent for dose rates ranging between 1200 MU/min and 2000 MU/min, and under-sensing or loss of sensing was more frequent for dose rates greater than 2000 MU/min.

Although any type of sensing abnormalities should be taken into consideration, over-sensing can become a more concerning issue for pacing-dependent patients.[122]

Several in vitro studies concerning CIED irradiation using FF beams have been conducted. [28–33] Mouton et al.[30] conducted an in vitro study using a Saturne 3 linac (CGR MeV-General Electric). The irradiation was performed at 18 MV and with different dose rates up to 8 Gy/min. They recommended a maximum dose rate of 0.2 Gy/min, rejecting the direct irradiation of the pacemaker, at a standard dose rate for tumor treatment (2 Gy/min). Hurkmans et al.[22] concluded that for conventional FF beams, the dose-rate effect (e.g., ranging from 1 Gy/min to 6 Gy/min at a depth corresponding to the maximum dose at a reference distance) on CIEDs is not significant because the dose rate at the CIED location is lower than the recommended maximum acceptable value.[30] Hurkmans and colleagues[22] further added that for FFF beams, the dose rate would be lower than 1 Gy/min, provided that the CIED is located outside of the treatment field. Thus, the dose-rate effect is rare. However, this study showed that in SBRT treatments with FFF beams and the VMAT delivery technique, the effect of a high dose rate is not always rare (if it is infrequent) when the ICD is in the close vicinity of the PTV.

To the best of our knowledge, only one in vitro study[71], in the form of an abstract, of ICDs in which the authors used FFF beams has been published. Irradiation was conducted with a cumulative dose of up to 150 Gy in the isocenter, [10 Gy*3 fractions] in five sets, with 6-, 10- and 18-MV beams. Our study attempted to imitate a real-world SBRT scenario, including clinical fractionation, dose rates and delivery techniques. However, a comparison between the ICD errors presented in this study and those reported by Gauter-Fleckenstein et al.[71] indicated a general agreement that during 6-MV FFF-VMAT, the risk of ICD malfunctions is low even when cardiac devices are located in the close vicinity of the PTV. According to our findings, ICD anomalies during 10-MV FFF-VMAT can occur even with irradiation at a lower cumulative dose in the isocenter, in contrast to the results from Gauter-Fleckenstein et al. [71]

There is no safe dose threshold below which no CIED damage occurs.[22,23,107] However, because increasing the cumulative dose increases the risk of failure, the consensus is that the cumulative dose received by CIEDs should be kept as low as possible.[22,78] CIED patients are usually risk categorized on the basis of the CIED cumulative dose and pacing dependency; the risk categories are low (the CIED dose is less than 2 Gy and the patient is not pacing dependent), medium (the CIED dose is less than 2 Gy and the patient is not pacing dependent), and high (the CIED dose is between 2 Gy and 10 Gy for a nonpacing-dependent patient, and pacing-dependent patients receive a CIED dose less than 2 Gy).[22,78]

In general, SBRT/SRS is applied to small treatment volumes; near the target volume, lower doses are produced by flattening filter-free-beam in comparison to that produced by the FF-beam.[66,68] In this

study, the ICD errors mostly occurred when the devices were positioned partially inside the beam and electronic circuit of ICD received at least 80% of the prescribed dose. However, two devices that were positioned outside the beam and were irradiated with 10-MV FFF-VMAT showed two errors at doses lower than 2 Gy.

In this study, ICDs were exposed to a high dose per fraction. Although this exposure can result in a higher ICD dose per fraction[20,22], the increased dose per fraction by itself is not a serious concern as long as the maximum accumulated dose to the devices is lower than the recommended value. However, the use of FFF beams with energies greater than 6 MV and high dose per fraction can increase the risk of ICD malfunctions, including inappropriate sensing and reprogramming, in close vicinity of the PTV. Accordingly, caution is needed in using FFF beams in CIED patients, in particular pacing-dependent patients.

As with other studies, this research is also subject to limitations. The first limitation of this study was that the tested ICDs were from only two different manufacturers, which limited the results and the analysis. Additionally, it was suggested that the device's projected battery life and current status were not appropriate surrogates in this test, and instead, actual measurements are required.

4.5 Conclusion

A retrospective analysis of patients with CIEDs who underwent radiotherapy at the Peter MacCallum Cancer Centre demonstrated an increase in the number of these patients who received conventional linac-based SBRT and SRS. Thus, some of the potential patient risk factors, such as a high dose per fraction, a high dose rate using FFF beams with two different energies, and delivery with an intensity-modulated technique, were investigated in this study.

The study showed that special attention should be paid to managing ICD patients undergoing SBRT with FFF beams. This consideration is particularly important for VMAT-SBRT with a high-dose-rate FFF beam with a beam energy greater than 6 MV. Correspondingly, it was found that with FFF beams, the dose-rate effect on an ICD positioned in the close vicinity of target may present issues not seen with conventional beams.

The results of this study and a recent review study[20] were used to update some of the policies applied to manage CIED patients undergoing SBRT/SRS at PeterMac. According to this update, for pacing-dependent patients, the use of FFF and 10 MV beams should be restricted if a significant dose spill to the device is expected.

Chapter 5: Monte Carlo and dosimetry study of out-of-field doses in a water phantom including depth of CIEDs

1. Introduction

The ultimate goal of radiotherapy is to deliver precisely high dose to the target, while reducing dose to normal tissues. To fully achieve this aim, all elements of the chain of RT have progressed and are still being developed, from target and organs-at-risk (OARs) delineation to plan verification, in an accurate manner [75,123,124].

One of the element of the chain of RT is treatment planning aiming to design the best strategy in order to establish a balance between objectives and constraints for the target and the OARs. Treatment planning systems (TPSs) accurately calculate and optimize in-field target doses [66]. However, they are not commissioned for out-of-field non-target doses. This is because sources of out-of-field radiations, such as collimator scatter, head leakage, and patient scatter, are usually underestimated by TPSs [66,125].

The out-of-field dose, generally, would be a concern to patients with cancer because it might increase the risk of secondary cancers, skin cancer, and cataract formation [66]. It specifically might be of concern to cancer patients with cardiac implantable electronic devices (CIEDs) due to the sensitivity of CIEDs to radiation doses. Thus, absorbed CIED dose, as one of the risk factor for CIED dysfunction, need to be accurately estimated [20,78,126].

The accuracy of different photon-beam treatment planning systems have been investigated either using dosimetry measurements or through Monte Carlo (MC) models using different MC radiation transport codes such as MCNP, Geant4/Gate, EGGnrc, and FLUKA [66,125].

Monaco, is one of the well-known MC-based treatment planning systems. Current algorithm within Monaco (Version 5) is the X-ray voxelized Monte Carlo (XVMC) for photon treatment. The modeling of the TPS was initially based on the virtual source model introduced by Sikora et al [127], considering three virtual sources such as primary photon source, secondary photon source and electron contamination source [128,129].

The main goal of this part of study is to model out-of-field doses from Elekta Synergy in a homogenous water phantom using MCNPX, as one of the most used and cited MC radiation transport codes in medical physics and radiotherapy [130–135]. Accordingly, the second goal is to compare the out-of-field doses at depth of CIED) obtained from Monaco, measurements and the model.

2. Methods and materials

2.1 Monte Carlo model

The MCNPX code [136] (Version 2.6, Los Alamos National Laboratory, Los Alamos, NM) was employed to simulate the head of an Elekta Synergy medical linear accelerator (Elekta oncology systems, Stockholm, Sweden). Full information of the beamline components was provided by the company in seven chapters including, general design description, radiation head, X-ray target, filters (for low and high energy), auto wedge filter and backscatter plate, ionization chamber, and mylar mirror.

However, ELEKTA does not supply full details of the head shielding, and available data in the literature [137] was used in our model, accordingly.

In this simulation, the geometry of the main major beamline components such as target, target block, as well as a 50 cm x 50 cm x 50 MP3 water phantom (PTW, Freiburg, Germany) were drawn by AutoCAD software in SAT format. A compatible tools with 3D CAD standard ACIS text (SAT), named the MCNP visual editor (MCNPXVised, version 2.6) was used to covert the SAT file into an MCNP input file [130].

In defining material compositions and density of each specific component, data were defined in data card section as indicated in manufacturer's document. As suggested by the literature [137], the materials used by manufacturers to make head shielding are similar, therefore the materials for shielding the head were used as suggested in the literature [137].

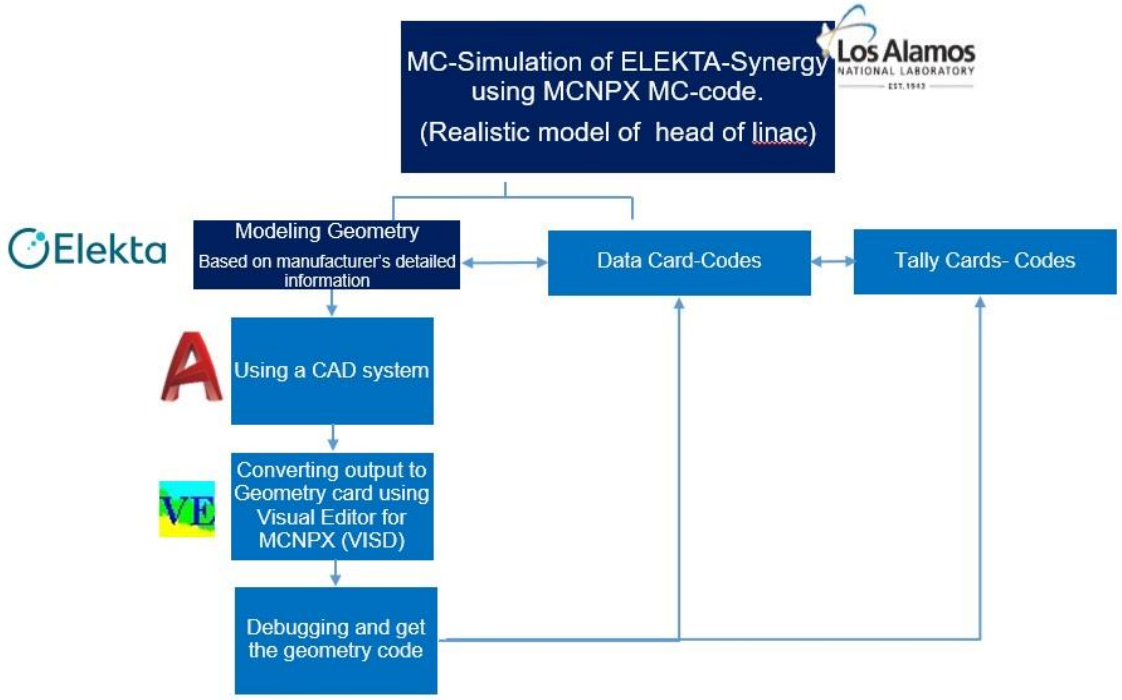

Figure 20: The procedure of simulation

In MCNPX, source is defined by "SDEF" card. This card has many variables or parameters to define all the characteristics that specify the source. Some of the defined variables used in this simulation is tabulated in the table 16:

Table 17: Variables used in the simulation of source

Variable	Meaning	Default
POS	reference point for positioning sampling	0, 0, 0
AXS	reference vector for EXT and RAD	no direction
EXT	Cell case: distance from POS along AXS. Surface case: cosine of angle from AXS	0
RAD	radial distance of the position from POS or AXS	0
PAR	type of particle source	emits = 1 (neutron) if MODE N or P or N P E; = 2 (photon)

		if MODE P; = 3 (electron) if MODE E
ERG	energy (MeV)	14 MeV
VEC	reference vector for VEC	Volume case: required unless isotropic. Surface case: vector normal to the surface with sign determoined by NRM.
DIR	μ, the cosine of the angle between VEC and UUU, VVV, WWW. The azimuthal angle is always sampled uniformly in [0, 2π]	Volume case: μ is sampled uniformly in [−1.1] (isotropic). Surface case: p(μ) = 2μ for μϵ [0, 1] (cosine distribution).

In source definition section, first the Gaussian energy spectrum and the spot size of the electron beam striking the target were selected based on the estimated values provided in ELEKTA MC document. The pre-defined Gaussian fusion energy spectrum in MCNPX (f=-4) was used [136].

$$p(E) = Ce^{-(\frac{E-b}{a})^2}$$

(Equation 4.1)

where a is the width in MeV and b is the average energy in MeV.

To obtain percentage dose deviation of less than 3% between measured and calculated practical range (Rp) and the depth of 50% maximum dose (R50) in PDD curves, these values. The suitable values were found through several trial and error. The peak energy of 6.5 MeV and FWHM 0.5 MeV were selected for 6 MV X-ray beam energy; they were 13.3 and 0.4 MeV for 15 MV X-ray beam energy.

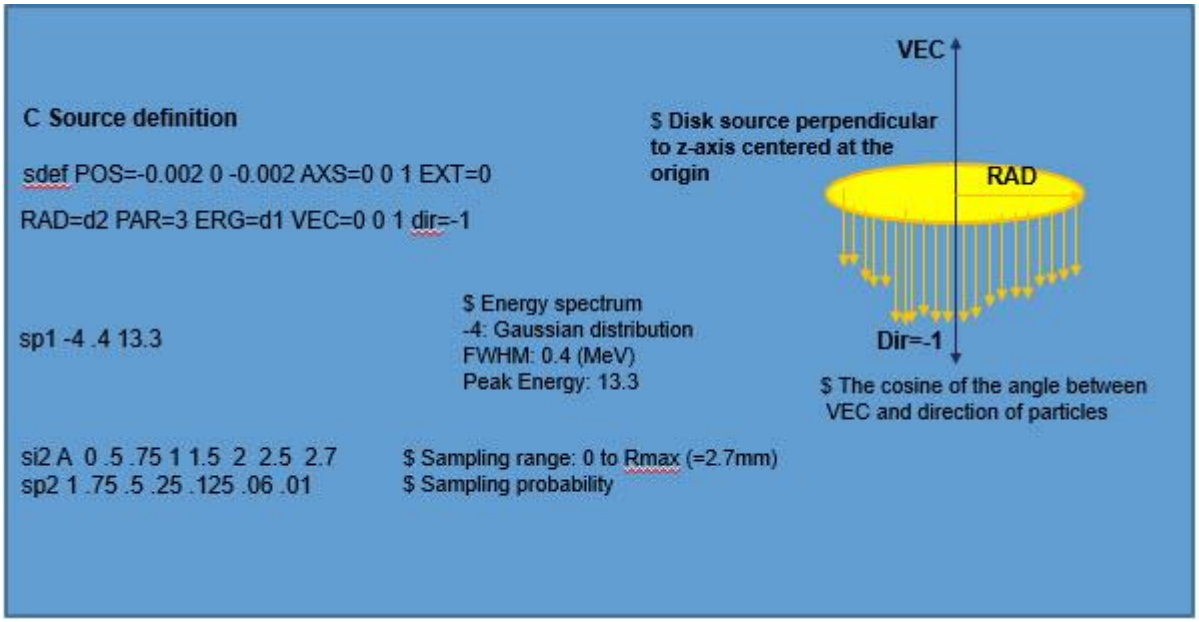

Figure 21: Source defenition

To validate the MC simulation, percentage depth dose curves and beam profiles were calculated at two depths (1 cm, and 10 cm) and they were compared against the corresponding measurements. Simulations and measurements were done at source-to-surface distance (SSD) 100 cm, for field size of 10 cm x 10 cm, with 6 MV and 15 MV. The gantry and collimator were set to zero. The central-axis of the beam in the water phantom were divided into 0.5 x 0.5 x 0.5 cm3 voxels [134,135].

Energy deposition from all types of particles in each voxel was scored using mesh tally type 3. In this tally particles are tracked through the independent mesh as part of the regular transport problem. The output is written as a text file for each mesh. Also, it is possible to use a conversion program, gridconv, which is available in MCNPX package to convert the output file into graphical analysis package.

There are some mandatory cards to define characteristics of each mesh tally, such as CORAn corra(n,1), corra(n,2), ... corra(n,N) CORBn corrb(n,1), corrb(n,2), ... corrb(n,N) CORCn corrc(n,1), corrc(n,2), ... corrc(n,N), where the CORAn, CORBn, and CORCn, cards were used to describe the three coordinates as defined by the mesh type [136]. In our model and in order to define the water phantom in rectangular meshes, CORAn were defined which represent planes perpendicular to the x-axis, CORBn are planes perpendicular to the y-axis, and CORCn are planes perpendicular to the z-axis.

The scored doses per source particles were normalized to the dose at depth of maximum dose (Dmax). The voxel sizes to score energy deposition in out-of-field doses were defined larger to

decrease statistical uncertainty [134,135]. They were 5 x 1 x 2 cm3 in-plane tallies and 1 x 5 x 2 cm3 in cross- plane tallies. Also, in order to reach the statistical uncertainty less than 1%, a sufficiently large number of particle (in the order of 10^9 primary electrons) was applied for all simulation.

Neutron fluxes from Synergy operating at 15 MV, for an iso-center and 30 cm from the iso-center, at the aforementioned depths for field size of 10 cm x 10 cm were calculated using tally (F5:n). The F5 is a point or ring detector tally which determines flux of particles at a specific point. The tally quantity scored in MCNPX is[136]:

$$\frac{W\ p(\Omega_p)e^{-\lambda}}{R^2}$$

(Equation 4.2)

and the physical quantity that corresponds to tally is

$$\phi_p = \int dE \int dt \int d\Omega\ \psi(r_p.\ \Omega.\ E.\ t)$$

(Equation 4.3)

Where W is particle weight, $p(\Omega_p)$ is probability density function for scattering (or starting) in the direction towards the point detector, R is distance to detector from a source or collision event, λ is total number of mean free paths from particle location to detector, ψ is angular flux familiar from nuclear reactor theory, $(r_p.\ \Omega.\ E.\ t)$ is particle position vector (cm), direction vector, energy (MeV), and time (sh; 1sh = 10-8 s). [136,138]

In order to reduce the statistical uncertainty and increase computing efficiency, different variance reduction techniques were used [139].From the specific truncation methods available in MCNPX, energy cut-off (CUT card) was used. For 6 MV photon beam simulation, the electron and photon cutoff energies were applied to 10 keV, while for photo-neutron simulation of 15 MV photon beam the energy cut-off were set to 5 MeV [134,135]. Geometry splitting from population control methods available in MCNPX was used and importance (IMP card) was assigned to each cell. From the modified sampling methods, bremsstrahlung production was biased in target materials for 15 MV photon using BBREM card [130–133]. The maximum number of particle histories used for 10 cm x 10 cm was 4 x 10^9. Photo-atomic and cross section data from MCPLIB04 [white]and ENDF/B-VI.8 [CSEWG] were used.

2.2 Measurements

2.2.1 Photon

Irradiation was delivered using a Elekta synergy linac (Elekta AB, Stockholm, Sweden) at University hospital of Trieste, Italy. The dosimetric measurements were performed in a water tank phantom (MP3, PTW-Freiburg, Germany).

First, the accuracy of the MC models for both 6 MV and 15 MV was verified at the central beam axis. Percentage doses and beam profiles at dmax and reference depth for photon calibration (10 cm) were measured.

The out-of-field dose profiles were measured using three different PTW (Freiburg, Germany) detectors such as synthetic single-crystal diamond detector (60003), PinPoint Ion Chambers (31014) and Semiflex 3D Ion Chamber (31021) in the water phantom with a step size of 3 mm in field and 1 mm in out-of-field. All the measurements were implemented using same geometric setup (gantry and collimator angle, SSD, field sizes and depth) as used in the simulations.

The dose profiles were measured at least three times in order to find out the random errors as well as positioning errors of the detector.

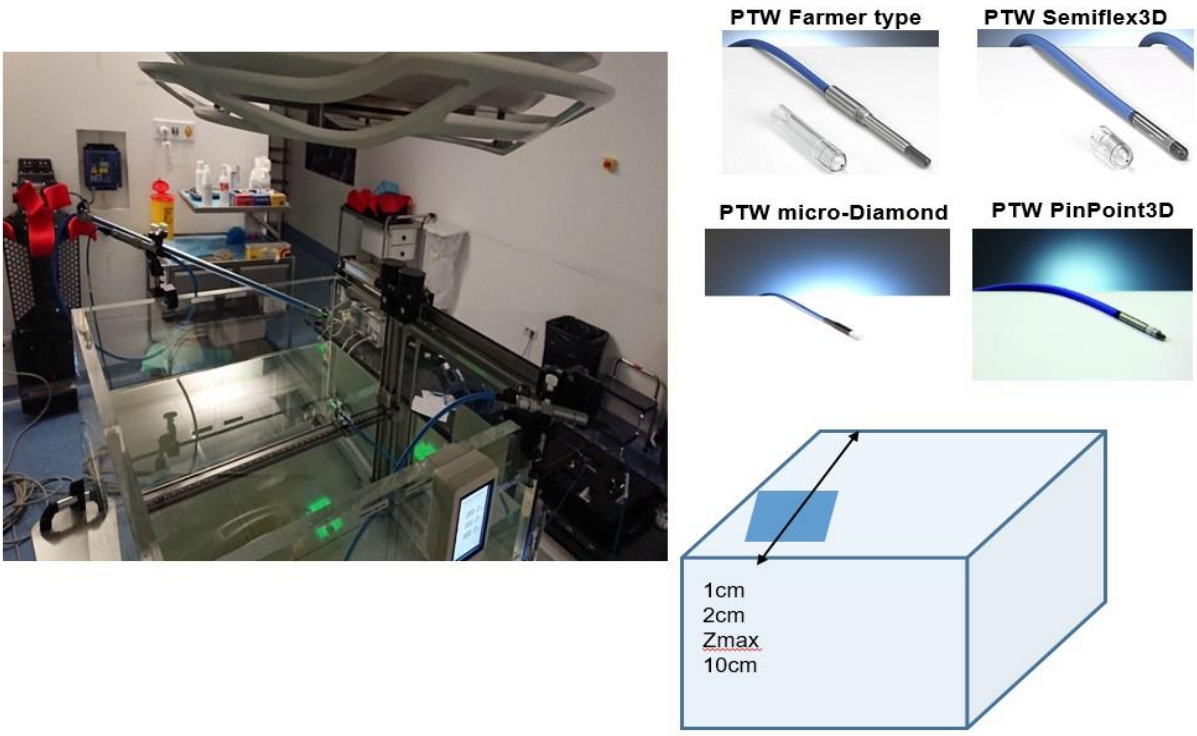

Figure 22: Phantom setups using four active dosimeters to measure dose profile up to 30 cm from the field edge.

2.2.2 Neutron

Bubble detectors are passive dosimeters made by metastable halocarbon droplets in an inert gel matrix. Since they are only sensitive to neutrons, they are suitable to measure neutron doses and fluences [140]. In this study, superheated drop dosimeters to measure neutron doses were used. Two types of superheated Bubble detectors (BTI Technologies, Inc., Chalk River, Canada) were used, namely BD-PND sensitive to fast neutrons (100 keV < E < 20 MeV) and BDT for thermal neutrons (E < 0.4 eV) [141].

A specific plastic holder was used to fix the bubble detectors in the rail shaft of the water phantom. The detectors placed at the iso-center, 15 cm and 30 cm outside the field in such a way that the center of the detectors were at the desired depth of this study [140].

Figure 23: The bubble detectors placed and fixed in arm of water tank using a special holder. The bubble detectors placed inside the beam, 15 cm and 30 cm out of the field at two depth of 1cm in which pacemaker is usually implanted. The SSD was 100cm, field size was 10x10cm of 15 MV photons.

In addition, neutron energy spectra were calculated using tally (F5:n) in MCNPX [136].

2.2.3 Treatment planning system (TPS)

A virtual water phantom with the exact size and same setup was simulated using Monaco TPS. The dose profiles from a 10x10 cm^2 field size at SSD=100 cm was calculated using the TPS in QA mode.

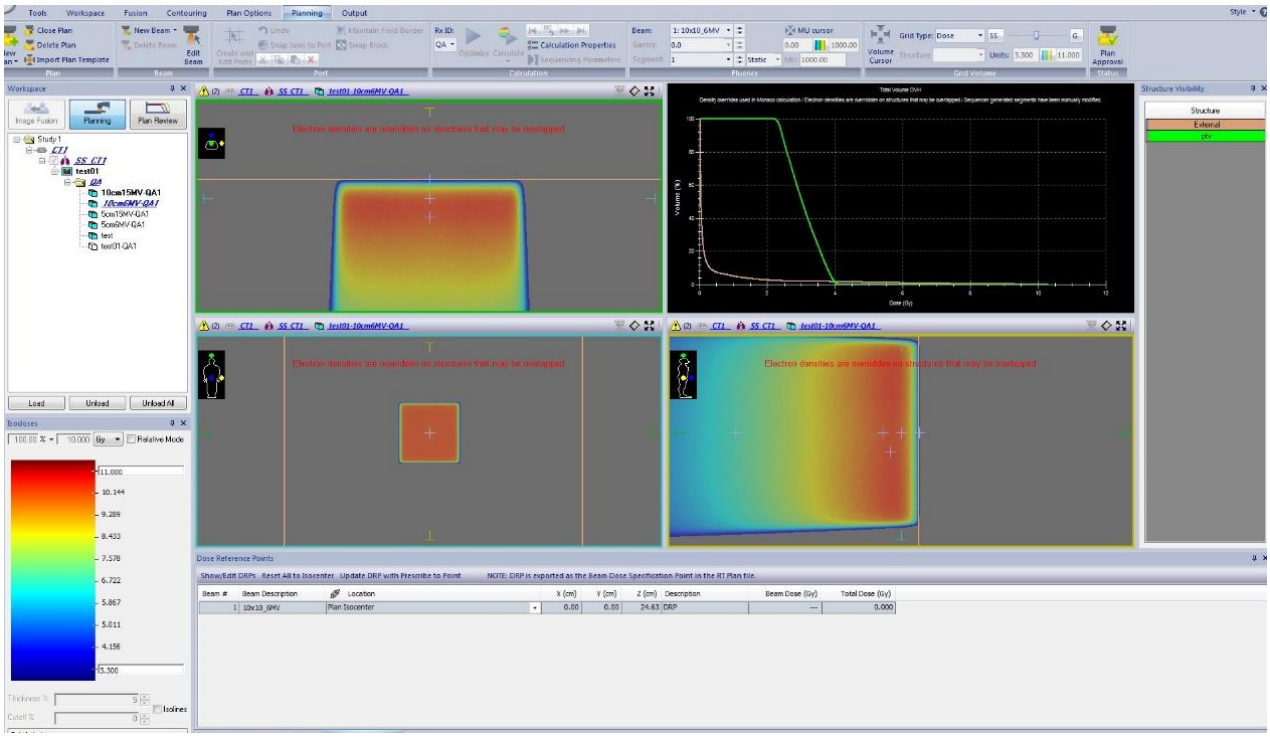

Figure 24: Dose calculation in water phantom using MONACO

The dose profiles were exported using dose export for comparison with those obtained from measurements and MCNPX. The calculations were computed using a $1 \times 1 \times 1$ mm^3 dose grid, dose uncertainty of 0.5% and beam statistical uncertainty of 1.0% per calculation for out-of-field doses.

2.3 Results

The figure 25 illustrates the different parts of MC simulation of synergy and the bunker using MCNPX and visualized by the MCNP visual editor (MCNPXVised).

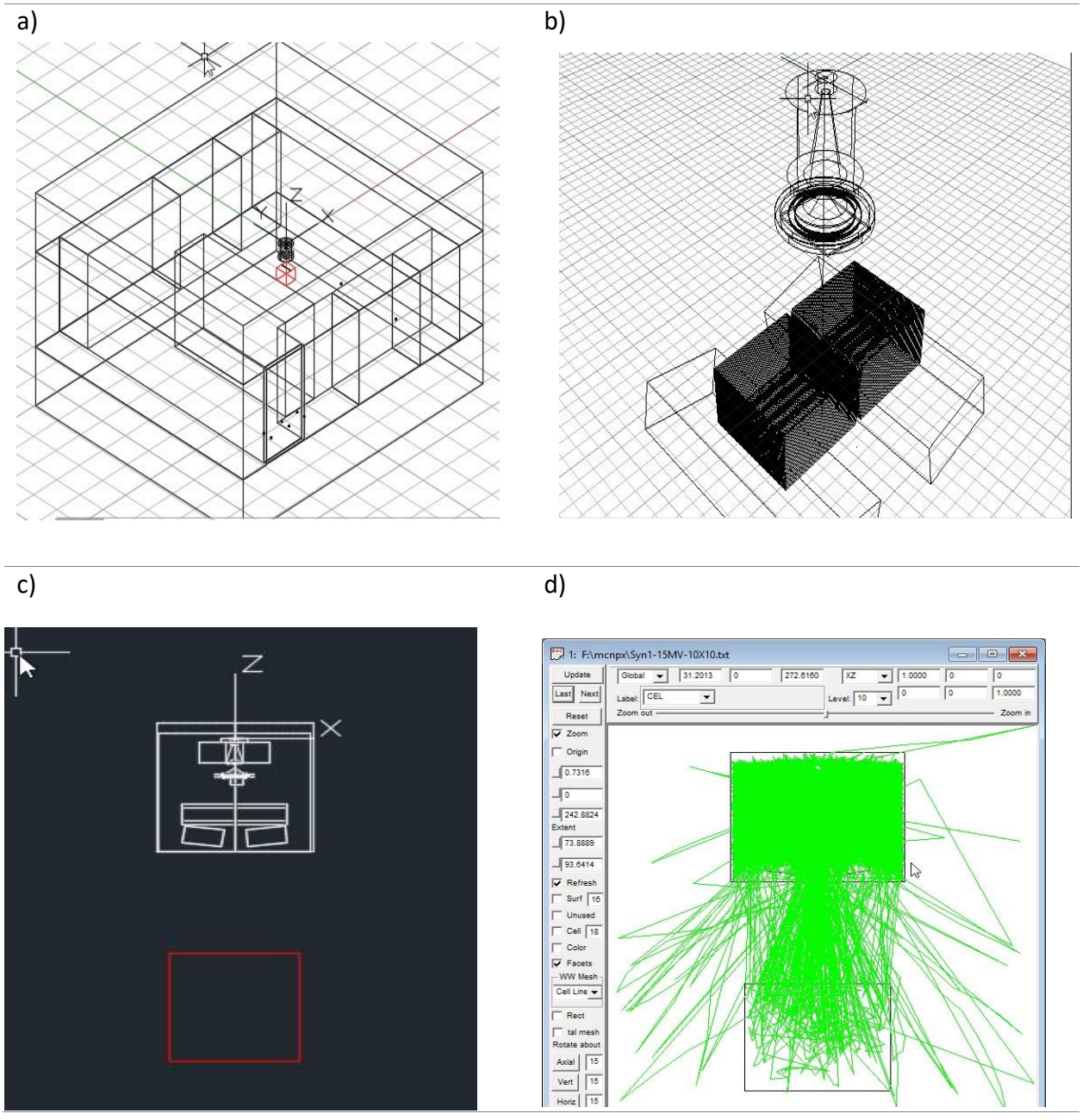

Figure 25(a) Linac Bunker modeling, b&c) sample of modeling of head in 2D and 3D view, d) sample of running MC-code using MCNPXVised

Figure 26 and 27 depict the comparisons between the MCNPX beam profiles calculations versus water phantom measurements for 6 MV and 15 MV photon beam at 10 cm depth.

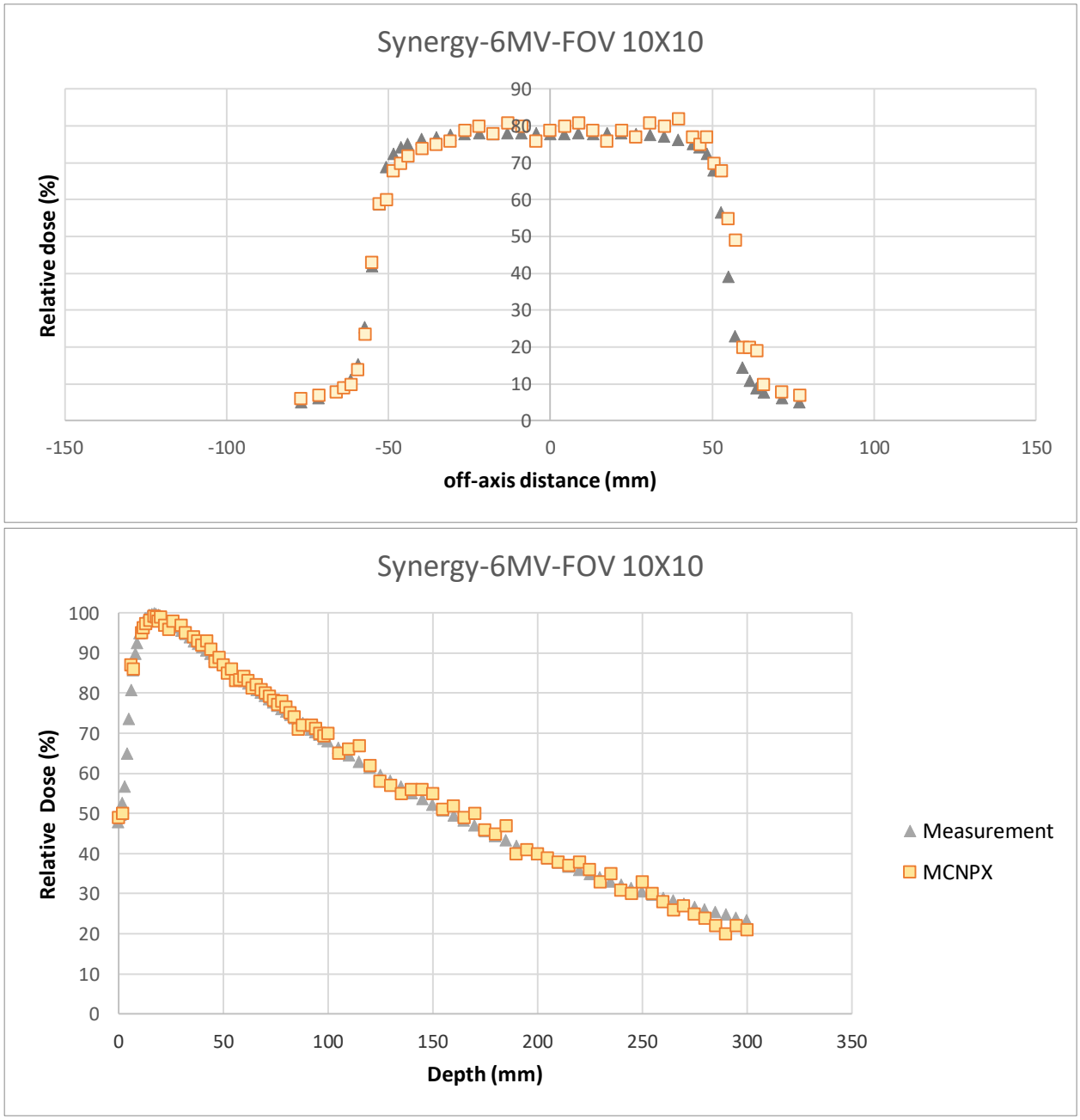

Figure 26: Validation of MCNPX calculations for 6MV photon thorough comparison with the corresponding experimental measurements.

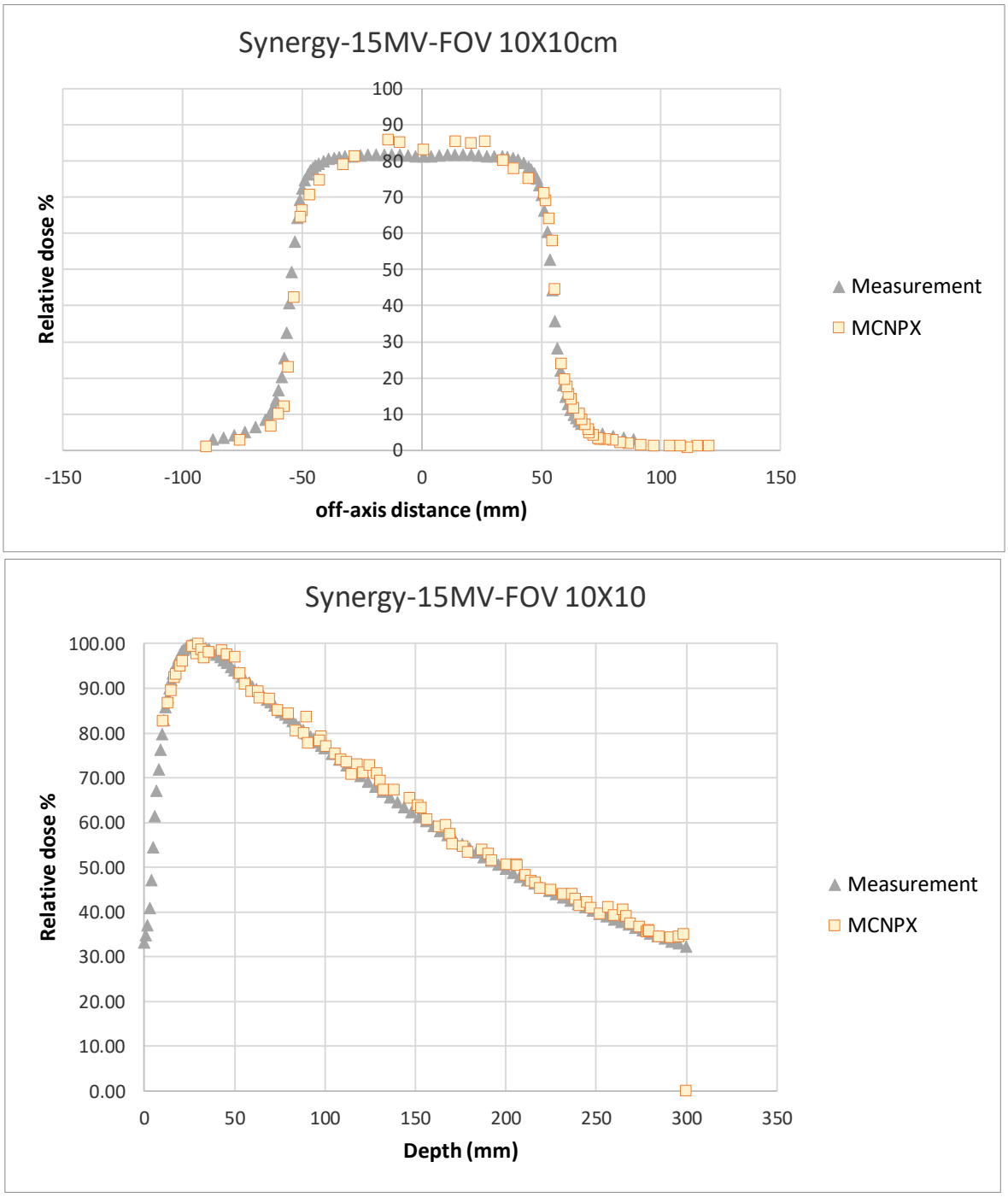

Figure 27: Validation of MCNPX calculations for 6MV photon thorough comparison with the corresponding experimental measurements.

The differences between measurement and simulation in build-up region were less than 13.5%, and for the rest of PDDs were less than 4%, there were 3-5% in 50-100% of beam, 8-12% in penumbra regions, less than 4% in umbra regions, and outside were 19-25%. Uncertainties were calculated less than 1% for 1 standard deviation.

The in-beam dose profiles at 10 cm measured by the diamond detector, a Pinoint, semiflex 3D, and Ion chamber were compared and the obtained results showed a good agreement till 250 mm distance from the iso-center. Although, agreement between dose profiles measured by detectors at CIED depth was reasonable, it was not as good as those obtained at clinical depth. A sample of these comparisons was illustrated in figure 28.

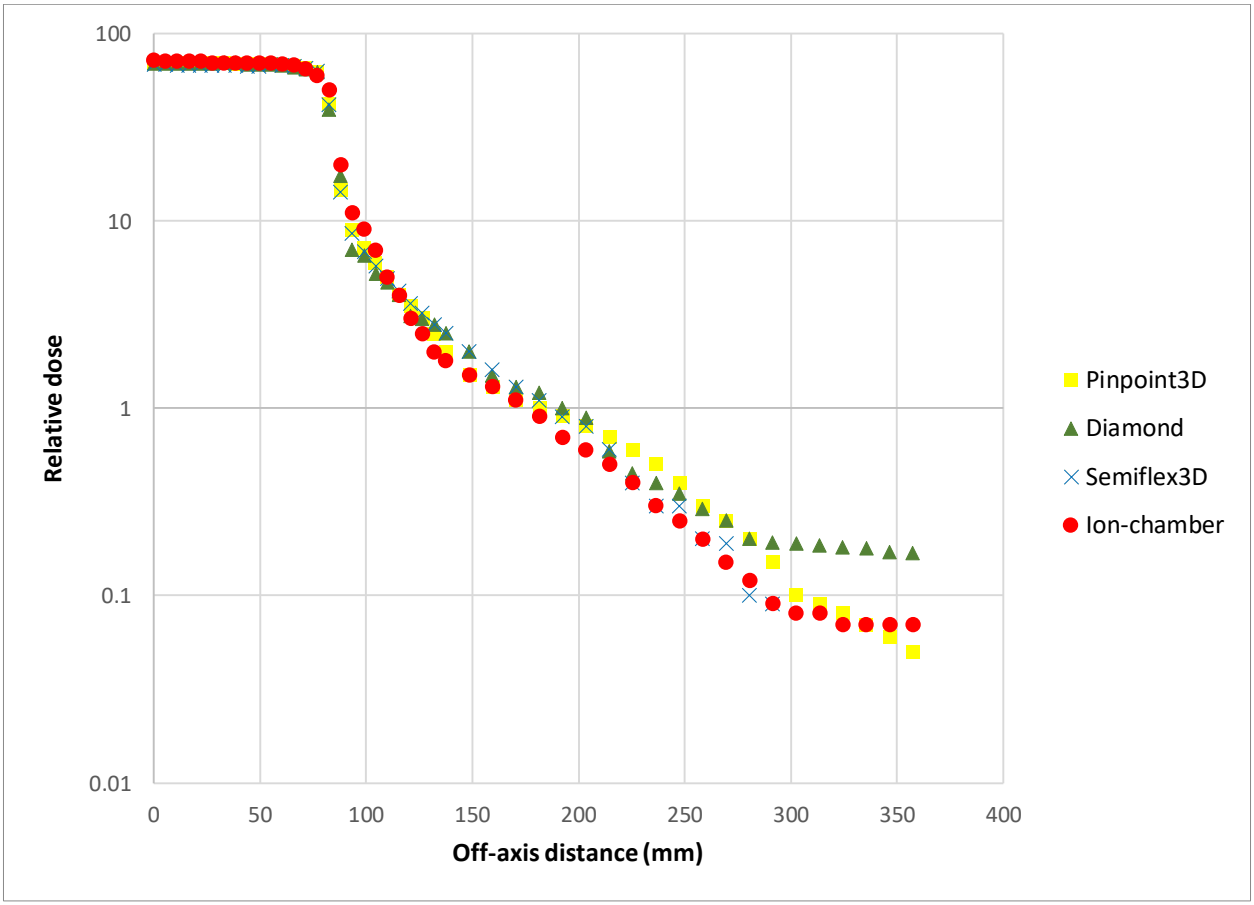

Figure 28: The in-beam dose profiles at 10 cm and 6MV measured by the diamond detector, a Pinoint, semiflex 3D, and Ion chamber

Figure 29 shows an example of the experiment reproducibility through measurements of dose profiles at least three times.

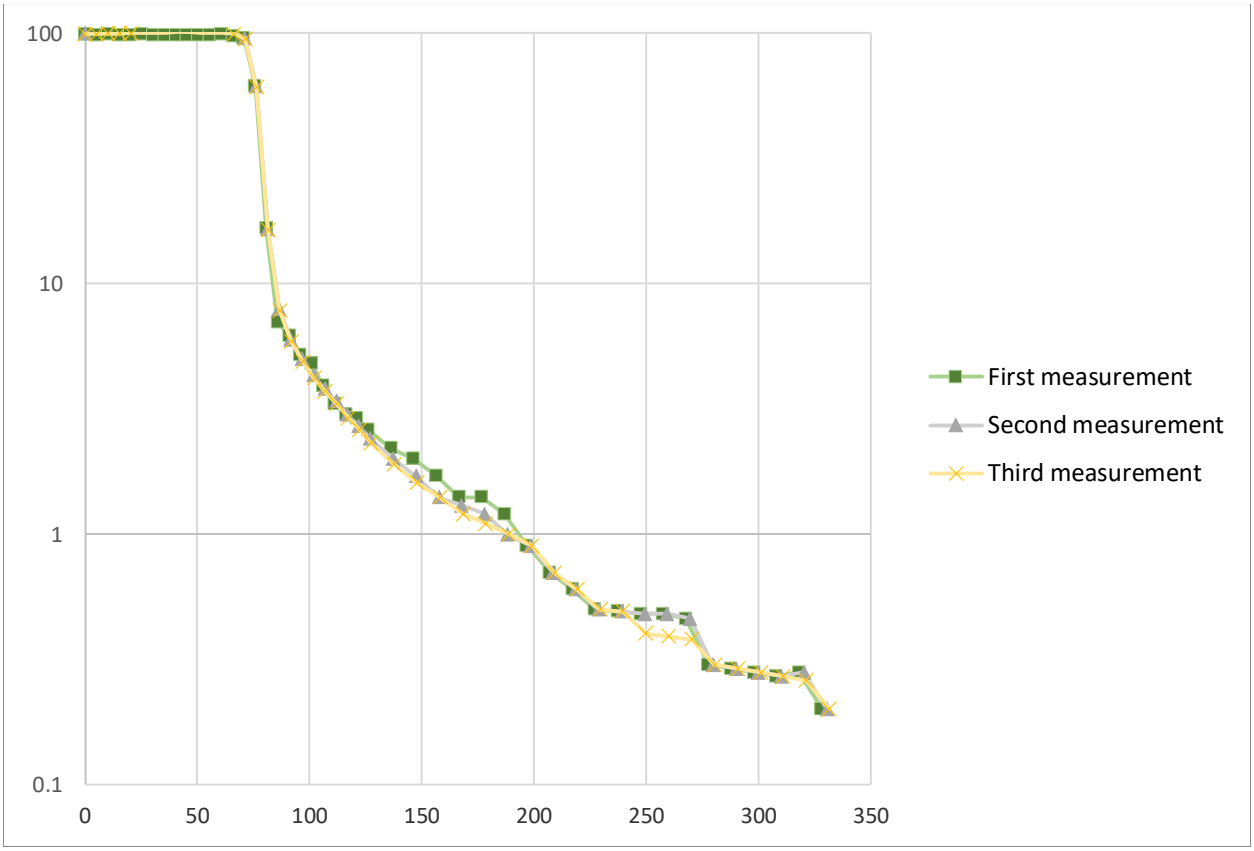

Figure 29: Comparison of three independent measurements of the in-beam dose profiles CIED depth cm and 6MV

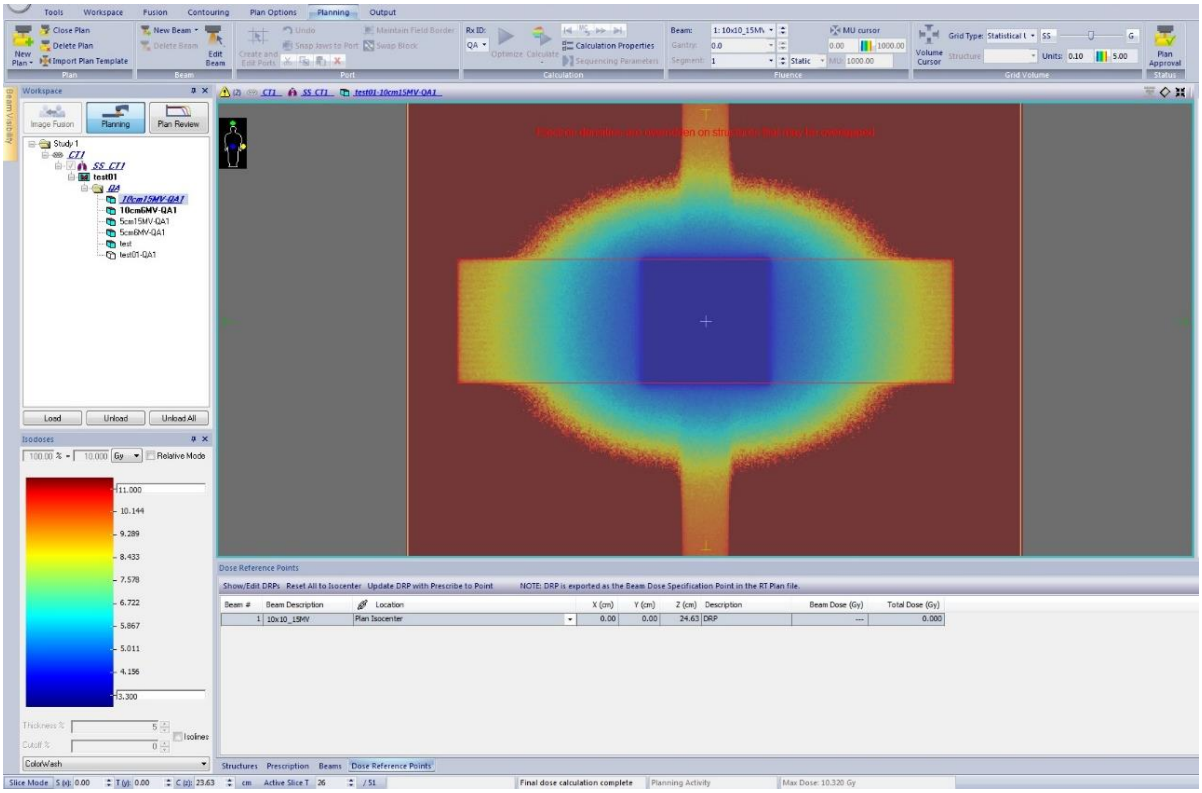

Figure 30: statistical uncertainty at depth of 10 cm for a 10x10 cm^2 field of 15 MV photons.

Figure 30 depicts statistical uncertainties calculated by MONACO for out-of-field doses. As expected, the uncertainty increases by increasing the distance from the field edge. The uncertainties at CIED depth is larger than uncertainties obtained at depth of 10 cm.

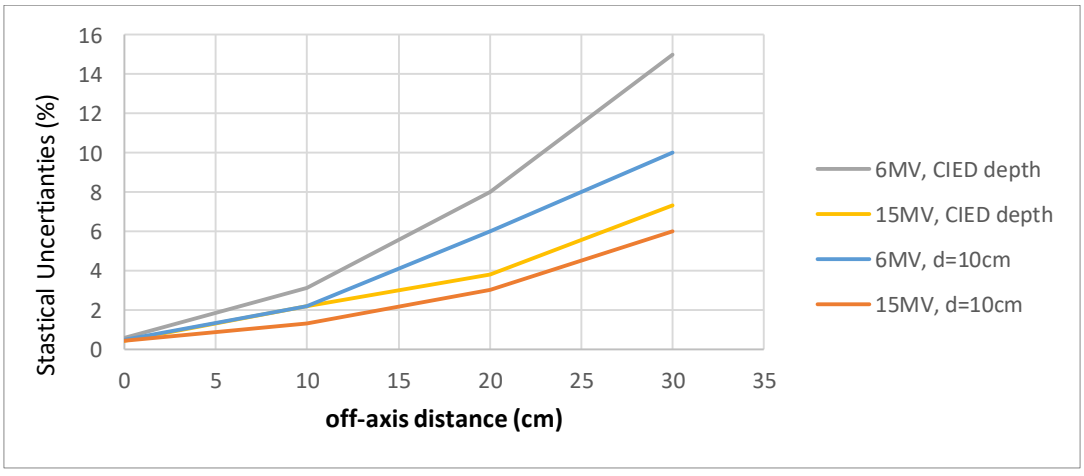

Figure 31: statistical uncertainty of dose calculated by Monaco treatment planning system

A comparison of in-beam profiles calculated by MCNPX, and the TPS and the corresponding beam profiles measured by diamond at a water depth of 10 cm were shown in Fig. 32 to 35.

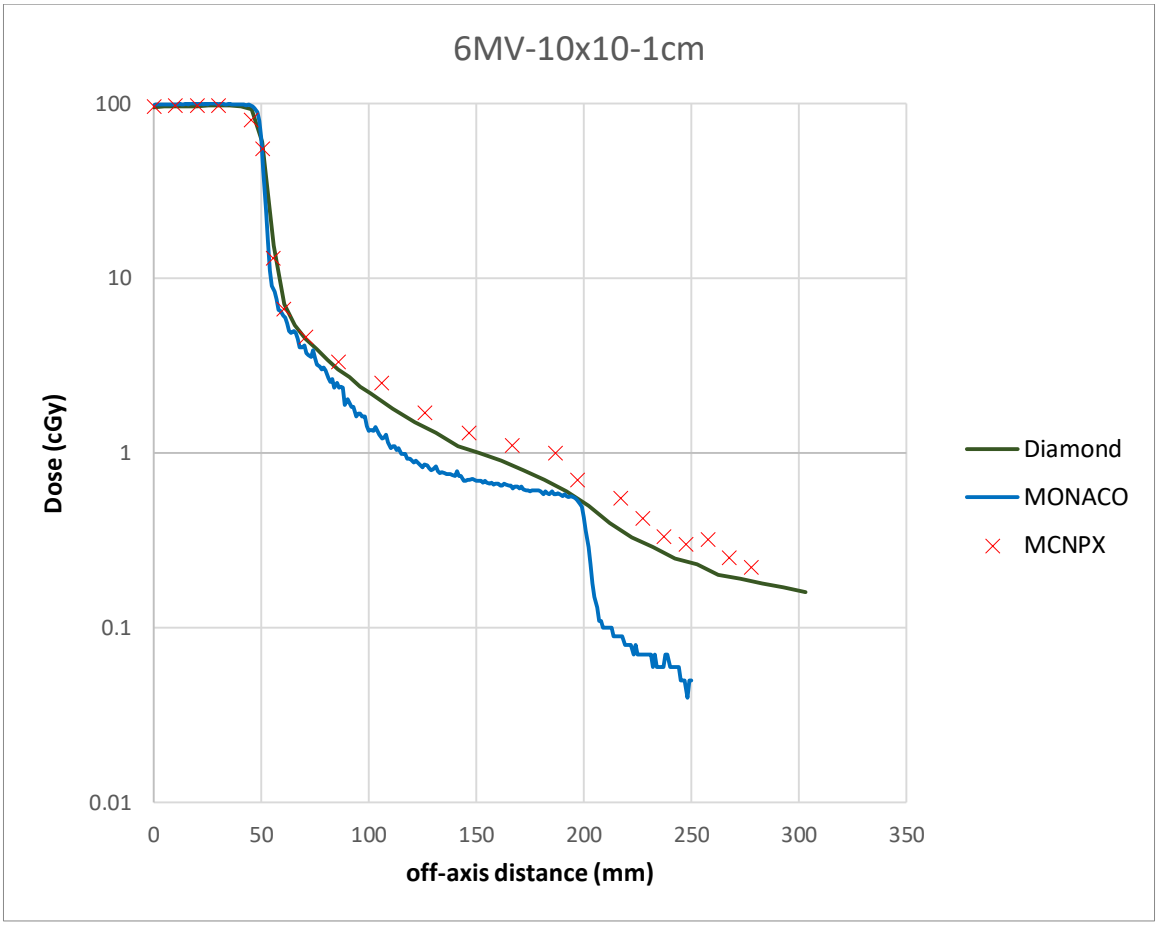

Figure 32: Comaparison of calculated and measured (in-line) dose profile for 10x10 cm^2 field size of 6MV at CIED depth

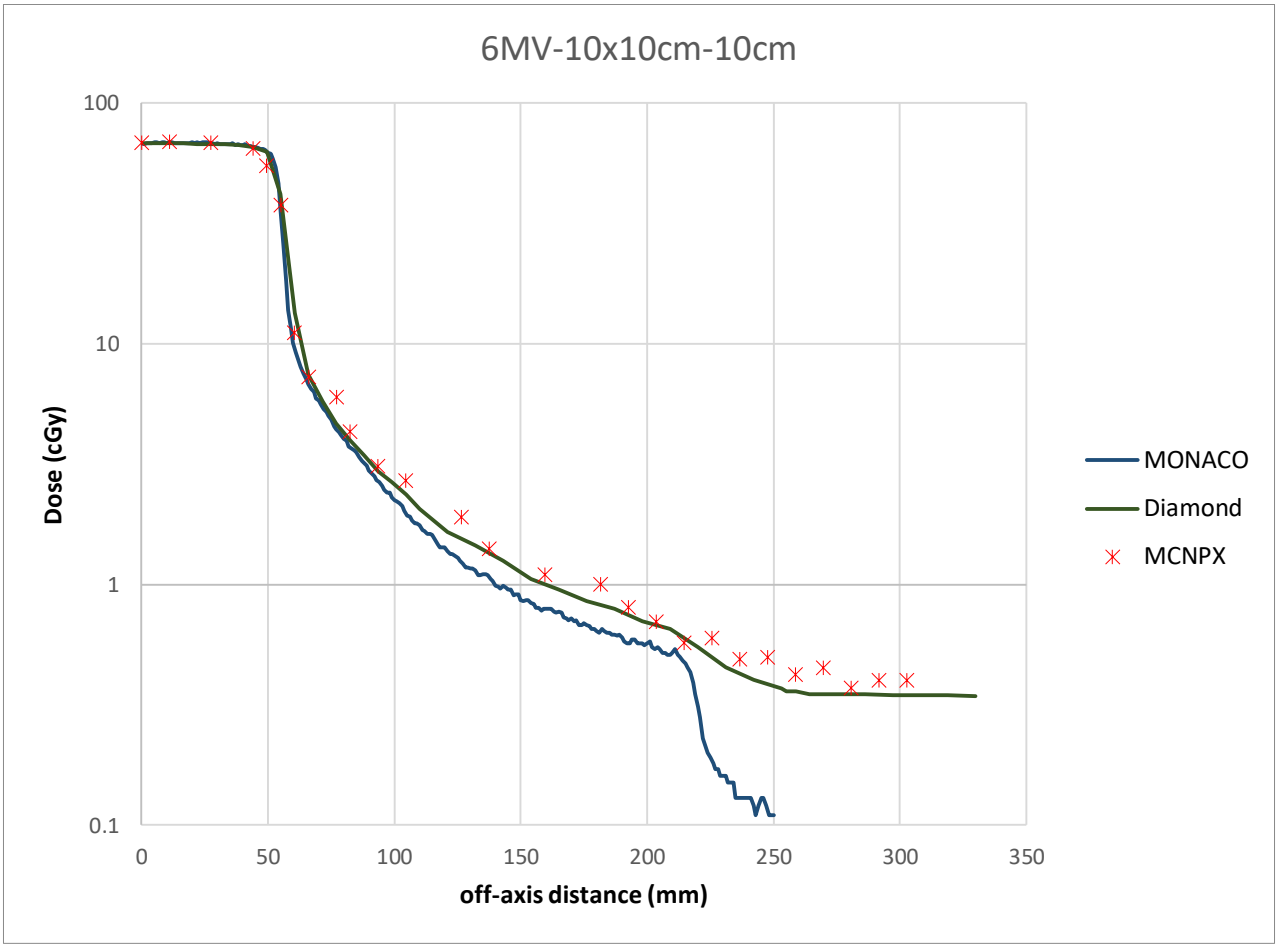

Figure 33: Comaparison of calculated and measured (in-line) dose profile for 10x10 cm^2 field size of 6MV at depth of 10cm

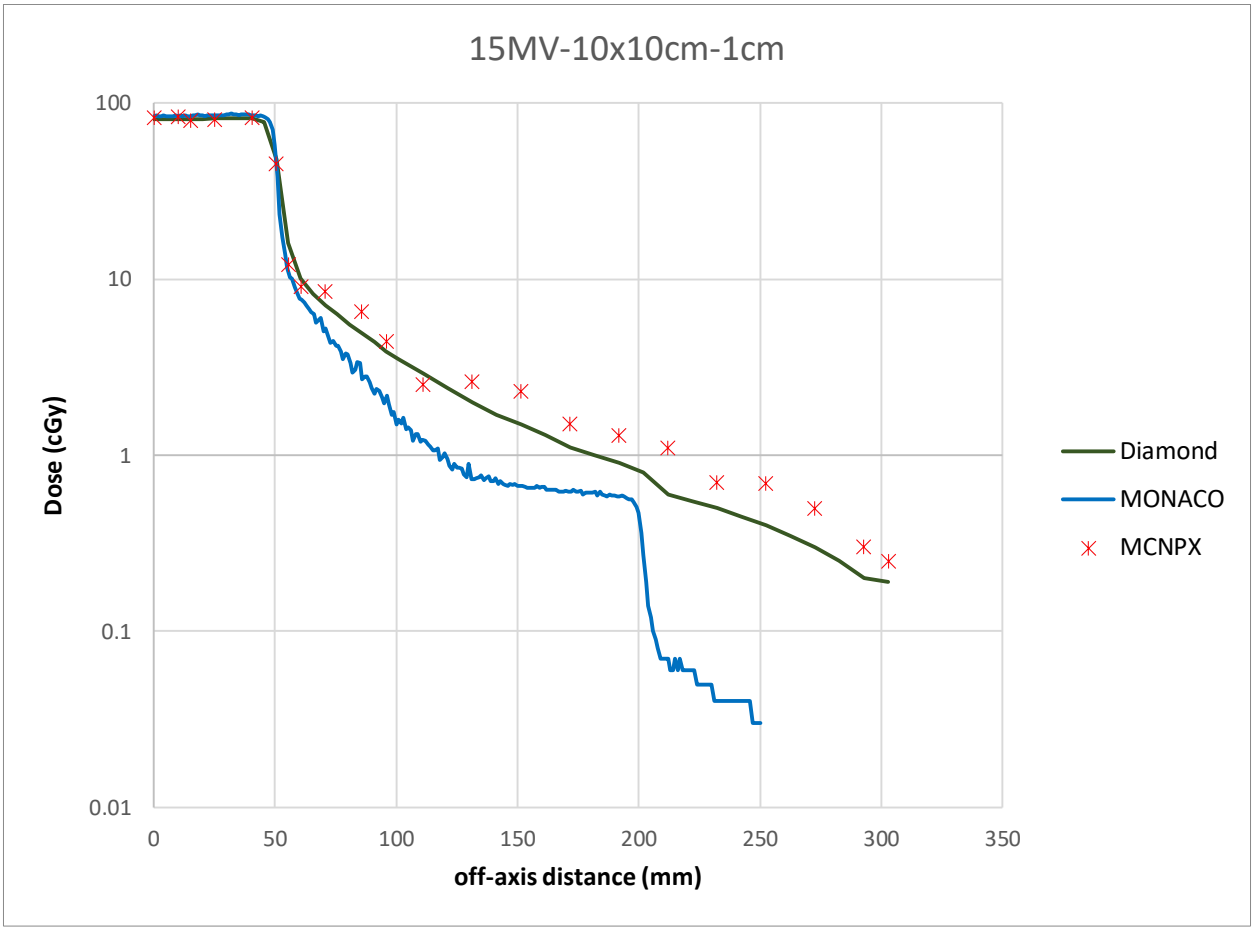

Figure 34: Comaparison of calculated and measured (in-line) dose profile for 10x10 cm^2 size of 15MV at depth of 10cm

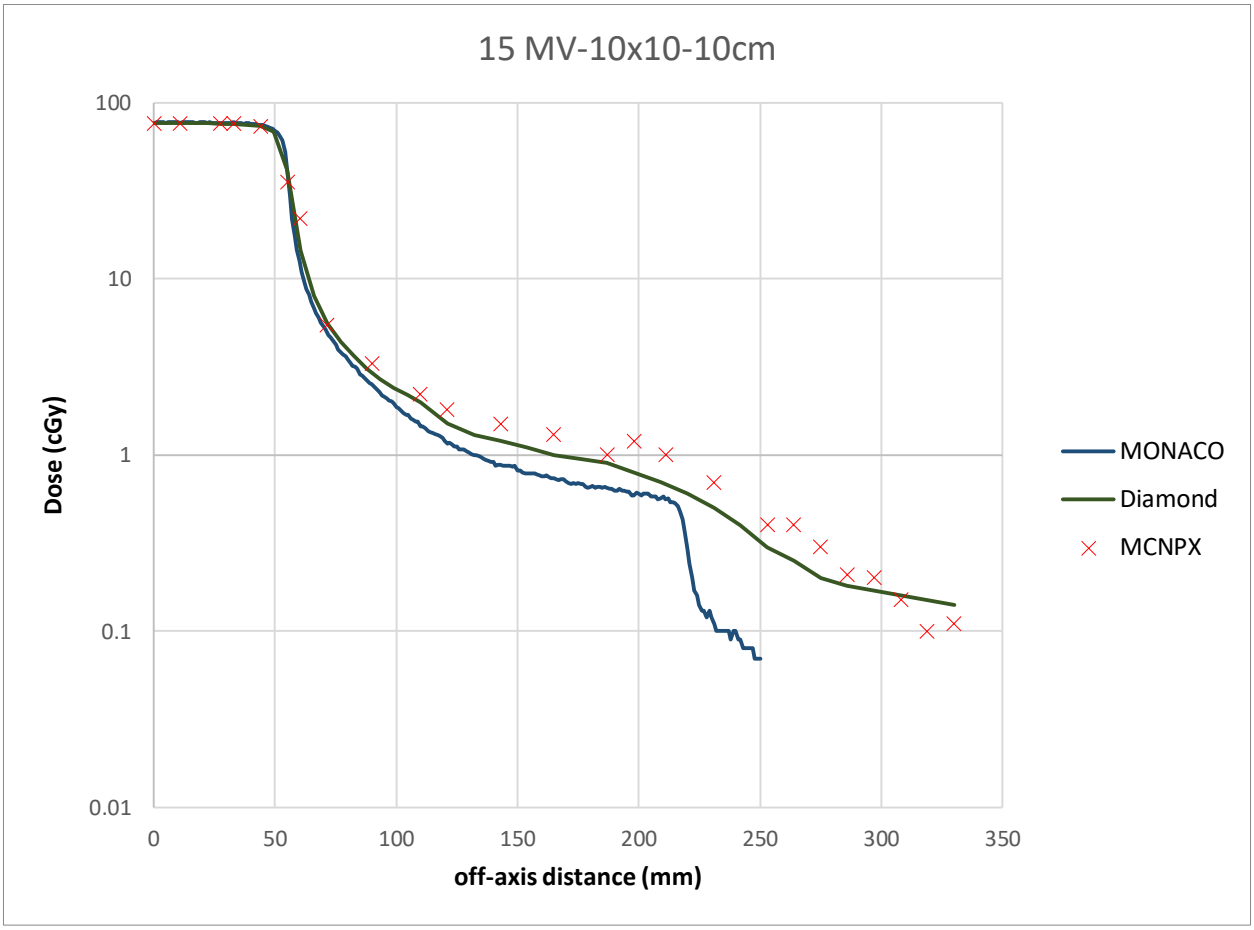

Figure 35: Comaparison of calculated and measured (in-line) dose profile for 10x10 cm² size of 15MV at depth of 10cm

The total neutron fluence and equivalent dose measured with the bubble dosiemters at CIED and clinical depth for a 10x10 cm² field of 15 MV photons were given in table 17.

Table 18: The neutron equivalent dose and fluences measured by bubble dosimeters

Depth	Off-axis distance	Equivalent dose mSV/Gy	$\emptyset(n/\boldsymbol{cm^2/MU})$
1cm	0	4.93	1.6E+04
	15	1.68	5.6E+03
	30	1.59	5.3E+03
10cm	0	0.27	9.1E+02
	15	0.11	3.5E+02
	30	0.08	2.99E+02

Finally, figure 36 shows neutron fluences calculated by MCNPX at CIED depth and depth of 10 cm for a 10x10 cm^2 field of 15 MV photons.

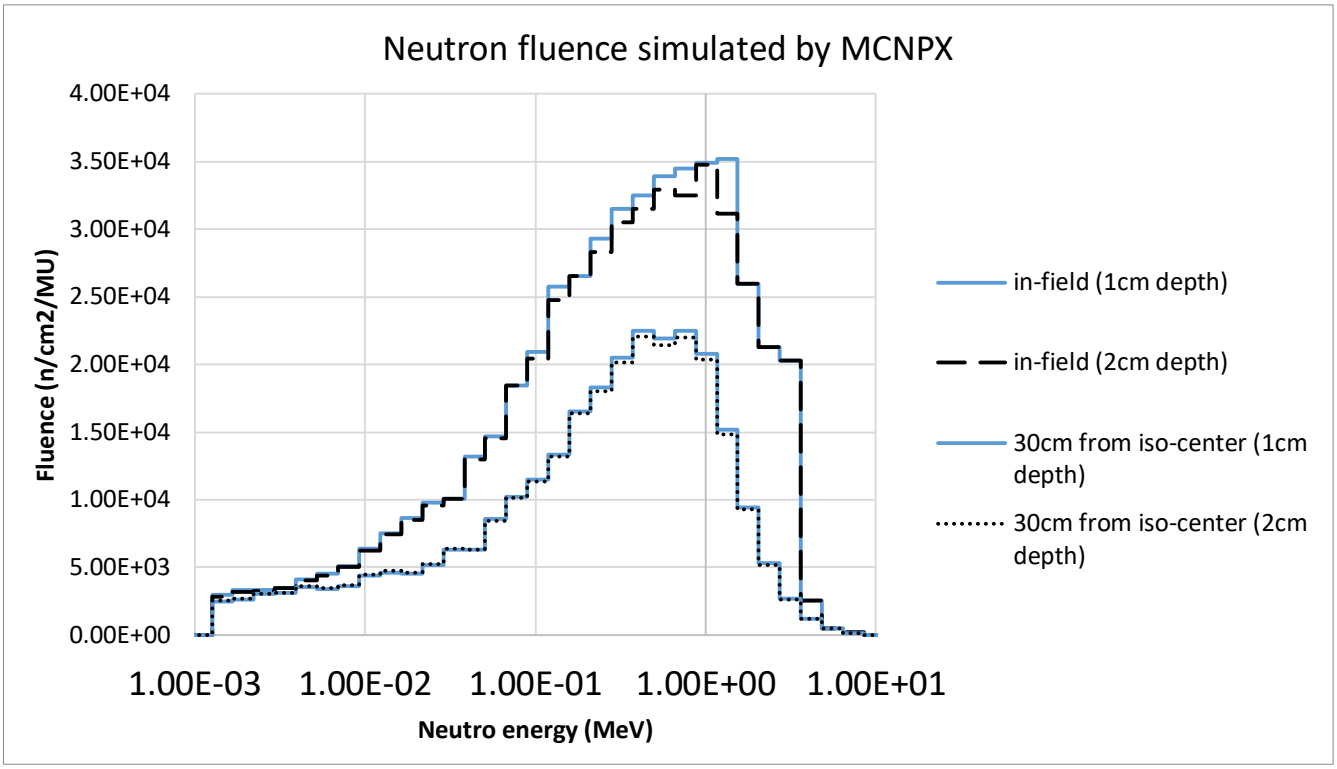

Figure 36: Calculated neutron fluences for or 10x10 cm2 field of 15 MV at CIED depth and depth of 10cm

2.4 Discussion and conclusion

The MC model of an Elekta Synergy was developed and benchmarked against measurement. The main goal was to investigate the accuracy of the out-of-field dose calculation in MONACO treatment planning system as a MC-based TPS.
Fig 28, indicates that there are slightly differences between the results obtained by the dosimeters, but the discrepancy was not more than 5% for the distance less than 20 cm from the field edge.

In general, for the measurements at 10 cm, there was a good agreement between the MC results and the measurements. however, this number was increased at 1 cm.

Figures 32 to 35, represent comparisons between all results obtained from the dosimeters as well as MCNPX with the results calculated by MONACO for 6 MV and 15 MV at 10 cm and 1 cm. It is seen that MONACO has a good accuracy for out-field-doses. According to the results, dose calculation discrepancy is in areas greater than 20 cm from the field edge where discrepancy

between the measurements and MCNPX with MONACO exceeding 35%. Although, this number is a bit more for the results at 1cm where the depth is less than dmax.

In this study, the out-of-field dose calculation accuracy of voxelized Monte Carlo (XVMC) algorithm used in MONACO (Version 5.0.1) was compared by a complete head MC-simulation of Eleketa Synergy. According to the results, although there was a very good agreement between results calculated by voxelized Monte Carlo (XVMC) algorithm and the results from MCNPX and detectors for out-of-field doses in general, it is seen that (XVMC) algorithm start to underestimate doses in the out-of-field areas greater than 20 cm from the field edge. This level of accuracy is very good, because some TPSs exhibit dose calculation inaccuracies in the out-of-field region exceeding 50–55% [30, 31], even in areas greater than 11.25 cm from the field edge.

Analyzing dose profiles in deep was not within scope of this study. However, some points should be noted based on the results. Based on the results, there were small differences among in-line beam profiles and cross-line beam profiles. This is due to the fact that usually profiles and out-of-field doses are directional dependence [140]. The results showed that discrepancy in the out-of-field doses at depth of CIED was not negligible compared to those obtained by clinical depth. This also discussed in a study by Kaderka et al [140], due to depth dependency of profiles.

As it is expected, for high energy photon of 15MV and at CIED depth, both neutron fluence and neutron equivalent doses decrease with increasing distance from the filed edge. According to ezzati et al [46,47], the probability of damage to a CIED from neutrons is related to the neutron equivalent dose rather than fluence. Our results showed that neutron equivalent dose reached a maximum in a depth between 1-2 cm where CIED is usually implanted.
As with other studies, our study has limitations to consider. One of the biggest limitation of this study was that it only focused on the statistic field. However, investigation of out-of-field doses for modulated fields would be of great value in order to compare the results in the clinical cases which can be addressed in future studies.

Reference

[1] Helland JR, Mond HG, Muff D. Lead Connection Systems and Standards for Cardiac Implantable Electronic Devices. Clinical Cardiac Pacing, Defibrillation and Resynchronization Therapy 2017:270–80. doi:10.1016/B978-0-323-37804-8.00009-2.

[2] Mond HG, Karpawich PP, editors. Pacing Options in the Adult Patient with Congenital Heart Disease. Malden, Massachusetts, USA: Blackwell Publishing; 2007. doi:10.1002/9780470750940.

[3] Campbell J. Campbell's physiology notes. Lorimer; 2009.

[4] Heart Information Center: Texas Heart Institute n.d. https://www.texasheart.org/heart-health/heart-information-center/topics/heart-anatomy/ (accessed October 1, 2019).

[5] Barold SS, Stroobandt RX, Sinnaeve AF, editors. Cardiac Pacemakers Step by Step. Malden, Massachusetts, USA: Blackwell Publishing, Inc.; 2004. doi:10.1002/9780470750728.

[6] Stroobandt RX, Barold SS, Sinnaeve AF. Implantable Cardioverter-Defibrillators Step by Step. Oxford, UK: Wiley-Blackwell; 2009. doi:10.1002/9781444303377.

[7] Silbernagl S, Despopoulos A, O'Sullivan G, Gay R, Rothenburger A. Color atlas of physiology. n.d.

[8] Khanna VK. Cardiac Pacemakers. Implantable Medical Electronics, Cham: Springer International Publishing; 2016, p. 267–92. doi:10.1007/978-3-319-25448-7_14.

[9] Khanna VK. Implantable Cardioverter Defibrillators. Implantable Medical Electronics, Cham: Springer International Publishing; 2016, p. 293–307. doi:10.1007/978-3-319-25448-7_15.

[10] BERNSTEIN AD, DAUBERT J-C, FLETCHER RD, HAYES DL, LUDERITZ B, REYNOLDS DW, et al. The Revised NASPE/BPEG Generic Code for Antibradycardia, Adaptive-Rate, and Multisite Pacing. Pacing and Clinical Electrophysiology 2002;25:260–4. doi:10.1046/j.1460-9592.2002.00260.x.

[11] MOND HG, FREITAG G. The Cardiac Implantable Electronic Device Power Source: Evolution and Revolution. Pacing and Clinical Electrophysiology 2014;37:1728–45. doi:10.1111/pace.12526.

[12] MOND HG, HELLAND JR, FISCHER A. The Evolution of the Cardiac Implantable Electronic Device Connector. Pacing and Clinical Electrophysiology 2013;36:1434–46. doi:10.1111/pace.12211.

[13] world health organization: Cardiovascular diseases (CVDs) n.d. https://www.who.int/news-room/fact-sheets/detail/cardiovascular-diseases-(cvds) (accessed October 1, 2019).

[14] Mond HG, Crozier I. The Australian and New Zealand Cardiac Implantable Electronic Device Survey: Calendar Year 2017. Heart, Lung and Circulation 2019;28:560–6.

doi:10.1016/J.HLC.2018.11.018.

[15] Raatikainen MJP, Arnar DO, Zeppenfeld K, Merino JL, Levya F, Hindriks G, et al. Statistics on the use of cardiac electronic devices and electrophysiological procedures in the European Society of Cardiology countries: 2014 report from the European Heart Rhythm Association. Europace 2015;17:i1–75. doi:10.1093/europace/euu300.

[16] Stella BM, Alessandro Z. ICD Implantation Practice Within Europe: How To Explain The Differences Beyond Economy? Journal of Atrial Fibrillation 2015;8:1262. doi:10.4022/jafib.1262.

[17] Bray F, Soerjomataram I. The Changing Global Burden of Cancer: Transitions in Human Development and Implications for Cancer Prevention and Control. The International Bank for Reconstruction and Development / The World Bank; 2015. doi:10.1596/978-1-4648-0349-9_CH2.

[18] Baskar R, Lee KA, Yeo R, Yeoh K-W. Cancer and Radiation Therapy: Current Advances and Future Directions. International Journal of Medical Sciences 2012;9:193. doi:10.7150/IJMS.3635.

[19] Stefanelli CB, Bradley DJ, Leroy S, Dick M, Serwer GA, Fischbach PS. Implantable cardioverter defibrillator therapy for life-threatening arrhythmias in young patients. Journal of Interventional Cardiac Electrophysiology : An International Journal of Arrhythmias and Pacing 2002;6:235–44.

[20] Aslian H, Kron T, Longo F, Rad R, Severgnini M. A review and analysis of stereotactic body radiotherapy and radiosurgery of patients with cardiac implantable electronic devices. Australasian Physical & Engineering Sciences in Medicine 2019;42:415–25. doi:10.1007/s13246-019-00751-8.

[21] Marbach JR, Sontag MR, Van Dyk J, Wolbarst AB. Management of radiation oncology patients with implanted cardiac pacemakers: Report of AAPM Task Group No. 34. Medical Physics 1994;21:85–90. doi:10.1118/1.597259.

[22] Hurkmans CW, Knegjens JL, Oei BS, Maas AJ, Uiterwaal G, van der Borden AJ, et al. Management of radiation oncology patients with a pacemaker or ICD: A new comprehensive practical guideline in The Netherlands. Radiation Oncology 2012;7:198. doi:10.1186/1748-717X-7-198.

[23] Gauter-Fleckenstein B, Israel CW, Dorenkamp M, Dunst J, Roser M, Schimpf R, et al. DEGRO/DGK guideline for radiotherapy in patients with cardiac implantable electronic devices. Strahlentherapie Und Onkologie 2015;191:393–404. doi:10.1007/s00066-015-0817-3.

[24] Zecchin M, Severgnini M, Fiorentino A, Malavasi VL, Menegotti L, Alongi F, et al. Management of patients with cardiac implantable electronic devices (CIED) undergoing radiotherapy. International Journal of Cardiology 2018;255:175–83.

doi:10.1016/j.ijcard.2017.12.061.

[25] Management of patients with cardiac implantable electronic devices during radiotherapy | eviQ n.d. https://www.eviq.org.au/clinical-resources/radiation-oncology/430-management-of-patients-with-cardiac-implantabl (accessed October 9, 2019).

[26] Zaremba T, Jakobsen AR, Søgaard M, Thøgersen AM, Riahi S. Radiotherapy in patients with pacemakers and implantable cardioverter defibrillators: a literature review. Europace 2016;18:479–91. doi:10.1093/europace/euv135.

[27] Hudson F, Coulshed D, D'Souza E, Baker C. Effect of radiation therapy on the latest generation of pacemakers and implantable cardioverter defibrillators: A systematic review. Journal of Medical Imaging and Radiation Oncology 2010;54:53–61. doi:10.1111/j.1754-9485.2010.02138.x.

[28] Zecchin M, Morea G, Severgnini M, Sergi E, Baratto Roldan A, Bianco E, et al. Malfunction of cardiac devices after radiotherapy without direct exposure to ionizing radiation: mechanisms and experimental data. Europace 2016;18:288–93. doi:10.1093/europace/euv250.

[29] Zaremba T, Jakobsen AR, Thogersen AM, Oddershede L, Riahi S. The effect of radiotherapy beam energy on modern cardiac devices: an in vitro study. Europace 2014;16:612–6. doi:10.1093/europace/eut249.

[30] Mouton J, Haug R, Bridier A, Dodinot B, Eschwege F. Influence of high-energy photon beam irradiation on pacemaker operation. Physics in Medicine and Biology 2002;47:2879–93.

[31] KAPA S, FONG L, BLACKWELL CR, HERMAN MG, SCHOMBERG PJ, HAYES DL. Effects of Scatter Radiation on ICD and CRT Function. Pacing and Clinical Electrophysiology 2008;31:727–32. doi:10.1111/j.1540-8159.2008.01077.x.

[32] Hurkmans CW, Scheepers E, Springorum BGF, Uiterwaal H. Influence of radiotherapy on the latest generation of pacemakers. Radiotherapy and Oncology 2005;76:93–8. doi:10.1016/J.RADONC.2005.06.011.

[33] Hashii H, Hashimoto T, Okawa A, Shida K, Isobe T, Hanmura M, et al. Comparison of the Effects of High-Energy Photon Beam Irradiation (10 and 18 MV) on 2 Types of Implantable Cardioverter-Defibrillators. International Journal of Radiation Oncology*Biology*Physics 2013;85:840–5. doi:10.1016/j.ijrobp.2012.05.043.

[34] Ferrara T, Baiotto B, Malinverni G, Caria N, Garibaldi E, Barboni G, et al. Irradiation of Pacemakers and Cardio-Defibrillators in Patients Submitted to Radiotherapy: A Clinical Experience. Tumori Journal 2010;96:76–83. doi:10.1177/030089161009600113.

[35] Gelblum DY, Amols H. Implanted Cardiac Defibrillator Care in Radiation Oncology Patient Population. International Journal of Radiation Oncology*Biology*Physics 2009;73:1525–31. doi:10.1016/j.ijrobp.2008.06.1903.

[36] Ferrara T, Baiotto B, Malinverni G, Caria N, Garibaldi E, Barboni G, et al. Irradiation of

pacemakers and cardio-defibrillators in patients submitted to radiotherapy: a clinical experience. Tumori n.d.;96:76–83.

[37] Gomez DR, Poenisch F, Pinnix CC, Sheu T, Chang JY, Memon N, et al. Malfunctions of Implantable Cardiac Devices in Patients Receiving Proton Beam Therapy: Incidence and Predictors. International Journal of Radiation Oncology*Biology*Physics 2013;87:570–5. doi:10.1016/j.ijrobp.2013.07.010.

[38] Makkar A, Prisciandaro J, Agarwal S, Lusk M, Horwood L, Moran J, et al. Effect of radiation therapy on permanent pacemaker and implantable cardioverter-defibrillator function. Heart Rhythm 2012;9:1964–8. doi:10.1016/j.hrthm.2012.08.018.

[39] Karnik AA, Helm RH, Chatterjee SB, Monahan KM. Abdominal implantable cardioverter-defibrillator placement in a patient requiring bilateral chest radiation therapy. HeartRhythm Case Reports 2016;2:395–8. doi:10.1016/j.hrcr.2016.04.009.

[40] Munshi A, Wadasadawala T, Kumar Sharma P, Sharma D, Budrukkar A, Jalali R, et al. Radiation therapy planning of a breast cancer patient with in situ pacemaker–challenges and lessons. Acta Oncologica 2008;47:255–60. doi:10.1080/02841860701678779.

[41] Elders J, Kunze-Busch M, Jan Smeenk R, Smeets JLRM. High incidence of implantable cardioverter defibrillator malfunctions during radiation therapy: neutrons as a probable cause of soft errors. EP Europace 2013;15:60–5. doi:10.1093/europace/eus197.

[42] GAROFALO R, EDE E, DORN S, KUTTLER S. Effect of Electronic Apex Locators on Cardiac Pacemaker Function. Journal of Endodontics 2002;28:831–3. doi:10.1097/00004770-200212000-00009.

[43] IRNICH W. Intracardiac Electrograms and Sensing Test Signals: Electrophysiological, Physical, and Technical Considerations. Pacing and Clinical Electrophysiology 1985;8:870–88. doi:10.1111/j.1540-8159.1985.tb05907.x.

[44] Chew K-M, Lau D. Pacemaker: Narrow pulses generation for design and sensitivity test. 2017 IEEE International Symposium on Medical Measurements and Applications (MeMeA), IEEE; 2017, p. 7–10. doi:10.1109/MeMeA.2017.7985840.

[45] Williams MR, Atkinson DB, Bezzerides VJ, Yuki K, Franklin K, Casta A, et al. Pausing With the Gauze. Anesthesia & Analgesia 2016;123:1143–8. doi:10.1213/ANE.0000000000001599.

[46] Ezzati AO, Studenski MT. Design of a neutron applicator to reduce damage in cardiac implantable electronic devices. The European Physical Journal Plus 2019;134:406. doi:10.1140/epjp/i2019-12851-3.

[47] Ezzati AO, Studenski MT. Neutron damage induced in cardiovascular implantable electronic devices from a clinical 18 MV photon beam: A Monte Carlo study. Medical Physics 2017;44:5660–6. doi:10.1002/mp.12581.

[48] Studenski MT, Xiao Y, Harrison AS. Measuring pacemaker dose: A clinical perspective.

Medical Dosimetry 2012;37:170–4. doi:10.1016/j.meddos.2011.06.007.

[49] Peet SC, Wilks R, Kairn T, Crowe SB. Measuring dose from radiotherapy treatments in the vicinity of a cardiac pacemaker. Physica Medica 2016;32:1529–36. doi:10.1016/j.ejmp.2016.11.010.

[50] Zaremba T, JAKOBSEN AR, SØGAARD M, THØGERSEN AM, JOHANSEN MB, MADSEN LB, et al. Risk of Device Malfunction in Cancer Patients with Implantable Cardiac Device Undergoing Radiotherapy: A Population-Based Cohort Study. Pacing and Clinical Electrophysiology 2015;38:343–56. doi:10.1111/pace.12572.

[51] Riley B, Garcia J, Guerrero T. The utilization of a 3-dimensional noncoplanar treatment plan to avoid pacemaker complications. Medical Dosimetry 2004;29:92–6. doi:10.1016/j.meddos.2004.03.013.

[52] Taylor ML, Kron T, Franich RD. A contemporary review of stereotactic radiotherapy: Inherent dosimetric complexities and the potential for detriment. Acta Oncologica 2011;50:483–508. doi:10.3109/0284186X.2010.551665.

[53] Brown JM, Brenner DJ, Carlson DJ. Dose Escalation, Not “New Biology,” Can Account for the Efficacy of Stereotactic Body Radiation Therapy With Non-Small Cell Lung Cancer. International Journal of Radiation Oncology*Biology*Physics 2013;85:1159–60. doi:10.1016/j.ijrobp.2012.11.003.

[54] Grant JD, Jensen GL, Tang C, Pollard JM, Kry SF, Krishnan S, et al. Radiotherapy-Induced Malfunction in Contemporary Cardiovascular Implantable Electronic Devices. JAMA Oncology 2015;1:624. doi:10.1001/jamaoncol.2015.1787.

[55] Scobioala S, Ernst I, Moustakis C, Haverkamp U, Martens S, Eich HT. A case of radiotherapy for an advanced bronchial carcinoma patient with implanted cardiac rhythm machines as well as heart assist device. Radiation Oncology 2015;10:78. doi:10.1186/s13014-015-0378-8.

[56] SOEJIMA T, YODEN E, NISHIMURA Y, ONO S, YOSHIDA A, FUKUDA H, et al. Radiation Therapy in Patients with Implanted Cardiac Pacemakers and Implantable Cardioverter Defibrillators: A Prospective Survey in Japan. Journal of Radiation Research 2011;52:516–21. doi:10.1269/jrr.10143.

[57] Corinna Bianchi Livia, Possanzini Marco, Brait Lorenzo, Bergantin Achille, Brambilla Alberto, Locatelli Maria Cristina FL. CyberKnife stereotactic radiotherapy in the treatment of patients with cardiac pacemaker/defibrillator n.d. http://therss.org/document/docdownload.aspx?docid=379.

[58] Riva G, Alessandro O, Spoto R, Ferrari A, Garibaldi C, Cattani F, et al. Radiotherapy in patients with cardiac implantable electronic devices: clinical and dosimetric aspects. Medical Oncology 2018;35:73. doi:10.1007/s12032-018-1126-3.

[59] Cakmak N, Yılmaz H, Sayar N, Erer B. [CyberKnife can cause inappropriate shock]. Turk

Kardiyoloji Dernegi Arsivi : Turk Kardiyoloji Derneginin Yayin Organidir 2012;40:714–8.

[60] Prisciandaro JI, Makkar A, Fox CJ, Hayman JA, Horwood L, Pelosi F, et al. Dosimetric review of cardiac implantable electronic device patients receiving radiotherapy. Journal of Applied Clinical Medical Physics 2015;16:254–63. doi:10.1120/jacmp.v16i1.5189.

[61] Ahmed I, Zou W, Jabbour SK. High dose radiotherapy to automated implantable cardioverter-defibrillator: a case report and review of the literature. Case Reports in Oncological Medicine 2014;2014:989857. doi:10.1155/2014/989857.

[62] Chow J C.L, Jiang R. Dosimetry of Pacemaker in VMAT for Lung SBRT. IFMBE Proceedings 2015;51:483–6. doi:10.1007/978-3-319-19387-8.

[63] Westover KD, Seco J, Adams JA, Lanuti M, Choi NC, Engelsman M, et al. Proton SBRT for Medically Inoperable Stage I NSCLC. Journal of Thoracic Oncology 2012;7:1021–5. doi:10.1097/JTO.0b013e31824de0bf.

[64] Ueyama T, Arimura T, Ogino T, Kondo N, Higashi R, Nakamura F, et al. Pacemaker malfunction associated with proton beam therapy: a report of two cases and review of literature-does field-to-generator distance matter? Oxford Medical Case Reports 2016;2016:omw049. doi:10.1093/omcr/omw049.

[65] Berlach DM, Beliveau-Nadeau D, Roberge D. Robotic radiosurgery and the “fingers of death.” Cureus 2011. doi:10.7759/cureus.33.

[66] Kry SF, Bednarz B, Howell RM, Dauer L, Followill D, Klein E, et al. AAPM TG 158: Measurement and calculation of doses outside the treated volume from external-beam radiation therapy. Medical Physics 2017;44:e391–429. doi:10.1002/mp.12462.

[67] Covington EL, Ritter TA, Moran JM, Owrangi AM, Prisciandaro JI. Technical Report: Evaluation of peripheral dose for flattening filter free photon beams. Medical Physics 2016;43:4789–96. doi:10.1118/1.4958963.

[68] Xiao Y, Kry SF, Popple R, Yorke E, Papanikolaou N, Stathakis S, et al. Flattening filter-free accelerators: a report from the AAPM Therapy Emerging Technology Assessment Work Group. Journal of Applied Clinical Medical Physics 2015;16:12–29. doi:10.1120/jacmp.v16i3.5219.

[69] Rieber J, Tonndorf-Martini E, Schramm O, Rhein B, König L, Adeberg S, et al. Establishing stereotactic body radiotherapy with flattening filter free techniques in the treatment of pulmonary lesions - initial experiences from a single institution. Radiation Oncology 2016;11:80. doi:10.1186/s13014-016-0648-0.

[70] Rodriguez F, Filimonov A, Henning A, Coughlin C, Greenberg M. Radiation-induced effects in multiprogrammable pacemakers and implantable defibrillators. Pacing and Clinical Electrophysiology : PACE 1991;14:2143–53.

[71] Gauter-Fleckenstein B, Tülümen E, Jahnke L, Nguyen J, Wenz F. Investigation of Mechanisms of Radiation-Induced CIED Failures With Flattening Filter-Free-VMAT.

International Journal of Radiation Oncology*Biology*Physics 2017;99:E661. doi:10.1016/j.ijrobp.2017.06.2196.

[72] Indik JH, Gimbel JR, Abe H, Alkmim-Teixeira R, Birgersdotter-Green U, Clarke GD, et al. 2017 HRS expert consensus statement on magnetic resonance imaging and radiation exposure in patients with cardiovascular implantable electronic devices. Heart Rhythm 2017;14:e97–153. doi:10.1016/j.hrthm.2017.04.025.

[73] Menten MJ, Wetscherek A, Fast MF. MRI-guided lung SBRT: Present and future developments. Physica Medica 2017;44:139–49. doi:10.1016/j.ejmp.2017.02.003.

[74] Crossley GH, Poole JE, Rozner MA, Asirvatham SJ, Cheng A, Chung MK, et al. The Heart Rhythm Society (HRS)/American Society of Anesthesiologists (ASA) Expert Consensus Statement on the Perioperative Management of Patients with Implantable Defibrillators, Pacemakers and Arrhythmia Monitors: Facilities and Patient Management. Heart Rhythm 2011;8:1114–54. doi:10.1016/j.hrthm.2010.12.023.

[75] Astaraki M, Severgnini M, Milan V, Schiattarella A, Ciriello F, de Denaro M, et al. Evaluation of localized region-based segmentation algorithms for CT-based delineation of organs at risk in radiotherapy. Physics and Imaging in Radiation Oncology 2018;5:52–7. doi:10.1016/j.phro.2018.02.003.

[76] Gupta T, Narayan CA. Image-guided radiation therapy: Physician's perspectives. Journal of Medical Physics, vol. 37, 2012, p. 174–82. doi:10.4103/0971-6203.103602.

[77] Bernier J, Hall EJ, Giaccia A. Radiation oncology: A century of achievements. Nature Reviews Cancer 2004;4:737–47. doi:10.1038/nrc1451.

[78] Aslian H, Delana A, Kaiser SR, Moretti E, Foti C, Bregant P, et al. A multicenter dosimetry study to evaluate the imaging dose from Elekta XVI and Varian OBI kV-CBCT systems to cardiovascular implantable electronic devices (CIEDs). Physica Medica 2018;55:40–6. doi:10.1016/J.EJMP.2018.10.013.

[79] Goyal S, Kataria T. Image Guidance in Radiation Therapy: Techniques and Applications. Radiology Research and Practice 2014;2014:1–10. doi:10.1155/2014/705604.

[80] Kawahara D, Ozawa S, Nakashima T, Suzuki T, Tsuneda M, Tanaka S, et al. Absorbed dose and image quality of Varian TrueBeam CBCT compared with OBI CBCT. Physica Medica 2016;32:1628–33. doi:10.1016/j.ejmp.2016.11.118.

[81] Alaei P, Spezi E. Imaging dose from cone beam computed tomography in radiation therapy. Physica Medica 2015;31:647–58. doi:10.1016/j.ejmp.2015.06.003.

[82] Tomic N, Devic S, Deblois F, Seuntjens J. Reference radiochromic film dosimetry in kilovoltage photon beams during CBCT image acquisition. Medical Physics 2010;37:1083–92. doi:10.1118/1.3302140.

[83] Amer A, Marchant T, Sykes J, Czajka J, Moore C. Imaging doses from the Elekta Synergy X-ray cone beam CT system. British Journal of Radiology 2007;80:476–82.

doi:10.1259/bjr/80446730.

[84] Islam MK, Purdie TG, Norrlinger BD, Alasti H, Moseley DJ, Sharpe MB, et al. Patient dose from kilovoltage cone beam computed tomography imaging in radiation therapy. Medical Physics 2006;33:1573–82. doi:10.1118/1.2198169.

[85] Osei EK, Schaly B, Fleck A, Charland P, Barnett R. Dose assessment from an online kilovoltage imaging system in radiation therapy. Journal of Radiological Protection 2009;29:37–50. doi:10.1088/0952-4746/29/1/002.

[86] Kan MWK, Leung LHT, Wong W, Lam N. Radiation Dose From Cone Beam Computed Tomography for Image-Guided Radiation Therapy. International Journal of Radiation Oncology Biology Physics 2008;70:272–9. doi:10.1016/j.ijrobp.2007.08.062.

[87] Zhang Y, Wu H, Chen Z, Knisely JPS, Nath R, Feng Z, et al. Concomitant Imaging Dose and Cancer Risk in Image Guided Thoracic Radiation Therapy Presented in part at the 56th Annual Meeting of the American Society for Radiation Oncology, San Francisco, CA, Sept 14-17, 2014. International Journal of Radiation Oncology Biology Physics 2015;93:523–31. doi:10.1016/j.ijrobp.2015.06.034.

[88] Winey B, Zygmanski P, Lyatskaya Y. Evaluation of radiation dose delivered by cone beam CT and tomosynthesis employed for setup of external breast irradiation. Medical Physics 2009;36:164–73. doi:10.1118/1.3036113.

[89] Hu N, McLean D. Measurement of radiotherapy CBCT dose in a phantom using different methods. Australasian Physical and Engineering Sciences in Medicine 2014;37:779–89. doi:10.1007/s13246-014-0301-x.

[90] Legge K, Greer PB, Keall PJ, Booth JT, Arumugam S, Moodie T, et al. Technical note: TROG 15.01 SPARK trial multi-institutional imaging dose measurement. Journal of Applied Clinical Medical Physics 2017;18:358–63. doi:10.1002/acm2.12151.

[91] Zecchin M, Severgnini M, Fiorentino A, Malavasi VL, Menegotti L, Alongi F, et al. Management of patients with cardiac implantable electronic devices (CIED) undergoing radiotherapy. A consensus document from Associazione Italiana Aritmologia e Cardiostimolazione (AIAC), Associazione Italiana Radioterapia Oncologica (AIRO), Associazione . International Journal of Cardiology 2018. doi:10.1016/j.ijcard.2017.12.061.

[92] Wolbarst AB. Management of radiation oncology patients with implanted cardiac pacemakers: Report of AAPM Task Group No. 34. Medical Physics 1994;21:85–90. doi:10.1118/1.597259.

[93] Wronski M, Pang G. TH-A-214-11: Dose to Implantable Cardiac Devices from Cone Beam CT. Medical Physics 2011;38:3844–5. doi:10.1118/1.3613476.

[94] Ming X, Feng Y, Chen Z, Zhang Y, Nath R, Deng J. Monte Carlo Estimation of Dose to the Cardiac Implantable Electronic Devices From a kVCBCT System Used in Image Guided Radiation Therapy. International Journal of Radiation Oncology*Biology*Physics

2013;87:S152. doi:10.1016/j.ijrobp.2013.06.393.

[95] Aslian H, Severgnini M, Bregant P LF. Imaging dose to cardiovascular implantable electronic devices (CIEDs) from the Elekta synergy X-ray cone beam CT system: a dosimetric study using gafchromic film XR-QA2. Australasian Physical & Engineering Sciences in Medicine 2018;41:268. doi:10.1007/s13246-017-0614-7.

[96] Shrimpton PC, Wall BF, Fisher ES. The tissue-equivalence of the Alderson Rando anthropomorphic phantom for X-rays of diagnostic qualities. Physics in Medicine and Biology 1981;26:133–9. doi:10.1088/0031-9155/26/1/013.

[97] White DR, Booz J, Griffith R V., Spokas JJ, Wilson IJ. Report 44. Journal of the International Commission on Radiation Units and Measurements 1989;os23:NP-NP. doi:10.1093/jicru/os23.1.Report44.

[98] DeWerd LA, Kissick M, editors. The Phantoms of Medical and Health Physics. New York, NY: Springer New York; 2014. doi:10.1007/978-1-4614-8304-5.

[99] Yan H, Guo F, Zhu D, Stryker S, Trumpore S, Roberts K, et al. On the use of bolus for pacemaker dose measurement and reduction in radiation therapy. Journal of Applied Clinical Medical Physics 2017:1–7. doi:10.1002/acm2.12229.

[100] Giaddui T, Cui Y, Galvin J, Yu Y, Xiao Y. Comparative dose evaluations between XVI and OBI cone beam CT systems using Gafchromic XRQA2 film and nanoDot optical stimulated luminescence dosimeters. Medical Physics 2013;40. doi:10.1118/1.4803466.

[101] Soares CG. Radiochromic film dosimetry. Radiation Measurements Med Phys 2007;41:100–2093. doi:10.1016/j.radmeas.2007.01.007.

[102] Menegotti L, Delana A. Radiochromic film dosimetry with flatbed scanners : A fast and accurate method for dose calibration and uniformity correction with single 2008:3078–85. doi:10.1118/1.2936334.

[103] Brady SL, Kaufman RA. Establishing a standard calibration methodology for MOSFET detectors in computed tomography dosimetry. Medical Physics 2012;39:3031–40. doi:10.1118/1.4712221.

[104] Devic S, Tomic N, Lewis D. Reference radiochromic film dosimetry: Review of technical aspects. Physica Medica 2016;32:541–56. doi:10.1016/j.ejmp.2016.02.008.

[105] Devic S. Radiochromic film dosimetry: Past, present, and future. Physica Medica 2011;27:122–34. doi:10.1016/j.ejmp.2010.10.001.

[106] Aldelaijan S, Alzorkany F, Moftah B, Buzurovic I, Seuntjens J, Tomic N, et al. Use of a control film piece in radiochromic film dosimetry. Physica Medica 2016;32:202–7. doi:10.1016/j.ejmp.2015.12.004.

[107] Bourgouin A, Varfalvy N, Archambault L. Estimating and reducing dose received by cardiac devices for patients undergoing radiotherapy. Journal of Applied Clinical Medical Physics 2015;16:411–22. doi:10.1120/jacmp.v16i6.5317.

[108] Sykes JR, Amer A, Czajka J, Moore CJ. A feasibility study for image guided radiotherapy using low dose, high speed, cone beam X-ray volumetric imaging. Radiotherapy and Oncology 2005;77:45–52. doi:10.1016/J.RADONC.2005.05.005.

[109] Ding GX, Munro P, Pawlowski J, Malcolm A, Coffey CW. Reducing radiation exposure to patients from kV-CBCT imaging. Radiotherapy and Oncology 2010;97:585–92. doi:10.1016/j.radonc.2010.08.005.

[110] Roxby P, Kron T, Foroudi F, Haworth A, Fox C, Mullen A, et al. Simple methods to reduce patient dose in a Varian cone beam CT system for delivery verification in pelvic radiotherapy. British Journal of Radiology 2009;82:855–9. doi:10.1259/bjr/37579222.

[111] Solberg TD, Siddon RL, Kavanagh B. Historical Development of Stereotactic Ablative Radiotherapy, 2012, p. 9–35. doi:10.1007/174_2012_540.

[112] Nagata Y. Introduction and History of Stereotactic Body Radiation Therapy (SBRT). Stereotactic Body Radiation Therapy, Tokyo: Springer Japan; 2015, p. 3–8. doi:10.1007/978-4-431-54883-6_1.

[113] Siva S, Bressel M, Murphy DG, Shaw M, Chander S, Violet J, et al. Stereotactic Abative Body Radiotherapy (SABR) for Oligometastatic Prostate Cancer: A Prospective Clinical Trial. European Urology 2018;74:455–62. doi:10.1016/j.eururo.2018.06.004.

[114] Siva S, Pham D, Kron T, Bressel M, Lam J, Tan TH, et al. Stereotactic ablative body radiotherapy for inoperable primary kidney cancer: a prospective clinical trial. BJU International 2017;120:623–30. doi:10.1111/bju.13811.

[115] Sohail MR, Eby EL, Ryan MP, Gunnarsson C, Wright LA, Greenspon AJ. Incidence, Treatment Intensity, and Incremental Annual Expenditures for Patients Experiencing a Cardiac Implantable Electronic Device Infection. Circulation: Arrhythmia and Electrophysiology 2016;9. doi:10.1161/CIRCEP.116.003929.

[116] Schoormans D, Pedersen SS, Dalton S, Rottmann N, van de Poll-Franse L. Cardiovascular co-morbidity in cancer patients: the role of psychological distress. Cardio-Oncology 2016;2:9. doi:10.1186/s40959-016-0019-x.

[117] Biasi G, Petasecca M, Guatelli S, Hardcastle N, Carolan M, Perevertaylo V, et al. A novel high-resolution 2D silicon array detector for small field dosimetry with FFF photon beams. Physica Medica 2018;45:117–26. doi:10.1016/j.ejmp.2017.12.010.

[118] Nakano H, Minami K, Yagi M, Imaizumi H, Otani Y, Inoue S, et al. Radiobiological effects of flattening filter-free photon beams on A549 non-small-cell lung cancer cells. Journal of Radiation Research 2018;59:442–5. doi:10.1093/jrr/rry041.

[119] Augustynek M, Korpas D, Penhaker M, Cvek J, Binarova A. Monitoring of CRT-D devices during radiation therapy in vitro. BioMedical Engineering OnLine 2016;15:29. doi:10.1186/S12938-016-0144-7.

[120] Siva S, Kron T, Bressel M, Haas M, Mai T, Vinod S, et al. A randomised phase II trial of

Stereotactic Ablative Fractionated radiotherapy versus Radiosurgery for Oligometastatic Neoplasia to the lung (TROG 13.01 SAFRON II). BMC Cancer 2016;16:183. doi:10.1186/S12885-016-2227-Z.

[121] Coolens C, Childs PJ. Calibration of CT Hounsfield units for radiotherapy treatment planning of patients with metallic hip prostheses: the use of the extended CT-scale. Physics in Medicine and Biology 2003;48:1591–603.

[122] Gertsch M. Pacemaker ECG. The ECG, Berlin, Heidelberg: Springer Berlin Heidelberg; 2004, p. 505–23. doi:10.1007/978-3-662-10315-9_29.

[123] Aslian H, Severgnini M, Cupardo F, Vidimari R, De Denaro M. EP-1562: VMAT pre-treatment verification using Octavius 4D system: from simple to more complex plans. Radiotherapy and Oncology 2016;119:S724–5. doi:10.1016/s0167-8140(16)32812-2.

[124] Aslian H, Sadeghi M, Mahdavi SR, Babapour Mofrad F, Astarakee M, Khaledi N, et al. Magnetic resonance imaging-based target volume delineation in radiation therapy treatment planning for brain tumors using localized region-based active contour. International Journal of Radiation Oncology Biology Physics 2013;87:195–201. doi:10.1016/j.ijrobp.2013.04.049.

[125] Huang JY, Followill DS, Wang XA, Kry SF. Accuracy and sources of error of out-of field dose calculations by a commercial treatment planning system for intensity-modulated radiation therapy treatments. Journal of Applied Clinical Medical Physics 2013;14:186–97. doi:10.1120/jacmp.v14i2.4139.

[126] Hurkmans CW, Knegjens JL, Oei BS, Maas AJ, Uiterwaal G, van der Borden AJ, et al. Management of radiation oncology patients with a pacemaker or ICD: A new comprehensive practical guideline in The Netherlands. Radiation Oncology 2012;7:198. doi:10.1186/1748-717X-7-198.

[127] Sikora MP. Virtual Source Modelling of Photon Beams for Monte Carlo Based Radiation Therapy Treatment Planning. 2011.

[128] Gholampourkashi S, Cygler JE, Belec J, Vujicic M, Heath E. Monte Carlo and analytic modeling of an Elekta Infinity linac with Agility MLC: Investigating the significance of accurate model parameters for small radiation fields. Journal of Applied Clinical Medical Physics 2019;20:55–67. doi:10.1002/acm2.12485.

[129] Clements M, Schupp N, Tattersall M, Brown A, Larson R. Monaco treatment planning system tools and optimization processes. Medical Dosimetry 2018;43:106–17. doi:10.1016/j.meddos.2018.02.005.

[130] Khaledi N, Dabaghi M, Sardari D, Samiei F, Ahmadabad FG, Jahanfarnia G, et al. Investigation of photoneutron production by Siemens artiste linac: A Monte Carlo Study. Radiation Physics and Chemistry 2018;153:98–103. doi:10.1016/j.radphyschem.2018.06.006.

[131] Khaledi N, Arbabi A, Sardari D, Rabie Mahdavi S, Aslian H, Dabaghi M, et al. Monte Carlo investigation of the effect of small cutouts on beam profile parameters of 12 and 14 MeV electron beams. Radiation Measurements 2013;51–52:48–54. doi:10.1016/j.radmeas.2013.01.019.

[132] Khaledi N, Aghamiri M, Aslian H, Ameri A. Tabulated square-shaped source model for linear accelerator electron beam simulation. Journal of Cancer Research and Therapeutics 2017;13:69–79. doi:10.4103/0973-1482.206235.

[133] Khaledi N, Arbabi A, Sardari D, Mohammadi M, Ameri A. Simultaneous production of mixed electron-photon beam in a medical LINAC: A feasibility study. Physica Medica 2015;31:391–7. doi:10.1016/j.ejmp.2015.02.014.

[134] Kry SF, Titt U, Followill D, Pönisch F, Vassiliev ON, White RA, et al. A Monte Carlo model for out-of-field dose calculation from high-energy photon therapy. Medical Physics 2007;34:3489–99. doi:10.1118/1.2756940.

[135] Kry SF, Titt U, Pönisch F, Followill D, Vassiliev ON, Allen White R, et al. A Monte Carlo model for calculating out-of-field dose from a Varian 6 MV beam. Medical Physics 2006;33:4405–13. doi:10.1118/1.2360013.

[136] MCNPX User's Manual, Version 2.7.0 | Request PDF n.d. https://www.researchgate.net/publication/263008961_MCNPX_User's_Manual_Version_270 (accessed November 25, 2019).

[137] Frontiers in Radiation Oncology. InTech; 2013. doi:10.5772/3065.

[138] Team MC. MCNP-A General Monte Carlo N-Particle Transport Code, Version 5 Volume I: Overview and Theory X-5 Monte Carlo Team. 2003.

[139] Zoubair M, El Bardouni T, El Gonnouni L, Boulaich Y, El Bakkari B, El Younoussi C. Application of variance reduction techniques in Monte Carlo simulation of clinical electron linear accelerator. Nuclear Instruments and Methods in Physics Research, Section A: Accelerators, Spectrometers, Detectors and Associated Equipment 2012;661:93–7. doi:10.1016/j.nima.2011.08.052.

[140] Kaderka R, Schardt D, Durante M, Berger T, Ramm U, Licher J, et al. Out-of-field dose measurements in a water phantom using different radiotherapy modalities. Physics in Medicine and Biology 2012;57:5059–74. doi:10.1088/0031-9155/57/16/5059.

[141] Alikaniotis K, Severgnini M, Giannini G, Milan V. MEASUREMENTS OF THE PARASITIC NEUTRON DOSE AT ORGANS FROM MEDICAL LINACS AT DIFFERENT ENERGIES BY USING BUBBLE DETECTORS. Radiation Protection Dosimetry 2018;180:267–72. doi:10.1093/rpd/ncx308.

Appendix: Published papers, and abstracts in journals until October 2019

6.1 The first full paper (APESM)

Australasian Physical & Engineering Sciences in Medicine
https://doi.org/10.1007/s13246-019-00751-8

REVIEW PAPER

A review and analysis of stereotactic body radiotherapy and radiosurgery of patients with cardiac implantable electronic devices

Hossein Aslian[1] · Tomas Kron[2] · Francesco Longo[1,3] · Roya Rad[4] · Mara Severgnini[5]

Received: 23 May 2018 / Accepted: 27 March 2019

Abstract
The implementation of stereotactic body radiation therapy (SBRT) and stereotactic radiosurgery (SRS) has greatly increased due to its convenience and advantages from perspectives ranging from radiobiology to radio physics. Because SBRT/SRS delivers high doses in few fractions, precise dose delivery to target volumes and sufficient sparing of adjacent organs at risk (OARs) are required. Achieving these conflicting objectives is challenging for all patients receiving SBRT/SRS and may be particularly challenging when SBRT/SRS is adopted for treating patients with cardiac implantable electronic devices (CIEDs) because cumulative doses in CIEDs must be limited. Published research considering the different aspects of stereotactic treatment in patients with CIEDs was reviewed to summarise their findings in the following sections: (I) conventional linear accelerator (linac)-based SBRT and SRS; (II) CyberKnife, Gamma-Knife, VERO and helical tomotherapy SBRT and SRS; and (III) proton therapy. A total of 65 patients who had CIEDs and underwent SRS, SBRT, or SABR treatments were identified in the reviewed studies. The functionality of the CIEDs was assessed for 58 patients. Of those, CIED malfunctions (such as data loss, mode change, and inappropriate shock) were reported in four patients (6.89%). This review highlights the available sparse information in the literature by posing questions for future research.

Keywords Stereotactic body radiotherapy (SBRT) · Stereotactic radiosurgery (SRS) · CyberKnife · Gamma-knife · Tomotherapy · Pacemaker · Implantable cardioverter defibrillator

Introduction

Stereotactic body radiotherapy (SBRT), which was more recently defined as stereotactic ablative body radiotherapy (SABR), is increasingly used in the treatment of different malignancies, including both primary and metastatic lung, liver, brain, vertebral, kidney and pancreatic tumours [1]. The increased use of SBRT is due to the possibility of achieving a highly localised dose distribution facilitated by the common use of non-coplanar beam deliveries, the explicit inclusion of motion management and the use of image guidance [2].

Although a higher dose per fraction can provide high rates of tumour control, it can increase the risk of long-term toxicity to normal tissues. Therefore, SBRT requires precise delivery of the dose to target volumes and sufficient sparing of adjacent organs at risk (OARs) [1, 2]. Achieving these conflicting objectives is challenging when planning radiotherapy for patients receiving SBRT/SRS and may be particularly challenging when SBRT/SRS is adopted for treating patients with cardiac implantable electronic devices (CIEDs).

The American Association of Physicists in Medicine (AAPM) report (TG34) was the earliest guideline published for the management of patients with CIEDs receiving general radiotherapy (RT) in 1994 [3]. Since

✉ Hossein Aslian
h-aslian@mail.com

1 Department of Physics, University of Trieste, Via Alfonso Valerio, 2, 34127 Trieste, Italy

2 Physical Sciences, Peter MacCallum Cancer Centre, Melbourne, Australia

3 Italian National Institute of Nuclear Physics (INFN), sezione di Trieste, Trieste, Italy

4 Viterbi School of Biomedical Engineering, University of Southern California, Los Angeles, CA, USA

5 Medical Physics Department, Azienda Sanitaria Universitaria Integrata di Trieste, Trieste, Italy

Published online: 04 April 2019

6.2 The second full paper (EJMP)

Physica Medica 55 (2018) 40–46

Contents lists available at ScienceDirect

Physica Medica

journal homepage: www.elsevier.com/locate/ejmp

Original paper

A multicenter dosimetry study to evaluate the imaging dose from Elekta XVI and Varian OBI kV-CBCT systems to cardiovascular implantable electronic devices (CIEDs)

Hossein Aslian[a,*], Anna Delana[b], Stefano Ren Kaiser[c], Eugenia Moretti[d], Claudio Foti[d], Paola Bregant[c], Mario de Denaro[c], Francesco Longo[a,f], Mara Severgnini[e]

[a] Department of Physics, University of Trieste, Trieste, Italy
[b] Department of Medical Physics, S. Chiara Hospital, APSS Trento, Italy
[c] Department of Medical Physics, Fondazione Poliambulanza, Istituto Ospedaliero, Brescia, Italy
[d] Department of Medical Physics, Azienda Sanitaria Universitaria Integrata di Udine, Italy
[e] Department of Medical Physics, Azienda Sanitaria Universitaria Integrata di Trieste, Trieste, Italy
[f] National Institute for Nuclear Physics (INFN), Sezione di Trieste, Trieste, Italy

ARTICLE INFO

Keywords:
Imaging dose
Cardiovascular implantable electronic devices
kV-Cone Beam CT System
Gafchromic XRQA2 film
MOSFET
TLD

ABSTRACT

The increasing use of daily CBCT in radiotherapy has raised concerns about the additional dose delivered to the patient, and it can also become a concern issue for those patients with cardiovascular implantable electronic devices (CIEDs) (Pacemaker [PM] and Implantable Cardioverter Defibrillator [ICD]). Although guidelines highly recommend that the cumulative dose received by CIEDs should be kept as low as possible, and a safe threshold based on patient risk classification needs to be respected, this additional imaging dose is not usually considered. Four centers with different dosimetry systems and different CBCT imaging protocols participated in this multicenter study to investigate the imaging dose to the CIEDs from Elekta XVI and Varian OBI kV-CBCT systems. It was found that although imaging doses received by CIEDs outside the CBCT field are negligible, special attention should be paid to this value when CIEDs are inside the field because the daily use of CBCT can sometimes contribute considerably to the total dose received by a CIED.

1. Introduction

Precise delivery of a prescribed dose to the target volume while sparing adjacent normal tissues is the ultimate goal of radiotherapy. To achieve this fundamental goal, all elements in the chain of radiotherapy process have been and are still being developed [1].

With the advent of the cone beam computed tomography (CBCT) system, radiotherapy and, more specifically, patient positioning have undergone significant changes. Because of noteworthy advantages of this system, including three-dimensional visualization of the body and enhanced visualization of soft tissue, it has become an important component of modern linear accelerator (LINAC) [2–4]. With the ever-increasing use of daily CBCT, additional imaging dose delivered to the patient has become a concern. Accordingly, there has been an increase in the number of research studies focusing on imaging dose due to CBCT in radiotherapy. Many aspects of this field have been investigated, ranging from dose measurements and calculations to cancer risk related to imaging dose [5–12]. Alaei and Spezi [3] presented a comprehensive systematic review of imaging dose associated with CBCT. The motivation behind this study was to review various methods for the measurements of imaging dose delivered by kilovoltage CBCT systems.

An updated literature review, however, showed that there is a lack of clinical and experimental data focusing on imaging dose to cardiovascular implantable electronic devices (CIEDs) from the CBCT systems. In addition, international and national guidelines for the management of patients with CIEDs receiving radiotherapy highly recommend that the cumulative dose received by CIEDs should be kept as low as possible, and a safe threshold based on patient risk classification needs to be respected [13–16]. Patients with CIEDs are usually categorized for risk on the basis of cumulative dose and pacing dependency into low (CIED dose is less than 2 Gy and the patients are not pacing dependent), medium (CIED dose is between 2 Gy and 10 Gy and the pacing-

* Corresponding author at: Via Alfonso Valerio, 2, Department of Physics, University of Trieste, 34127 Trieste, Italy.
E-mail addresses: h-aslian@mail.com (H. Aslian), anna.delana@apss.tn.it (A. Delana), stefano.renkaiser@poliambulanza.it (S.R. Kaiser), eugenia.moretti@asuiud.sanita.fvg.it (E. Moretti), claudio.foti@asuiud.sanita.fvg.it (C. Foti), paola.bregant@asuits.sanita.fvg.it (P. Bregant), mario.dedenaro@asuiud.sanita.fvg.it (M. de Denaro), francesco.longo@ts.infn.it (F. Longo), mara.severgnini@asuits.sanita.fvg.it (M. Severgnini).

https://doi.org/10.1016/j.ejmp.2018.10.013
Received 23 February 2018; Received in revised form 2 October 2018; Accepted 15 October 2018

6.3 The first published abstract in APESM

O27 In-vivo dosimetry with gafchromic EBT3 film for TBI treatments: clinical implementation and dosimetric review

S. Zawlodzka[1]

[1]Radiation Oncology Mater Centre, Brisbane, Australia. (sylwia.zawlodzka-bednarz@health.qld.gov.au [Presenting author])

Introduction Total body irradiation (TBI) was implemented in our clinic in 2014 for paediatric patients in preparation for the stem cell or bone marrow transplant. TBI treatments are planned using a dedicated TBI beam model (Pinnacle[3] TPS) and delivered using modulated arc TBI (MATBI) technique. The treatment goal is to deliver a homogenous dose 12 Gy/6fr to the entire body with ± 10% acceptable uniformity variation.
To verify dose delivered during TBI treatments an in-vivo dosimetry protocol using Gafchromic EBT3 film was implemented.
Method To facilitate the use EBT3 film for patient in-vivo dosimetry extensive testing was performed including film stability, reproducibility, dose rate and angular dependency, surface dose accuracy and film accuracy for prolonged dose delivery. In addition a departmental protocol for film preparation and analysis was developed.
Since 2014 twelve patients have been treated using the MATBI technique. For every patient in-vivo films were placed for the first fraction at eleven standard positions and additional locations as requested by the radiation oncologist. In total dose for 137 locations was measured and compared with prescribed dose and TPS dose.
Results For all patients the average percentage difference ± SD between measured and prescribed dose was − 1.3 ± 3.8% for umbilicus, 3.6 ± 7.0% for eyes, 3.4 ± 4.9% for neck, − 1.9 ± 3.3% for lumbus, − 1.8 ± 4.5% for knees and + 0.3 ± 7.9% for heels. The largest variation between measured and prescribed dose was observed for extremities (heels) where the range of percentage differences was from − 12.2% to 21.2%. However in such cases measured dose was in agreement with TPS dose.
Conclusion Gafchromic EBT3 film has been successfully implemented for patient in-vivo dosimetry during TBI treatments.

O28 Imaging dose to cardiovascular implantable electronic devices (CIEDs) from the Elekta synergy X-ray cone beam CT system: a dosimetric study using gafchromic film XR-QA2

H. Aslian[1], **M. Severgnini**[2], **P. Bregant**[2], **F. Longo**[1,3]

[1]Department of Physics, University of Trieste, Trieste, Italy. (hossein.aslian@phd.units.it [Presenting author]). [2]Medical Physics Department, Azienda Sanitaria Universitaria Integrata di Trieste, Trieste, Italy. (mara.severgnini@asuits.sanita.fvg.it), (paola.bregant@asuits.sanita.fvg.it). [3]INFN, sezione di Trieste, Trieste Italy. (francesco.longo@ts.infn.it)

Introduction Since the threshold of cumulative dose received by CIEDs (Pacemaker and Implantable Cardioverter Defibrillator) needs to be respected, the goal is to investigate the imaging dose to the CIEDs from XVI CBCT system.
Method The dosimetry system included GafChromic XR-QA2 and a Radcal ionization chamber calibrated for radiation qualities RQR 9. The film was cut into pieces and they were precisely calibrated free in air. To simulate the exact situation of the real patient an anthropomorphic phantom was used and the CIEDs were placed in the Alderson's left clavicular region. A 1-cm thick bolus was placed over the CIEDs to account for the patient's skin over the device. Different standard CBCT-imaging protocols were applied: Head & Neck, Chest and symmetry left and right in which CIEDs were inside the field and prostate and pelvis in which CIEDs were outside the field. In addition, Copper shielding was used, wherever it was necessary, for the purpose of imaging dose reduction due to its less noise affection compared to lead.
Results The measurements indicated the average imaging doses to PM and ICD ranged between the following values: (H&N-36.6 mAs: 0.004–0.03 cGy), (Chest-264 mAs: 0.345–0.386 cGy), (Symmetry-312 mAs; left: 1.61–1.77 cGy; and right: 0.86–0.911 cGy), (Pelvis-1056 mAs: 0.044–0.059 cGy), (Prostate-1689 mAs: 0.018-0-022 cGy) respectively. The dose profile along craniocaudal direction showed a large penumbra region and a dramatic decrease in imaging dose (around 66%) by increasing the distance between CIEDs and field edge. While a much less dramatic decrease along mediolateral direction was seen. Copper shielding significantly decreased CBCT dose (almost 60%) but increased the image noise especially in location of CIEDs.
Conclusion Although dose received by CIEDs outside the CBCT field imaging is low, a special attention should be paid to this value when CIEDs are inside the CBCT field since it can make a noticeable contribution to the total cumulative dose received by CIED. In that case, applying a dose reduction strategy (like shielding) might be suggested.

References
1. Giaddui T, Cui Y, Galvin J, Chen W, Yu Y, Xiao Y (2012) Characteristics of Gafchromic XRQA2 films for kV image dose measurement. Med Phys 39 (2): 842–850
2. Wronski M, Pang G (2011) Dose to Implantable Cardiac Devices from Cone Beam CT. Med Phys 38(6): 3844–3845
3. Ming X, Feng Y, Chen Z, Zhang Y, Nath R, Deng J (2013) Monte Carlo Estimation of Dose to the Cardiac Implantable Electronic Devices From a kVCBCT System Used in Image Guided Radiation Therapy. Int Jou Radiat Oncol Biolo Physic 87(2): S152

Acknowledgements The first author would like to acknowledge the financial support from University of Trieste and European Social Fund (FSE-S3/2, project code: FP1683026001) to perform this study.

O29 Impact of an in vivo dosimetry system using TLDs across a large radiotherapy department

P. Lonski[1], **R. Antony**[1], **L. Marsh**[1], **T. Kron**[1]

[1]Department of Physical Sciences, Peter MacCallum Cancer Centre, Melbourne Australia. (Peta.Lonski@petermac.org [Presenting author]), (Rachitha.Antony@petermac.org), (Linda.Marsh@petermac.org), (Tomas.Kron@petermac.org).

Introduction In vivo dosimetry is an important quality assurance tool in many radiotherapy centres. It was the aim of this work to assess the impact of a novel in vivo TLD service at the Peter MacCallum Centre, which services 4 campuses. The new in vivo service was implemented in June 2015 and includes assessment of a range of modern and complex treatment techniques.
Method High sensitivity LiF:Mg,Cu,P TLD chips were used to perform surface dose verification measurements on patients undergoing external beam radiotherapy using high energy photons, electrons, and lower energy superficial and deep therapies (S/DXRT). In vivo dosimetry is requested by radiation therapists, oncologists and occasionally initiated by physicists. A TLD system was established according to the methodology outlined in reference 1.

6.4 The second published abstract in EJMP

tion gives a general overview of the guideline including insights about this recent update.

Methods. The guideline focuses on the measurement of objective image quality parameters and radiation output from any kind of CBCT device, including applications in dental radiology, C-arms and guidance systems in radiotherapy. Indications to use commercial or non-commercial phantoms and software are given, as well as to use ionization chambers or solid state dosemeters. The new EURADOS appendix includes an extensive review of patient dose data from recent research papers, organized by application and dose indicators: CTDI, DAP, effective dose, entrance surface dose, CTDIw, absorbed dose, D1-D2 and air kerma. The DIN has reviewed the details of the standards 6868–161 and 6868–15 for acceptance and constancy tests in dental CBCT. Individual comments have helped to clarify the measurements of radiation output and the methods to measure the modulation transfer function. Some colleagues have stressed the informative value of the appendices.

Results. The comments received were reviewed by the authors of the corresponding sections and discussed by the group in virtual meetings before being published as an update. The mentioned additions are meant to keep the document alive. They respond to questions raised by physicists that are starting to use the protocol inside and outside Europe.

Conclusions. The first presentation in the ECMP in Athens was followed by international presentations at ESTRO, ECR, IOMP and IRPA and national presentations in Italy, Spain, UK, Germany and other countries. Thanks to these voluntary efforts, physicists around the world are using and improving the document together. We also welcome your participation in this session and your feedback.

https://doi.org/10.1016/j.ejmp.2018.06.248

[OA177] Contribution of the medical physicist to the italian consensus document on management of patients with cardiac implantable devices (CIED) undergoing radiotherapy and future development from aifm wotking group

Mara Severgnini[a,*], Loris Menegotti[b], Anna Delana[b], Tiziana Malatesta[c], Mariagrazia Quattrocchi[d], Hossein Aslian[e], Francesca Pietrobon[f], Stefano Andreoli[g], Federica Cattani[h], Stefano Ren kaiser[i], Moretti Eugenia[j], Claudio Foti[j], Maria Daniela Falco[k], Francesco Guerriero[l], Sonia Recanello[l], Aldo Valentini[m], Michele Stasi[n]

[a] *Azienda Sanitaria Universitaria Integrata DI Trieste, Medical Physics, Trieste, Italy*
[b] *Hospital S. Chiara, Azienda Provinciale Per I Servizi Sanitari, Trento, Italy*
[c] *Ospedale "San Giovanni Calibita" Fatebenefratelli, Medical Physics Department, Rome, Italy*
[d] *Usl Nord Ovest Toscana, Medical Physics Department, Lucca, Italy*
[e] *University of Trieste, Department of Physics, 34123, Italy*
[f] *Ospedale S.Martino, Medical Physics Department, Belluno, Italy*
[g] *Asst Papa Giovanni XXIII, Fisica Sanitaria, Bergamo, Italy*
[h] *Istituto Europeo DI Oncologia, Medical Physics Department, Milan, Italy*
[i] *Fondazione Poliambulanza – Istituto Ospedaliero, Medical Physics, Brescia, Italy*
[j] *Azienda Sanitaria Universitaria Integrata DI Udine, Medical Physics Department, Udine, Italy*
[k] *Policlinico Ss. Annunziata, Medical Physics Department, Chieti, Italy*
[l] *Azienda Ulss3 Serenissima, Medical Physics Department, Mestre Ve, Italy*
[m] *Hospital S. Chiara, Azienda Provinciale Per I Servizi Sanitari, Trento, Italy*
[n] *A.O. Ordine Mauriziano, Medical Physics Department, Turin, Italy*
* Corresponding author.

Purpose. The management of patients with CIED receiving radiotherapy (RT) is challenging and requires a structured multidisciplinary approach. In order to stratify the risk of patients and approaching RT sessions appropriately, a consensus document from Associazione Italiana Aritmologia e Cardiostimolazione (AIAC), Associazione Italiana Radioterapia Oncologica (AIRO), Associazione Italiana Fisica Medica (AIFM) has been published on the International Journal of Cardiology in 2018. Along this line, the AIFM working group is promoting specific measurements to better investigate the role of RT on CIED.

Methods. In Consensus document potential radiation interactions on CIED such as recommendations for the estimation of the dose to the device are described and a multidisciplinary review of in vivo and in vitro data is presented.

Further, a multi-center study to evaluate IGRT dose, neutron contamination assessment, and photon out-of-field dose are still being performed. To measure out-of-field dose to CIEDs two phantoms were created and sent to centers working with different treatment planning systems (TPS).

Results. Preliminary results show that the use of daily CBCT can add a considerable contribution to CIED dose up to 50 cGy like lung 4D protocol.

Neutron contamination of photon and electron beams of energies ranging from 6 to 18 MV measured with REM counters show that neutron production for 10 MV photon beam is not negligible. It confirms that neutron produced by electron beam has to be taken into account for beam energy higher than 15 MeV. Comparisons between calculated and measured out-of-filed dose along with examining the behavior of different dosimeters are being studied.

Working group is performing measurement to confirm that, in absence of out-of-field TPS commissioning, in vivo dosimetry is still recommended in the case of short distance CIED-field edge or dose close to 2 Gy.

Conclusions. A detailed approach for safe management of RT patients with CIEDs is now available with important implications for clinical practice. Only a multidisciplinary approach between medical physicists, radiation oncologists and electrophysiologists can really reduce the risk of malfunctions in patient with CIED undergoing RT. Results of the AIFM working group try to provide valuable support and further indications in this regard.

https://doi.org/10.1016/j.ejmp.2018.06.249

[I178] EANM/EARL harmonization strategies in PET quantification: From daily practice to multicentre oncological studies

Bernhard Sattler[a,*], Ronald Boellaard[b]

[a] *University Hospital Leipzig, Department of Nuclear Medicine, Leipzig, Germany*
[b] *University Medical Center Groningen, Nuclear Medicine and Molecular Imaging, Groningen, Netherlands*
* Corresponding author.

Quantitative positron emission tomography (PET-) imaging is essential for staging and tracking subtle processes like pathophysiologic change and therapy response in oncological diseases. The accuracy of PET-quantification decisively depends on the correct system calibration involving all corrections that are implicitly necessary using the full ring PET Detector setting in 3D mode. Basically, these

6.3 The third published abstract in EJMP

features robustness, for each metric and reduced activity level, relative changes from FTA image, paired Wilcoxon tests and Intraclass Correlation Coefficient (ICC) were computed taking FTA features values as the ground truth. SUVmean was computed in the lesions at each activity level and its average relative changes from FTA were considered as benchmarks for texture features stability.

Results. The choice of contouring and SUV resampling methods results in different features changes at lower activity levels from FTA. Focusing on Variable VOI and R025, at 1.5 MBq/kg, 35/55 features showed both non-statistically significant differences from FTA image (paired Wilcoxon test, p-value < 0.01) and ICC > 0.85. At lowest activities (1.5, 1.2, 0.6 MBq/kg), about half of the features changed from FTA values less than the corresponding SUVmean changes (2%, 3%, 9%) using Variable VOI-R025.

Conclusions. Specific PET texture features can be reliably extracted from low-activity images in pediatrics for tumor biologic heterogeneity characterization depending on tracer activity level, SUV resampling and lesion delineation strategies.

https://doi.org/10.1016/j.ejmp.2018.06.217

[OA146] Underestimation of 68GA PET/CT quantification caused by activity overestimation using default calibrator settings

Tom Sanderson [a,*], James Solomon [b], Chris Nottage [b], John Dickson [a]

[a] *University College London Hospital, Institute of Nuclear Medicine, London, United Kingdom*
[b] *Colchester Hospital University NHS Foundation Trust, Nuclear Medicine, Colchester, United Kingdom*
* Corresponding author.

Purpose. It is desirable to achieve accurate quantification in PET/CT imaging as routinely assessed using SUV measurement, including for Gallium-68 (^{68}Ga) labelled tracers.

A PET/CT scan of a uniformly filled ^{68}Ga phantom on a GE D710 scanner unexpectedly resulted in a low SUV_{mean} of 0.88, outside of the local tolerance of $1.0 \pm 5\%$. A possible cause of underestimation of quantification is inaccuracy of the activity measurement of ^{68}Ga in the dose calibrator associated with the PET/CT scanner.

Methods. A source of ^{68}Ga (maximum activity of 599 MBq in 4ml in a P6 vial) was measured in 5 Capintec CRC-55t calibrators (including that used with the D710 PET/CT scanner) using the default ^{68}Ga pre-set calibrator factor of 416. The source was then measured in an externally located Fidelis secondary standard calibrator. Based upon the results, manual adjustments were made to the Capintec factors to match the decay corrected Fidelis measurement. A repeat PET/CT scan of a uniformly filled ^{68}Ga phantom was then performed.

Results. The cross-calibration results showed that the 5 Capintec calibrators systematically overestimated the activity measurement by 8–9% compared to the Fidelis when using the default factor of 416. The factors were adjusted to 457–463 to match the decay corrected Fidelis measurement.

After adjustment of factors, a repeat uniform phantom scan resulted in a SUV_{mean} of 0.97, within the local tolerance.

Conclusions. Underestimation of PET/CT quantification of ^{68}Ga was caused by overestimation of ^{68}Ga activity measurement using the pre-set dose calibrator factor settings on a Capintec CRC-55t. Improvement in quantification accuracy was achieved by adjusting the calibrator factor based upon an external cross-calibration. Similar results have been recently reported by a group in Australia [1].

We recommend SUV checks using a uniform phantom and regular calibrator cross-calibration exercises for all isotopes used clinically or in clinical trials for quantitative PET/CT imaging.

References

[1] Bailey et al., Accuracy of dose calibrators for gallium-68 pet imaging: unexpected findings in a multi-centre clinical pre-trial assessment, J Nucl Med, 2018, 10.2967/jnumed.117.202861.

https://doi.org/10.1016/j.ejmp.2018.06.218

[I147] New approaches in radiotherapy: Spatial fractionation of the dose

Yolanda Prezado *

Centre National de la Recherche Scientifique, Imagerie et Modelisation Pour la Neurobiologie et la Cancerologie, New Approaches in Radiotherapy, Orsay, France
* Corresponding author.

Cancer is responsible for one out of four deaths in Europe. *Radiotherapy (RT)* has a key role in cancer treatment. In fact, about half of the patients will receive RT at some point during their illness. The therapeutic use of ionizing radiation has been largely guided by the goal of directly eliminating all cancer cells while minimizing the toxicity to adjacent tissues. Nowadays, technological advances in radiation delivery, including image guidance and particle therapy (i.e. proton therapy), have notably improved tumor dose conformation, thus reducing the dose to the organs-at-risk. Despite remarkable advancements, the dose tolerances of normal tissues continue to be the main limitation in RT and still compromise the treatment of some radioresistant tumors, tumors close to a sensitive structure (e.g. central nervous system (CNS)) and pediatric cancer. Therefore, why not to change the strategy? Why not make use of the evolving wealth of biological knowledge to seek for new approaches that might substantially increase the normal tissue resistance? One possible way to overcome this limitation is to employ new modes of radiation dose deposition that activate biological processes different from those in standard radiotherapy. An example is the spatial fractionation of the dose. This lecture will give a general overview about this strategy. Different studies on the challenging dosimetry of the very small (submillimetric) field sizes used will be presented. Some of the promising results obtained in the pre-clinical studies will be shown: a very significant increase in tolerance doses (doses of up to 100 Gy in a single fraction) and the remission of extremely aggressive tumors, such as gliomas, even with a very heterogeneous dose coverage, are observed. The biological mechanisms, which are not completely known, seem to contradict the classic RT paradigms. Its exploration offers a whole new horizon of both scientific research and potential future clinical practice. The spatial fractionation of the dose could especially benefit paediatric oncology (central nervous system), whose treatments are limited to the high risk of complications in the development of the infants.

https://doi.org/10.1016/j.ejmp.2018.06.219

[OA148] A multi-center dosimetry study to evaluate imaging dose from Elekta XVI and varian OBI KV-CONE beam CT systems to cardiovascular implantable electronic devices (CIEDS)

Hossein Aslian [a,*], Anna Delana [b], Stefano Ren kaiser [c], Eugenia Moretti [d], Claudio Foti [d], Paola Bregant [e], Mario De Denaro [e], Francesco Longo [f], Mara Severgnini [e]

[a] *University of Trieste, Physics, Trieste, Italy*
[b] *Hospital S. Chiara, Azienda Provinciale Per I Servizi Sanitari, Trento, Italy*

[c] Fondazione Poliambulanza – Istituto Ospedaliero, Medical Physics, Brescia, Italy
[d] Azienda Sanitaria Universitaria Integrata DI Udine, Medical Physics, Udine, Italy
[e] Azienda Sanitaria Universitaria Integrata DI Trieste, Medical Physics, Trieste, Italy
[f] University of Trieste, INFN, Sezione DI Trieste, Trieste Italy, Physics, Trieste, Italy
* Corresponding author.

Purpose. By increasing the use of daily CBCT, additional delivered imaging dose to the patient became a matter of concern. This can also raise concerns about patients with CIEDs since accumulated dose to these devices highly needs to be limited. The aim of this study is to investigate the imaging dose to the CIEDs from Elekta XVI and Varian OBI kV-CBCT systems performed by a multi-institutional study.

Methods. Four geographically separated centers with different CBCT imaging systems and three different dosimetric measurement methods including Gafchromic films, metal-oxide-semiconductor field-effect transistor (MOSFET) and thermoluminescence dosimeters (TLDs) participated in this multi-center study. At each center an anthropomorphic phantom (Alderson RANDO phantom) was used and the CIED was placed in the alderson's left clavicular region using the same setup. The dosimeter was fixed on top of the device over which a 1-cm thick bolus was used to simulate patient's skin. Different standard CBCT-imaging protocols which are commonly used in clinical practice of each center were applied namely, Head&Neck (HN), Chest, Thorax, Symmetry, Prostate and Pelvis.

Results. The maximum values of imaging doses were found once CIEDs were inside the CBCT field. They were between the following values: HNS20 (XVI):2.57 mGy/100 mAs, Thorax (OBI):2.92 mGy/100 mAs, ChestM15-left (XVI): 1.52 mGy/100 mAs, Symmetry-left (XVI): 5.67 mGy/100 mAs. However, they received much lower dose once the CIEDs were not inside the field.

Conclusion. This study shows that although imaging doses received by CIEDs outside the CBCT field is negligible, a special attention should be paid to this value when CIEDs are inside the CBCT field because daily use of CBCT can make a considerable contribution to the total dose received by CIED. Based on the obtained results, it is possible that in some protocol like symmetry total imaging dose to CIED in a 30-fraction reach as high as 50 cGy. Therefore in such cases, this additional imaging dose should not be ignored when classifying CIED patients into risk groups.

https://doi.org/10.1016/j.ejmp.2018.06.220

[OA149] Influence of treatment couch in the secondary MU calculation for VMAT prostate treatments

Eva Maria Ambroa Rey[a,*], Roberto Gomez Pardos[a], David Navarro Giménez[a], Julia García-Miguel Quiroga[a], Antoni Ramirez[b], Montserrat Colomer Truyols[a]

[a] Medical Physics Unit, Radiation Oncology Department, Consorci Sanitari de Terrassa, Terrassa (Barcelona), Spain
[b] Consorci Sanitari de Terrassa, Radiation Oncology, Terrassa, Spain
* Corresponding author.

Purpose. Monitor unit (MU) verification of the treatment planning system (TPS) using an independent procedure is a very important component of volumetric modulated arc therapy (VMAT) quality assurance (QA) program.

The study was aimed to compare accuracy of monitor unit verification with and without treatment couch, for VMAT prostate treatments.

Methods. The accuracy of dose computation by Monaco TPS (v5.10) is checked by independent secondary check software (PTW-Diamond version 6.0). Diamond performs calculation based on modified Clarkson method, which integrates the primary and the scatter components of the radiation dose to a point from all individual and segmental subfields.

Dicom files exported from Monaco include RTplan, dose, patient contour and treatment couch structures. Diamond compares results against the TPS. Also, the couch used was Elekta iBEAM evo Couchtop modeled with a density of 0.1 g/cm3 for inner part of foam and 0.5g/cm3 for the carbon fiber shell.

A total of 60 patients treated with a single arc of 6MV were included in this study. For every patient MU verification was performed with and without the treatment couch.

Results. From 60 patients, the average of MU difference was 0.04% taken into account the treatment couch and 1.23% without the couch, being the maximum found deviation of 3.41% and 4.65% respectively. These differences were statistically significant (p value: 0.00011). The introduction of the treatment couch improves the Diamond results in approximately 68% of the cases.

Conclusions. We can conclude that including the treatment couch in the Diamond MU calculations results in a better QA outcome than when the table is not included.

We can finish up by saying that incorporate the treatment couch is essential to correctly assess the errors in MU calculations.

https://doi.org/10.1016/j.ejmp.2018.06.221

[OA150] Influence of extrafocal dose in the out-of-field dose distribution in a paediatric anthropomorphic phantom, irradiated with a FFF beam and a 120 HD MLC – Monte Carlo simulations and gafchromic EBT3 dose distribution

Firass Ghareeb[a,*], Jorge Eduardo Oliveira[a], Sofia Silva[b], Joana Lencart[c], Joao Santos[d]

[a] Instituto Português de Oncologia Do Porto Francisco Gentil- Epe, Research Center, Porto, Portugal
[b] Medical Physics Service, Portuguese Oncology Institute of Porto (Ipo Porto), Medical Physics Service, Porto, Portugal
[c] Instituto Português de Oncologia Do Porto Francisco Gentil- Epe, Medical Physics Service, Porto, Portugal
[d] Ipopfg, Epe, Servico de Fisica Medica, Research Center, Porto, Portugal
* Corresponding author.

Purpose. Since paediatric patients have higher life expectancy than adults and tend to receive higher secondary organ doses due to geometrical factors, secondary induced cancer due to out-of-field dose among paediatric patients is thus an increased concern. This work focusses on the influence of extrafocal dose in the out-of-field dose distribution using a paediatric anthropomorphic phantom. Monte Carlo simulations (Penelope) and Gafchromic EBT3 2D dose distribution measurement will be assessed.

Methods. A 5-year pediatric phantom (hypothetical brain lesion) was irradiated by Varian TrueBeam 120HD MLC linac, using four 6MV Flattening Filter Free (FFF) static fields. A cranio-caudal beam was employed. The plan was simulated by Monte-Carlo (MC) simulation using PRIMO software. The 2D dose distributions at several distances from the isocenter were measured using Gafchromic EBT3 films. The results were evaluated using 2D Gamma index on PTW-Verisoft software. MC simulations were previously validated by gamma index method (98% of points <1; 2mm, 2%).

Results. Dose distributions were evaluated at 10, 15 and 17.5 cm away from the isocenter. The maximum local measured doses were 3.5, 1.6 and 1cGy per Gy at the isocenter respectively. A well-defined rectangular shaped dose distribution was noticed in the films located at 15 and 17.5 cm from the isocenter. The same shape was also detected in all the MC simulations of the same planes. The rectangular shape was not observed in the TPS (Acuros nor AAA). The center